Finite Element Analysis on the behaviour of multi-storey steel frame with concrete slabs against progressive collapse under fire conditions.

By

NENE NTETHELELO SYABONGA

Submitted in partial fulfilment of the academic requirements for the degree of

Master of Science in Civil Engineering

School of Civil Engineering, Surveying & Construction

University of KwaZulu-Natal

Durban

4 December 2020

Supervisor: Georgios Drosopoulos

COLLEGE OF AGRICULTURE, ENGINEERING AND SCIENCE

DECLARATION 1 – SUPERVISOR

As the Candidate's Supervisor I agree to the submission of this thesis. Signed

……..……...

DECLARATION 2 - PLAGIARISM

I, Ntethelelo Syabonga Nene declare that

1. The research reported in this thesis, except where otherwise indicated, is my original research.
2. This thesis has not been submitted for any degree or examination at any other university.
3. This thesis does not contain other persons' data, pictures, graphs or other information, unless specifically acknowledged as being sourced from other persons.
4. This thesis does not contain other persons' writing, unless specifically acknowledged as being sourced from other researchers. Where other written sources have been quoted, then:

a. Their words have been re-written but the general information attributed to them has been referenced

b. Where their exact words have been used, then their writing has been placed in italics and inside quotation marks and referenced.

5. This thesis does not contain text, graphics or tables copied and pasted from the Internet, unless specifically acknowledged, and the source being detailed in the thesis and in the References sections.

Signed

……..……....

Acknowledgements

Firstly, I would like to thank the **Almighty wonderful God** for giving me the strength and the resources to perform this study as well as giving me the love to do what I do.

Secondly, I would like to express my deepest gratitude to each any member of the **Nene family** back home for their unconditional love and support throughout my studies since preschool till now. They believed so much in me which led me to believe more in myself and my capabilities. In particular, I would love to thank my **late grandmother** who raised me and sacrificed a lot to make sure that I became a better man. My love for you is deeper than pacific and Indian ocean combined.

Thirdly, I would also love to thank **Dr. G. Drosopoulos** for being a great mentor for my research. I am thankful for the patience, guidance, discussions and responses of how to use the program and all the information shared since my undergraduate degree till this day.

In addition, I would love to thank everyone for their love, support, and their motivation during everyday struggles, I am so humbled by everyone who made even the slightest effort to ensure that I achieve my dreams.

Lastly, I would like to thank the **University of KwaZulu-Natal** for giving me the chance to conduct my thesis through provisions of necessary resources and as well sharping me to be one of the future civil engineers.

This is dedicated to my **late grandmother and young sister; I love you guys' infinity squared**.

"Sthenjwa, Mandlokovu wena owaseNgweni"

"I have no special talents. I am only passionate curious." - Albert Einstein

Abstract

This research was conducted to study the behaviour of a multi-storey steel frame with concrete slabs against progressive collapse under fire conditions. An implicit coupled thermomechanical analysis was executed using a commercial finite element modelling, ANSYS while considering the computational effort and the simulation time required to solve the models. A three-dimensional steel frame model was modelled using line bodies while concrete slabs were modelled with shell elements. The research studies the collapse modes and load redistribution action of the steel frame exposed to elevated temperatures. Two fire scenarios were investigated namely, (i) heating individual ground floor columns at various location i.e., corner, short edge, long edge and interior column (ii) four columns being heated at the same time within the same compartment (also referred as compartment fires).

The findings illustrate that when individual columns are heated, the steel frame does not show any signs of progressive collapse; however, the premature local buckling was observed on the heated columns. This was due to material softening or an increase in compression on the heated column. The interior column was more likely to cause progressive collapse. This was due to column load-ratio i.e., the interior columns carry twice the loads in comparison with the perimeter columns. For compartments, no progressive collapse was observed for all the scenarios; however, premature local failure was observed for all the heated columns and for some non-heated columns. For corner and interior compartment fire, non-heated perimeter columns showed premature local failure due to the lateral movement caused by the sagging of slabs above the upper floor of the ground floor column under tension forces.

The global progressive collapse was restrained by the load redistribution action which transferred the loads which were previously carried by the buckled column to the surrounding structural elements. In addition, more loads were transferred along the short span because the stronger axis (x-axis) was orientated along the short span. Hence, loads are more likely to be transferred to the axis with the greater stiffness (stronger axis). In conclusion, the collapse modes were influenced by the fire location and the load redistribution action.

Table of Contents

List of Figures

List of Tables

List of Abbreviations

2D	Two-Dimensions
3D	Three Dimension
ANSYS	Analysis System (Finite element Modelling Software)
AutoCAD	Computer-Aided design (CAD)
°C	Degrees Celsius
FE	Finite Elements
GPa	Gigapascal
J	Joules
K	Kelvin
KN	kilo-Newtons
m	metres
m^2	metres squared
Mpa	Megapascal
N	Newtons
Pa	Pascal
UDL	Uniform Distributed Loading

Chapter 1: Introduction

1.1 Motivation

The recent fire events such as the collapse of the World Trade Centre in USA, New York (2001), Windsor building in Spain, Madrid (2005) and many more, have caused a high level of interest for research in fire structural engineering. Since the early 1900's, there has been a growth in fire events which has led to consider fire engineering as an important part of the design. In 2015, the National Fire Protection Association in the United States reported that, "494000 structural fire events have been reported that year, which led to 2860 civilian deaths, 13425 injuries and a cost of $9.8 billion in property damage". Steel is among the most utilized material throughout the world, based on its advantages such as that it is economical, durable, ductile, versatile and recyclable. Furthermore, in reinforced concrete structures, steel is used as tension reinforcement. However, despite these advantages mentioned above, steel has one major disadvantage, that it is very vulnerable to fire (Awatade, Pise, Japatap, Pawar, Kadam, Deshmukh & Mohite, 2016).

Structural steel tends to lose its strength and stiffness extremely when subjected to higher temperatures i.e., 500°C or more. This means that steel is a good thermal conductor of heat as well as electricity, unlike concrete which has a low thermal conductivity hence concrete is a good insulator material. According to Walls (2016), the exact behaviour of structural steel is complex and there are a lot of uncertainties hence it is unclear what level of precision can be achieved in fire engineering. According to Oosthuizen (2010), a great number of effects have significantly influenced the capacity of these structural elements, which includes the end member support conditions, thermal restrains provide by the connections, the surrounding cooler structure elements, and the bracing system.

Generally, fire grows in a compartment and atmospheric gas temperatures tend to differ within the compartment which then leads to temperature differences in the members within the compartment. Oosthuizen (2010) states that, "the temperature of members at elevated temperatures can be uniform, non-uniform or have a temperature gradient along their length or possess their temperature along the cross section". The structural capacity is mainly affected by the dispensation of temperature within the members. In addition, mid-span members such as beams, or columns tend to heat at higher rates in comparison to the joints which can experience lower temperatures between 62-88 % (Oosthuizen, 2010). According to Jiang, Li and Usmani (2014), progressive collapse is defined as "spread of the first local damage to the

adjacent structural components resulting to global collapse or affecting the structure very largely to cause collapse". Progressive collapse is generally unlikely to occur because when it happens it means the structure has bizarre loading pattern to cause the local failure and lacks the sufficient redundancy, continuity or even ductility to restrict the spreading of failure (Jiang *et al.* 2014). This is due to the fact that the redundant structure has alternative-load paths or excess exterior supports to provide structural stability. Therefore, it prevents local or global failure through the alternative-load transfer paths, as the loads from the failure structure are transferred to the surrounding members. In seismic or wind loading scenarios, the bracings are generally used as one of the measures to improve the lateral response. However, the same theory can be applied in a fire scenario against progressive collapse of the framed structure, but relevant studies are not sufficient.

There are many ways to protect the steel material to sustain its structural integrity. Currently, the fire resistance rating tests (also known as furnace tests) are formally utilized to check the fire resistance of structural elements such as columns, beams or connections. However, the unprotected structural steel elements of a complicated global structure tend to behave well under fire condition in comparison with individual elements. This is because of the capacity of the global structure to transfer fire loads to the cooler surrounding structure (Awatade *et al.* 2016). Furthermore, Oosthuizen (2010) stated that, it is more logical to design a structure that can resist fire loads instead of designing the structure at normal temperatures and subsequently applying fire protection.

Due to the lack of knowledge of the exact behaviour of steel material under fire conditions, it is significant that structural steel elements are studied in detail, especially as part of a global structure, in order to produce designs which are sustainable and can survive the extreme thermal loads. Furthermore, the isolated structures such as beams, or column generally behave differently under fire events compared to global system structure. Thus, it becomes necessary to study the global structural system. This research is intended to study the behaviour of multi-storey steel structures against progressive collapse under fire conditions using finite elements modelling, ANSYS.

1.2 Research Questions

- How does a multi-storey steel structure behave when it is exposed to high temperatures?
- Which collapse mode will occur when various column locations with different load ratios are exposed to high temperatures?

- Which collapse mode will occur when various compartment locations are exposed to high temperatures?
- Will the structural framework experiences global collapse when the different fire locations are exposed to elevated temperatures?

1.3 Aims and Objectives

1.3.1 Aims

- To investigate the fire resistance of a multi-storey steel frame with concrete slabs exposed to elevated temperatures using the finite element modelling software, ANSYS.
- To investigate the collapse modes of a multi-storey steel frame with concrete slabs under fire conditions using ANSYS.

1.3.2 Objectives

- To examine the performance of fire resistance of a multi-storey steel building when various columns are heated at different locations.
- Evaluate and examine the performance of fire resistance of a multi-storey steel building when various fire compartments are heated.
- Evaluate and analyse the possible collapse modes of a multi-storey steel frame under fire conditions.
- To assess the influence of column load ratios of an unprotected multi-storey structural steel under fire exposure.
- To study the load redistribution action when the structural steel elements are exposed to heat.
- To validate and extend to the existing knowledge in the field of fire engineering through the use of finite elements modelling packages, ANSYS.

1.4 Limitations

The study is to be constructed on the finite element analysis program ANSYS, due to the associated financial constraints of performing the laboratory/experimental tests which are more expensive and assumed to be more reliable. The model was created using line bodies because it requires less computational efficiency and time rather than modelling a three-dimensional prototype. This may lead to unconservative results and the equivalent strains (Von misses) parameter which is utilized to observe failure in structural element is not support for line bodies. For this study, an implicit analysis was used for modelling due to financial and computational

constraints. However, an explicit analysis is more competent for this kind of study due to its accuracy and competency against complex non-linear problems of this magnitude. The couple thermo-mechanical analysis is programmed such that the thermal actions are applied firstly and afterwards, the mechanical loads are applied onto a heated structure using a Newton-Raphson iterative method. This is unrealistic in real life situations; however, this will not yield unconservative results. This is due to the fact that in realistic case where fire load is applied after a stable mechanical solution, the results may be a collapse or stable structure, depending on the magnitude and length of the thermal load. Considering that in this study, the thermal load is first applied, the output of mechanical solution which follows is not guaranteed to be a stable equilibrium. If yes, both cases should not differ and if no, the adopted approach will not give us direct information about the collapse history and time during the thermal, accidental loading.

1.5 Methodological Approach

Robson (2007) defined the methodology as the system of recommendations which are used to solve a presented problem with the use of components such as tools, techniques etc. There are three different methodological approaches namely, the qualitative, the quantitative and lastly, the triangulation methodological approach.

A qualitative methodological approach is basically representing the research information by using descriptions, words, and characteristics to record and analyse any social issue (Bless, Higson-Smith & Kagee, 2006). In simple terms, qualitative methodology is defined as a scientific approach to obtain and analyse information without any use of numerical data. Quantitative methodology is known as the scientific approach which is based on numerical data (Kothari, 2004). This involves gathering and analysing the information using mathematical, statistical and/or computational tools. The outputs obtained are presented by using tables, graphs, or any scientific presentations. Lastly, the triangulation methodology is the combination of both the qualitative and quantitative methodology to obtain information and observations which look at various factors (Bless *et. al*, 2006). This method allows more balance between the two methods hence the researcher can get more reliable findings and conclusions.

For this study, a triangulation methodology approach was adopted, which is a combination of both the quantitative and qualitative methodology approach. Also, the triangulation methodology is referred as mixed-methods approach. This means that the limitations of each

research methodology are reduced, and the reliability of the study is improved significantly (Bless *et. al*, 2006). The quantitative research utilized in this study is through the development of numerical models, utilizing graphs and tables to represent the findings. The qualitative methodology was applied through the collection of all the background information of the study and the observations. In addition, all the non-numerical information that was collected through qualitative research was utilized to explain the findings and making recommendations for future research.

1.6 Structure of the Research

The research thesis is divided into six sections. A short introduction and a summary at the end of each chapter is provided. The outline for the study is presented as follows:

Chapter 1

This chapter provides a short introduction to explain the topic further and the motivation for conducting this research. Furthermore, the research questions, the aims and objectives, methodological approach, and limitations are also discussed in this chapter.

Chapter 2

The chapter consists of the theoretical background that is associated with the behaviour of multi-storey steel buildings exposed to elevated temperatures including steel and concrete material properties. The chapter starts by introducing the behaviour of steel structures under fire conditions and then explores case studies of past fire events. Furthermore, the fire resistance categories, fire curves and a brief introduction to fire design resistance is presented on this chapter.

Chapter 3

Chapter 3 demonstrates the steps which are taken when running a simulation with the finite element modelling software, ANSYS. The limitations of the program are also stated in this section and a brief summary is provided in the end.

Chapter 4

Chapter 4 illustrates the methodological procedure which was followed when analysing the multi-storey steel building model in ANSYS program. This includes the materials properties used during the study and as well as the different models which were developed.

Chapter 5

Chapter 5 consists of the results which were obtained by following the methodological procedure stated in chapter 4. Graphical solutions are utilized to represent the results, then a brief discussion is provided to explain the results into further details.

Chapter 6

Chapter 6 contains the conclusion for the whole study where the outcomes of the conducted research are discussed in relation to the objectives. Recommendations for future studies are also provided in this section. Furthermore, additional data such as raw data which was used during the simulation was attached in the appendices section.

Chapter 2: Literature Review

2.1 Introduction

For the past decades, there has been increase in cases of steel structures collapse due to fire incidents, which has caused a major loss to both the economy of the country (property damage) and the citizens (death, injuries etc.). The collapse of steel structures also caused an alert to study fire engineering into detail. This chapter aims to construct the moral of the study and as well to give more insight on the topic. This includes the relevant fire theoretical background, the steel and concrete material properties, an introduction to fire resistant principles and past reviews of past fire events. In this chapter, section 2.2 establishes the basic summary of how fire can affect steel structures, also it provides an overview of past fire incidents. Section 2.3 gives a discussion of the structural steel and the concrete's material properties at elevated temperatures. Furthermore, section 2.4 and section 2.5 present heat mechanisms, fire curves models and the basic fire resistance design. Lastly, a brief summary of the chapter is presented at the end of the chapter to summarize the key points of this chapter.

The analytical methods in this study are founded on numerical expressions obtain from verified theoretical data and are acquired from a several credited fire engineering tests which were conducted.

2.2 Effects of fire on structural steel structures

2.2.1 Overview

Steel structures normally perform "sufficiently" under fire situations; however, their exact behaviour is not fully understood since the performance of individual structural steel members' is slightly different from that of the global structure (Qin, 2016). The term "sufficiently" mentioned above, refers to the capacity of the structure to allow deformations but resist the collapse of the global structure under fire situations. According to Qin (2016), a more quantifiable way of evaluating the "sufficiency" of steel structures under fire exposure or any related extreme hazards is by coordinating a life cycle cost assessment.

The main reason why there is a lack of full understanding of the behaviour of steel structures at elevated temperatures is because at high temperatures, the steel loses its strength and stiffness very drastically, which then needs certain testing and simulations abilities. From the structural engineers' point of view, the main effect is the reduction of steel strength and strength with increasing temperatures which could cause collapse of the global structure. On the other the

hand, from the simulation point of view, the problem is composite and needs simulation of 1) fire behaviour, 2) the transfer of heat to the structure and the nearby structural elements, 3) the structural behaviour where considerable deformations are to be anticipated (Qin, 2016).

Generally, the fire resistance of any structural steel element is basically the time taken by the structural element to resist the combination of mechanical and thermal loads when subjected to the standard fire tests. Oosthuizen (2010), further explains that the fire resistance tests are related to the time taken by structural elements to reach their critical temperature. The standard fire resistance tests are understood to fall within the safety limits hence in case of the fire event, people and belongings can be evacuated. However, the focus must shift to make designs which can survive these extreme temperatures and prevent damage of structural buildings.

Several factors influence the behaviour of steel structures under fire conditions which then makes it complex to predict the "real conditions" of these members. As mentioned above, individual members tend to behave differently under fire standard tests compared to global system structure. Furthermore, the EN 1993-1-2 (2005) proposed a standard heat transfer model which over predicts the increase of temperature because it does not consider the influence of combustion products on the heating rates for structural elements. According to Kang-Hai, Wee-Saing, Zhan-Fei & Guang-Hwee (2007), the Cardington tests showed that the structural members in a global structure heated up in a slower heating rate than in comparison with the standard fire tests. Furthermore, from the findings of the experimental tests, it was observed that the global and isolated column both experienced axial and rotational restraints.

Kang-Hai *et al.* (2007) also mentions that the column imperfections and as well as load eccentricities had a major effect on the collapse time of these members by greatly reducing it. In addition, the axial restrains influences the increase of column axial loads which then lead to a reduction of collapse time. Fire compartments tests are utilized in multi-storey buildings to prevent the spread of fire into the whole structure. Generally, the members under fire conditions are surrounded by the cooler structural members which provides more load paths options hence disallowing the collapse of the global structure. The surrounding cooler members are assumed to disallow the thermal expansion (by inducing additional internal forces and moments) of the members under fire exposure. These members exposed to thermal expansion will have a reduced failure strength, however, Davies & Wang (2003) mentioned that these additional internal forces had no influence on the collapse loads of columns.

The structural steel will experience a loss of strength and stiffness when it is exposed to increasing temperatures which can lead to permanent deformations and collapse of the structure. According to Qin (2016), under uniform loading, a steel structure will experience permanent deformation when the temperature is at least 450 ℃ due to creep. At lower temperatures, there is no reduction of strength and stiffness, however, only in a statically indeterminate structure.

The upcoming sections are aimed to provide the related background information for this research, including the past major fire events. The past fire events are discussed into detail to highlight the behaviour of structural steel when exposed to fire conditions. Furthermore, the material properties, natural fire curves, heat transfer mechanisms and the basic principles of fire-resistant design are elaborated.

2.2.2 Major Past Fire events

Experimental testing and analytical simulations are key factors to fully understand the behaviour of structural steel at elevated temperatures. However, due to lack of technical constraints related to experimental testing or the numerical simulations, it has been difficult to fully understand the behaviour of structural steel under fire conditions. Hence, it is very critical to study past fire scenarios to obtain the basic behaviour of the structural steel. In addition, several experiments have been carried out on the steel members, connections and as well as the materials, however, it has been difficult to carry these experiments on the global structure and determine how the global structure behaves under fire conditions due to a greater number of constraints including costs of experiments.

2.2.2.1 Broadgate Phase 8 Fire, London, UK (1990)

In 1990, the 14-storey incomplete steel frame building in London, England was ignited with fire. An estimated area of 40m by 20m was damaged and could not be repaired, but the global structure did not collapse as it redistributed the loads to the adjacent structural members. Furthermore, the composite floor slab maintained its strength during the fire duration. It was reported that most of the steel framework had no fire protection and was easily exposed to fire. The British steel investigators found that the steel framework temperature did not go above 600℃ and the connections reached only a maximum 540℃.

Steel without any protection indicated signs of local buckling mainly because it was vulnerable to fire. Steel beams which showed signs of permanent deformation were observed to undergo local buckling near the supports. According to report by Newman in 2000, the behaviour was

mainly affected by mechanical restraints versus thermal expansion and it extended to the surrounding cooler members. In addition, it was reported that no permanent deformation occurred in the columns which were largely exposed to compartment fires.

Figure 2.1: Local Column Buckling after fire exposure (Qin, 2016).

2.2.2.2 Churchill Plaza Fire, Basingstoke, UK (1991)

In 1991, the 12-storey Mercantile Credit Insurance building in Basingstoke, England was ignited with fire due to glazing problems. Fire started on the 8th floor then quickly spread to the 10th floor due the glazing failure mechanisms (see Figure 2.2). The building was standing since 1988 and it was designed for fire protection by applying the 90 minutes standard fire resistance curves. Fire repelling insulators were applied to the composite steel floors. Also, heat repelling boards were utilized to protection the steel columns against fire events. After the fire incidents, researchers found that the fire protection system played a very crucial part to ensure that the whole structure does not collapse. According to Preston & Kirby (1998), no permanent deformations were observed on both the steel frames and the connections.

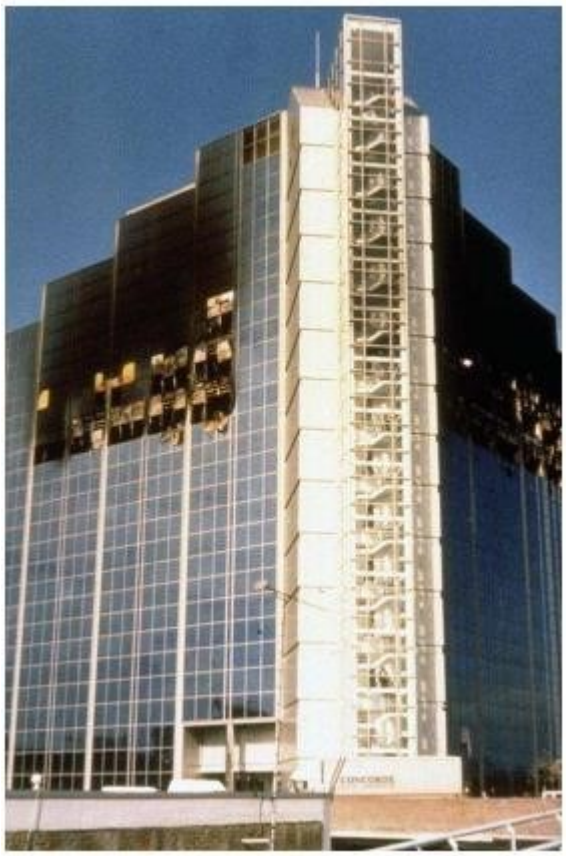

Figure 2.2: Church Plaza fire (Qin, 2016).

2.2.2.3 Windsor Building, Madrid, Spain (2005)

On the 12th of February 2005, the Windsor building in Madrid, Spain was ignited with fire which lasted between 18 and 20 hours long. The fire started approximately at 11 pm on the 21st floor of the 32nd story building and then spreading onto the above floors. The fire was then observed spreading onto the lower floors by 9 am, and a few hours afterwards the fire was uncontrollable.

The building had a 40m by 25m floor plan and it was composed of a composite structural steel with reinforced concrete. The building was constructed using the 1970 Spanish design code and has been standing since 1979. The building was under renovation when fire occurred, which involved installation of fire protection specifications. Renovation was completed on the first 17th stories and the remaining top floors had no fire protection.

A reported by the NILIM (2005) suggested that the following partial collapses and phenomena related to the structural response of the building:

(1) Steel columns which were exposed to elevated temperatures buckled because of the reduction of the steel material properties at high temperatures.

(2) The buckled columns distributed its axial loading onto the adjoining members.
(3) The developing fire caused more columns to buckle but the waffle slabs acted as a cantilever to prevail structural collapse.
(4) The fire spread onto the members, and the waffle slabs collapsed when they reached their maximum load carrying capacity.
(5) The floor failure caused failure for the remaining floors and then the waffle slabs failed at the connection towards the centre.

Floors without any fire protection showed enough signs of collapse but the reinforced concrete core prevented the global collapse of the whole structure by maintaining its strength. Figure 2.3 shown below, demonstrates the different states of the building during the fire incident.

Figure 2.3: Windsor Building Fire (Qin, 2016)

2.3 Material Properties

Most construction materials tend to lose rapidly their strength and their stiffness with increasing temperatures. Hence, studies on the material properties are very crucial to fully understand its behaviour at elevated temperatures. Therefore, this section discusses thermal and mechanical properties of structural steel with increasing temperatures. Moreover, concrete's material properties are also briefly summarised on this section.

2.3.1 a) Thermal Properties of Steel

The thermal properties are very significant to understand the behaviour of steel materials and this involves properties such as thermal expansion, specific heat, thermal conductivity and the density.

2.3.1.1 Thermal Expansion

Thermal expansion is defined as the phenomenon where a material changes in length, area and volume due to temperature changes. According to the laws of thermodynamics, when a material is heated, the atoms gain more kinetic energy which increases motion for the particles and causes more collisions between the atoms. Generally, the linear expansion is defined as the change in length divided by original length and it is used for solid materials. Furthermore, when the steel material is under high temperatures, it elongates and when is subject to low temperatures, it lessens. The equations below are utilized to calculate the thermal linear expansion (Eurocode 3, 2001).

- For temperatures between 20 °C and 750 °C:
  $\Delta l/l = 1.2 \times 10_5 T_s + 0.4 \times 10_{-8} T_{s2} - 2.416 \times 10_{-4}$
- For temperatures between 750 °C and 860 °C:
  $\Delta l/l = 1.1 \times 10^{-2}$
- For temperatures between 860 °C and 1200 °C:
  $\Delta l/l = 2 \times 10^5 T_s - 6.2 \times 10^{-3}$

Where:

l = Length at 20 °C

Δl = Elongation due to increase in temperature

T_s = Steel Temperature [°C]

Figure 2.4 below shows the thermal expansion versus temperature graph for the steel (Eurocode 3, 2001). The change of slope observed between 750 °C and 860 °C is due to the transformation phase which is taking place within the steel. Awatade *et al* (2016) states that for elementary calculation models, the slope for the thermal expansion versus temperature can be assumed to be linear with no discontinuities. The equation below can be utilized to calculate the thermal strain (Eurocode 3, 2001).

$$\text{Thermal Strain} = 14 \times 10^{-6} (T_S - 20)$$

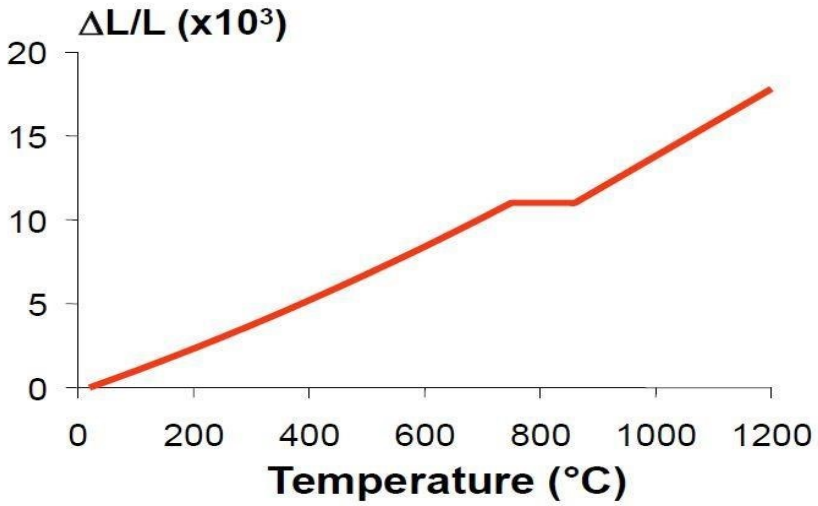

Figure 2.4: Thermal expansion of steel with increasing temperature (Eurocode 3, 2001).

2.3.1.2 Specific Heat

The capacity of the material to take in heat by either chemical or physical action is defined as the specific heat for that material. Eurocode 3 (2001) clearly states for a structural steel, its ability absorb heat does not depend on the chemical and mechanical constitution, however, it is only dependent to the changing temperature.

The equations below are utilized to calculate the specific heat for the steel material at different temperatures (Eurocode 3, 2001).

- For temperatures between 20 °C and 600 °C:
  $C_s = 425 + 7.73 \times 10^{-1} T_s + 0.4 \times 10^{-8} T_s^2 - 2.22 \times 10^{-6} T_s^3$ J/kg.K
- For temperatures between 600 °C and 735 °C:
  $C_s = 666 + 1300/ (2738 - T_s)$ J/kg.K
- For temperatures between 735 °C and 900 °C:
  $C_s = 545 + 17820/ (T_s - 731)$ J/kg.K
- For temperatures between 900 °C and 1200 °C:
  $C_s = 650$ J/kg. K

Where:

C_s = Specific heat of steel [J/kg.K]

T_s = Steel Temperature [°C]

For easy calculation models which do not consider the effect of temperature, a numerical value of 600 J/kg.K is adopted for the specific heat. Furthermore, if the temperature is above 900℃, then a numerical value of 650 J/kg is used. Below, a specific heat versus temperature graph is demonstrated on Figure 2.5 (Eurocode 3, 2001). It should be noted that at 730 ℃, there is a change in chemical composition for the steel which results a summit specific heat.

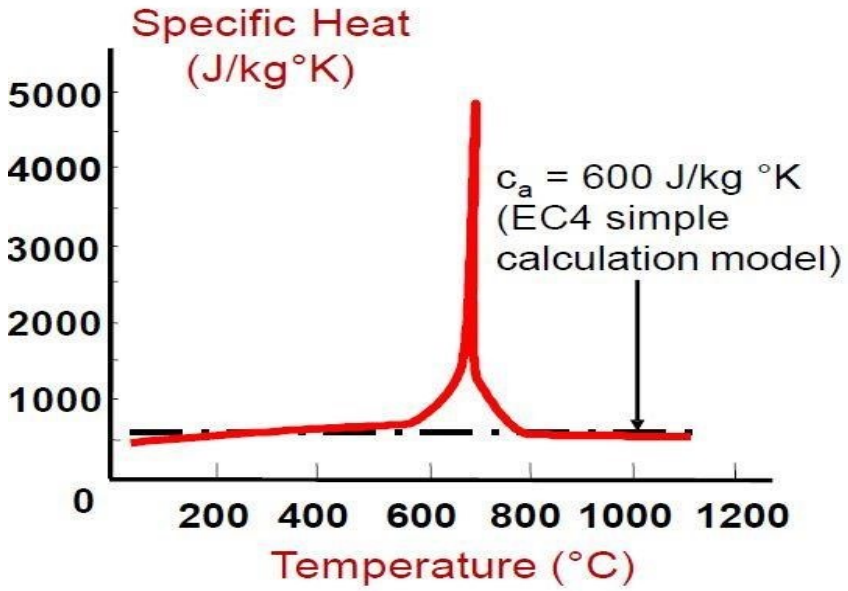

Figure 2.5: Specific heat of steel with increasing temperature (Eurocode 3, 2001).

2.3.1.3 Thermal Conductivity

According to Awatade *et al.* (2016), thermal conductivity is elucidated as the capability of the material to conduct heat. Scientifically, it can be expressed as "quotient of the heat flux to the temperature gradient". In any steel material, thermal conductivity is directly proportional to the varying temperature. In addition, according to the second law of thermodynamics, when an isolated system experiences a change in temperature, heat tends to flow from a higher concentration to low concentration to ensure a constant temperature distribution throughout the material (Vassart *et al.* 2014).

The thermal conductivity at different temperatures can be calculated by using the equations shown below which were adopted from the Eurocode 3 (2001).

- For temperatures between 20 ℃ and 800 ℃:
  Thermal conductivity (λ /κ) = 54 – 3.33 $\times 10^{-2}\, T_S$ W/m.K

- If the temperature lies in between 800 °C and 1200 °C:
- Thermal conductivity (ƛ /κ) = 27.3 W/m.K

Where:

T_S = Steel temperature [°C] ƛ /κ =
Thermal conductivity [W/m.K]

Generally, most steel materials are completely disintegrated when the temperature is above 1200 °C thus the thermal conductivity above this temperature is not defined. However, in the case where a thermal analysis is performed and the temperature is above 1200 °C, a numerical value of 27.3 W/m.K can be employed. Furthermore, in a simple calculation model where the influence of temperature is not taken into account, a numerical value of 45 W/m.K can be employed.

Figure 2.6 demonstrates the thermal conductivity of a steel material. The thermal conductivity of a steel material experiences a steady reduction between 20 °C and 800 °C then above 800°C, it remains steady at one numerical value approximately 27.3 W/m.K.

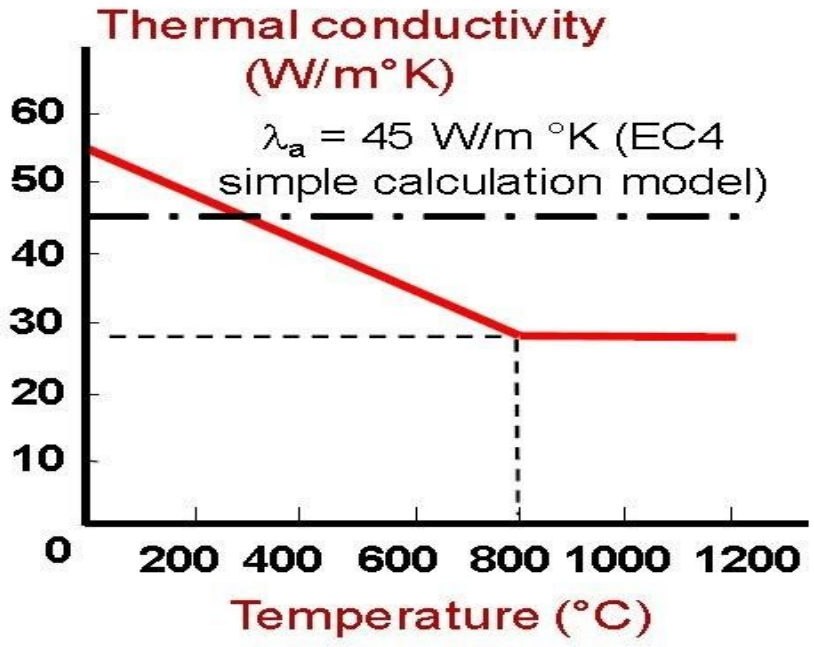

Figure 2.6: Thermal conductivity of steel with temperature (Eurocode 3, 2001).

2.3.1.4 Density

Density is expressed as the ratio of the mass of the material and its volume. The density of a steel varies with the temperature however it results in minimal changes in comparison with other thermal properties for the steel which are described above. Generally, a numerical value of 7850 kg/m^3 is mainly adopted for most steels and it is assumed to be steady (Eurocode 3, 2001).

2.3.2 b) Mechanical Properties of Steel

2.3.2.1 Stress

In simple terms, the stress is expressed as the quotient of the force and the cross-sectional area of an object. Stress is a measure of strength (Hibbler, 2014). Most structural failures are related to stress failures thus it is important to study the stresses of any material in detail. Parson (2018), states that there are six vital stresses which are namely, bending, shear, tensile, compressive, torsion and lastly, fatigue stress. In addition, the way a force is applied on any material illustrates which type of stresses will occur on that material. Figure 2.7 illustrates the direction of the induced normal stresses due to the application of corresponding forces.

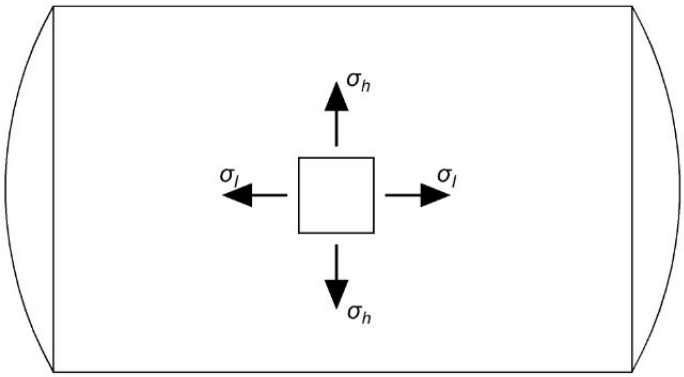

Figure 2.7: Direction of the induced stresses as a resultant of the applied forces.

2.3.2.2 Strain

Strain is expressed as the quotient of the change in length and the original length due to the applied load. Hibbler (2014) states that the strain is a measure of deformation. As described above, strain due to temperature changes is referred to as thermal strain. Strains consists of a various component and are illustrated in the equation below (Eurocode 3, 2001).

$$\varepsilon_t = \varepsilon_{th} + (\varepsilon_\theta + \varepsilon_{tr} + \varepsilon_c) + \varepsilon_r$$

Where:

ε_t = the total strain

ε_{th}= the thermal strains caused by the elongation of steel

ε_θ = the strain caused by the stresses

ε_{tr} = the strain caused by the transient and non-uniform heating pattern for concrete

ε_r = the strain caused by the residual stresses in steel

Figure 2.8 below illustrates the creep strain as a function of the temperatures tested in tension. The figure below clearly shows that the strain is directly proportional to the temperature of the steel as well as the stress level. In addition, it can be observed that the effect of temperature occurs between 400°C and 500°C, where the curves change their slope into a linear vertical shape due to increasing temperature. Eurocode 3 (2001) states the significance of creep deformation because of their effect on the structural steel when it comes near its collapse.

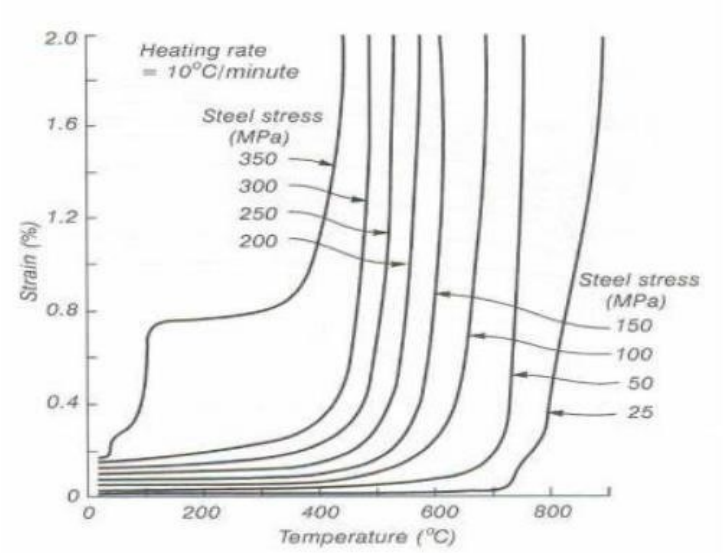

Figure 2.8: Creep strains with increasing temperature (EN 1991-1-2, 2002).

2.3.2.3 Stress-Strain Relationship

The stress-strain relationship (as shown on Figure 2.9) illustrates the different phases a material undergoes when a load is applied to it. Two classical experiments are performed to obtain this relationship, namely the tension and the compression test. From the stress-strain diagrams, two important factors namely, the elastic modulus (Young's modulus) and yield strength were discovered. For a steel, it is found that tension and the compression tests yield almost the same

relationship. Hibbler (2014) states that most materials obey the Hooke's Law, which states that in an elastic region, the stress is directly proportional to the strain.

Figure 2.9 illustrates the stress strain diagram for the structural steel (0.2% Carbon steel) with increasing temperatures. In addition, it can be seen from the Figure below that both the yield strength and the modulus of elasticity (Young's modulus) are greatly reduced with the increasing temperature.

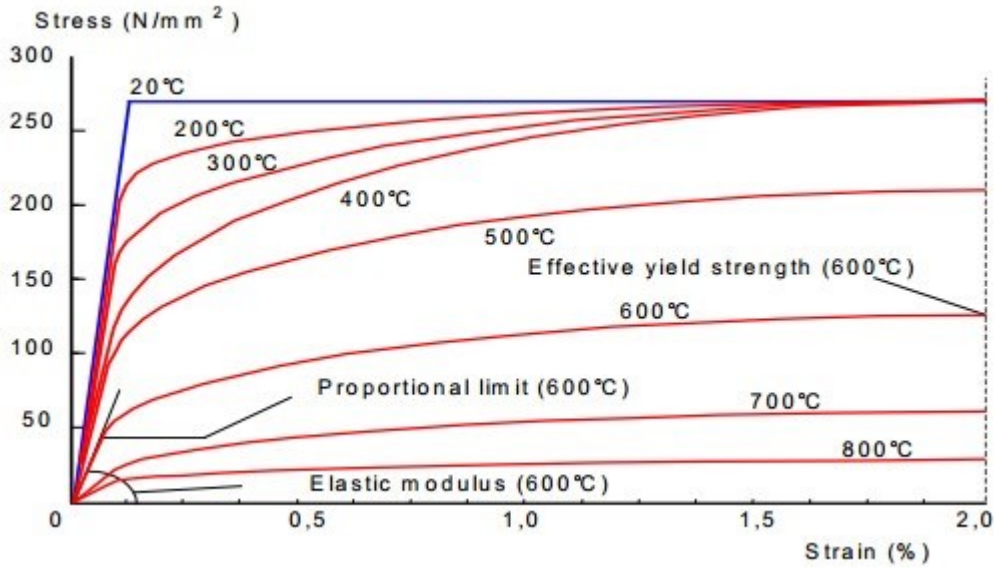

Figure 2.9: Stress-strain relationship with increasing temperature (EN 1993-1-2, 2005).

Figure 2.10 below illustrates two graphs which indicate the strength and stress-strain behaviour of the structural steel with increasing temperatures, adopted from the Eurocode 3 (2001). The graph on the left-hand side indicates the reduction of both the effective yield strength and the elastic modulus with increasing temperature while the graph on the right-hand side indicates the normalised stress-strains with increasing temperatures. From the Figure below (left), it can be clearly seen that at 600 °C, the effective yield strength (indicated by the red line graph) of the structural steel diminishes by over 50 % and the elastic modulus (indicated by the green line graph) diminishes by at least 70 % (Eurocode 3, 2001).

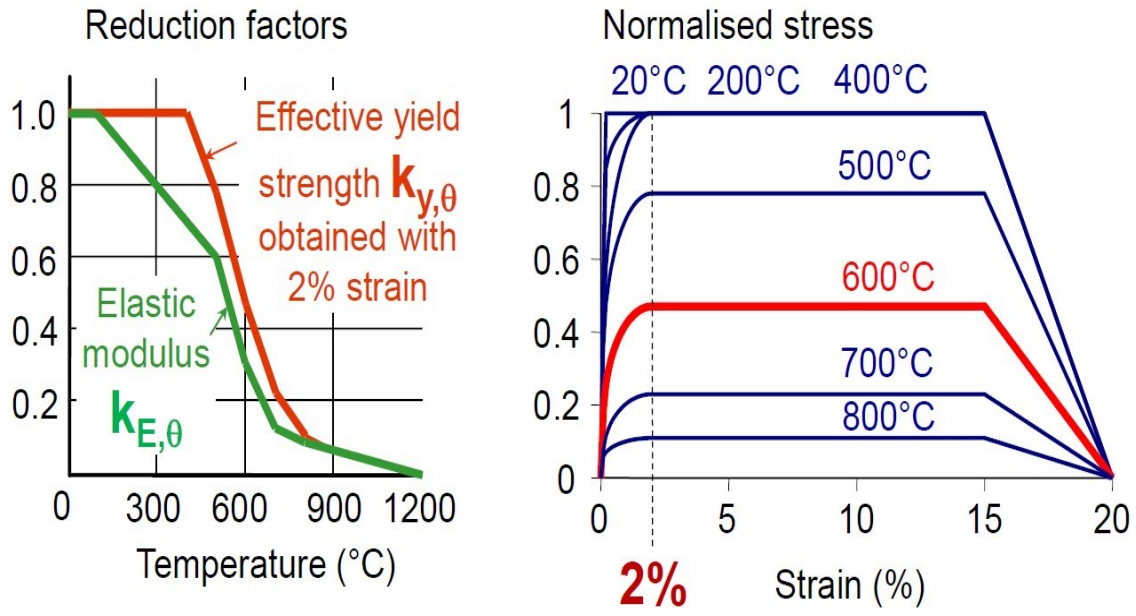

Figure 2.10: Mechanical properties of steel with increasing temperature (Eurocode 3, 2001)

Figure 2.11 and Table 2.1 below summarise the structural steel mechanical properties which are utilized in simple and complex calculation models. It should be noted that the data from the Table below is expressed in terms of the reduction factors and that temperature is considered.

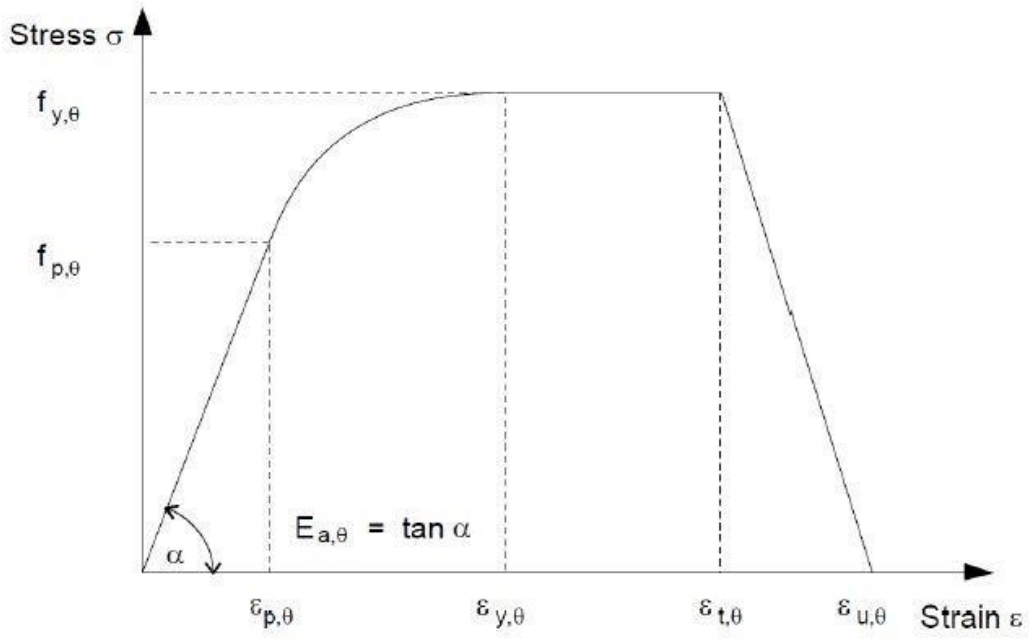

Figure 2.11: Stress-strain curve (Hibbler, 2014)

Where

$f_{y,\theta}$ = Effective yield strength

$f_{P,\theta}$ = Proportional limit

$\varepsilon_{a,\theta}$ = Slope of the linear elastic range

$\varepsilon_{p,\theta}$ = Strain at the proportional limit

$\varepsilon_{y,\theta}$ = Yield strain

$\varepsilon_{t,\theta}$ = Limiting strain for yield strength

$\varepsilon_{u,\theta}$ = Ultimate strain

Table 2.1: Reduction factors for stress-strains relationship for Carbon steel exposed to high temperatures (Eurocode 3, 2001).

Steel temperature θ_a	Reduction factors at temperature θ_a relative to the value of f_y or E_a at 20 °C		
	Reduction factor (relative to f_y) for effective yield strength $k_{y,\theta} = f_{y,\theta}/f_y$	Reduction factor (relative to f_y) for proportional limit $k_{p,\theta} = f_{p,\theta}/f_y$	Reduction factor (relative to E_a) for the slope of the linear elastic range $k_{E,\theta} = E_{a,\theta}/E_a$
20 °C	1,000	1,000	1,000
100 °C	1,000	1,000	1,000
200 °C	1,000	0,807	0,900
300 °C	1,000	0,613	0,800
400 °C	1,000	0,420	0,700
500 °C	0,780	0,360	0,600
600 °C	0,470	0,180	0,310
700 °C	0,230	0,075	0,130
800 °C	0,110	0,050	0,090
900 °C	0,060	0,0375	0,0675
1000 °C	0,040	0,0250	0,0450
1100 °C	0,020	0,0125	0,0225
1200 °C	0,000	0,0000	0,0000
NOTE: For intermediate values of the steel temperature, linear interpolation may be used.			

2.3.2.4 Modulus of elasticity

As described above, the Hooke's law is an important quantity, and it is commonly known as the modulus of elasticity. In simple terms, the modulus of elasticity is explained as the quotient of the stress and the strain within the elastic region where the material can safely return to its original shape (Hibbler, 2014). Moreover, the modulus of elasticity is sometimes referred to as the Young's modulus or the Tensile modulus.

Figure 2.12 below illustrates the behaviour of the elastic modulus and as well as the strength of the structural steel when it is subjected to stresses. In addition, from Figure 2.10, it was observed that at approximately 600 ℃, the steel rapidly lost 70% of its stiffness and 50% of the effective yield strength (Eurocode 3, 2005).

2.3.2.5 Plasticity Region

The Plastic zone is often referred to as the "non-linear zone" in the stress-strain diagram and this zone does not obey the Hooke's law. In the plastic zone, the material will be subjected to permanent deformations and can never return to its original shape (Hibbler, 2014). Figure 2.12 below illustrate the life cycle of the steel material when loads are applied to it.

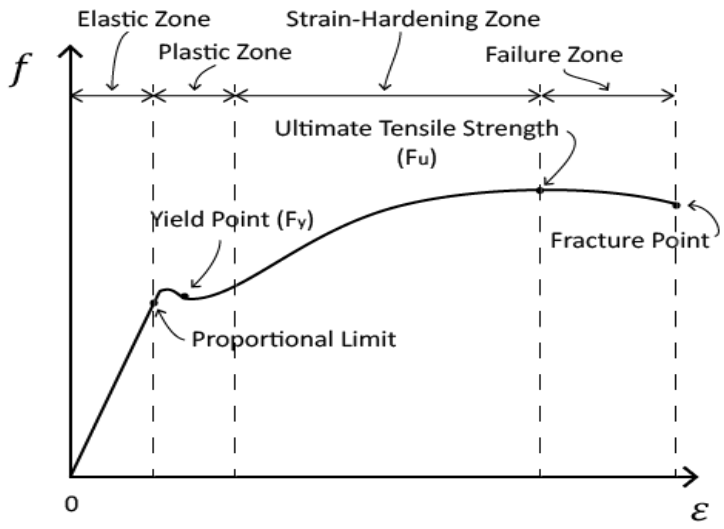

Figure 2.12: Different zones in a steel material (Adapted from online sources).

2.3.2.6 Von Misses

The von misses yield stress is commonly known as the Equivalent stress. It is defined as the peak stress that is expected before the material starts yielding. Long, McAllister, Gross & Hurley (2010) describes that the theory of von misses' states that a system of loads will induce

yielding of a material when the distortion energy is the same or bigger than the material yield limit. The theory of von misses only applies to the plastic region of ductile materials (such as steel) as it describes the maximum stress expected before yielding starts to occur. Generally, most finite elements modelling packages present their results using the von misses' stresses.

2.3.3 Concrete material Properties

This sub-section aims to highlight the mechanical and thermal properties for concrete material. Most construction materials are affected by elevated temperatures thus it is significant to study their properties at elevated temperatures in order to understand their behaviour.

2.3.3 a) Thermal Properties

The thermal and mechanical properties of concrete such as the thermal elongation, specific heat, thermal conductivity, density, and stress-strain relationship are summarised on the subsections below.

2.3.3.1 Thermal Elongation

The thermal elongation for a normal weight concrete is influenced by the increasing temperature. In simple models, the thermal expansion increases linearly with the increasing temperatures (Simms, 2016). The thermal strain for normal weight concrete with siliceous aggregates can be calculated by using the following equations (Eurocode 4, 2005):

$$\text{Thermal Strain} = -1.4 \times 10^{-6} + 9 \times 10^{-6}.T_S + 2.3 \times 10^{-11}.T_S^3 \qquad \text{for } 20°C \leq T_S \leq 700°C$$

$$\text{Thermal Strain} = 14 \times 10^{-3} \qquad \text{for } 700°C \leq T_S \leq 1200°C$$

Figure 2.13 below demonstrates the thermal elongation of concrete with siliceous aggregates for both simple and exact models.

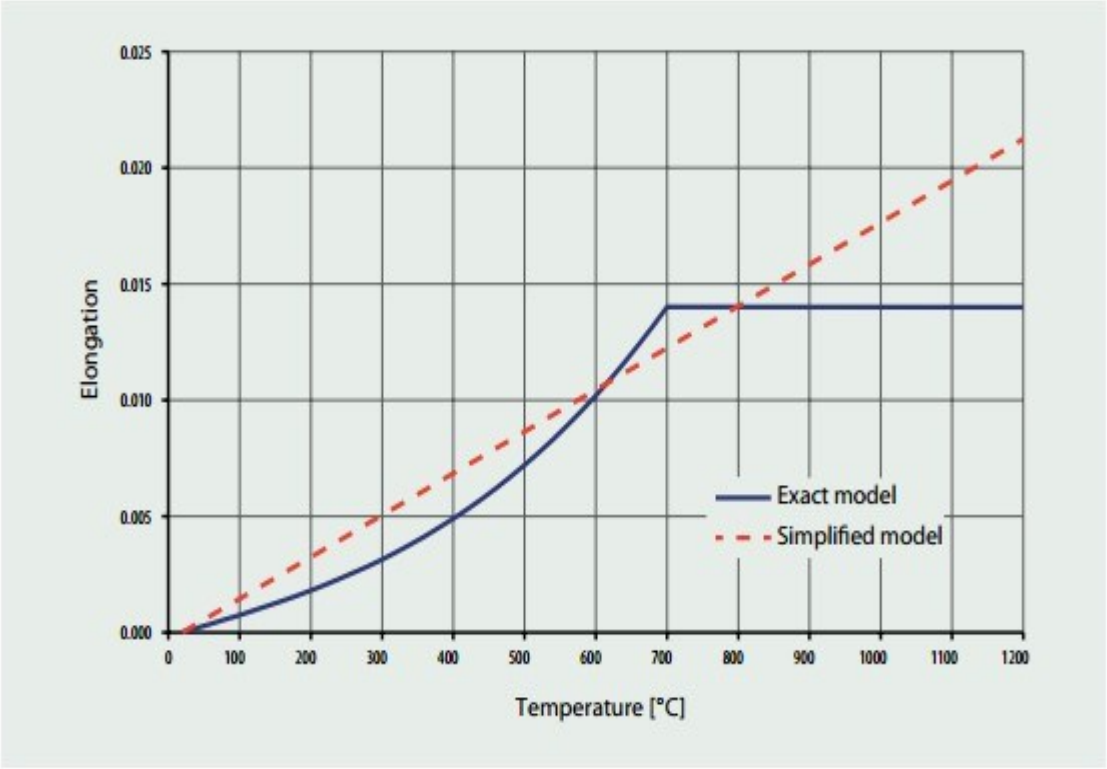

Figure 2.13: Concrete's thermal elongation as function of temperature (Simms, 2016).

2.3.3.2 Specific Heat

In simple models, the specific heat for normal weight concrete (either with siliceous or calcareous aggregates) is regarded to not be influenced by the concrete temperatures. However, to completely model the behaviour of concrete under fire condition, the effect of temperature must be considered in the analysis. In the case when the moisture content is not included in the analysis then a numerical value of 915 J/kg.K can be assumed. Also, if the effect of temperature is not taken into account, then the concrete's specific heat can be assumed to be a constant value of 915 J/kg.K (Simms, 2016). Below, are the numerical values for specific heat values of concrete at different moisture content (Eurocode 4, 2005):

C_s= 1470 J/kg.K for u=1.5%

C_s= 2020 J/kg.K for u=3.0%

C_s= 5600 J/kg.K for u=10%

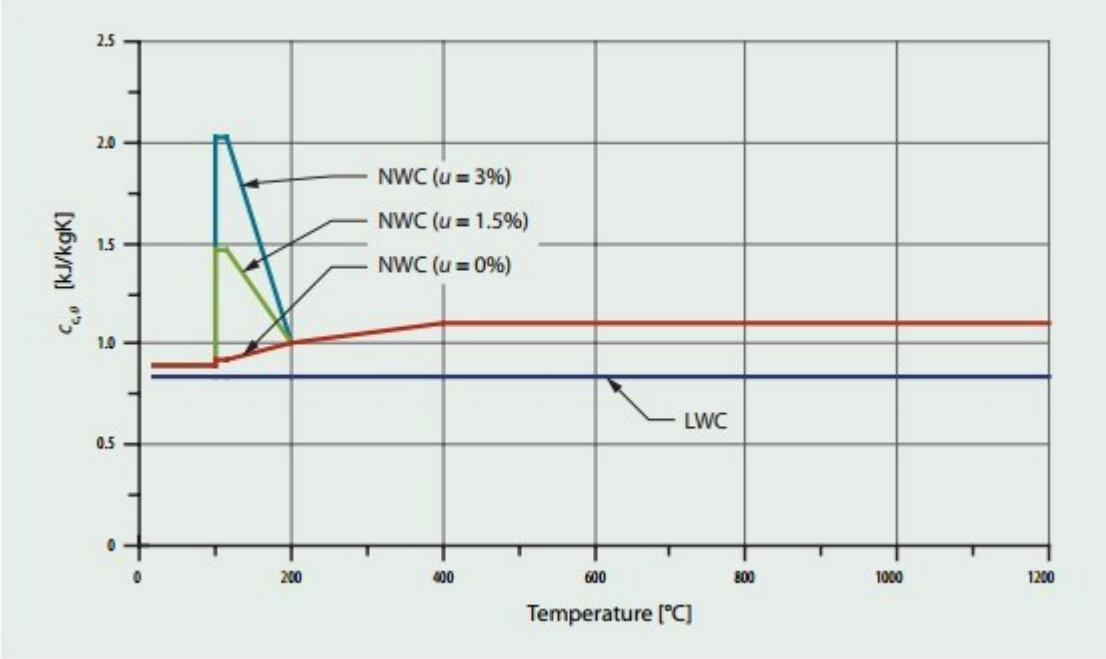

Figure 2.14: Specific heat of concrete as function of temperature (Simms, 2016).

2.3.3.3 Thermal Conductivity

Thermal conductivity of normal weight concrete is defined by the upper and lower limits values which are shown in the expression below (Eurocode 4, 2005):

Upper limit: Thermal conductivity (λ_c) = 2 – 0.2451 (T_S/100) + 0.0107 (T_S/100)^2 W/m.K

Lower limit: Thermal conductivity (λ_c) = 1.36 – 0.136 (T_S/100) + 0.0057 (T_S/100)^2 W/m.K

Note that: Both equations are used for temperatures between 20°C - 1200 °C.

Figure 2.15 below illustrates the relationship of thermal conductivity for both lower and upper limits with increasing temperature. The EN 1994-1-2 (2005) suggests that the upper limit must be utilized in all events.

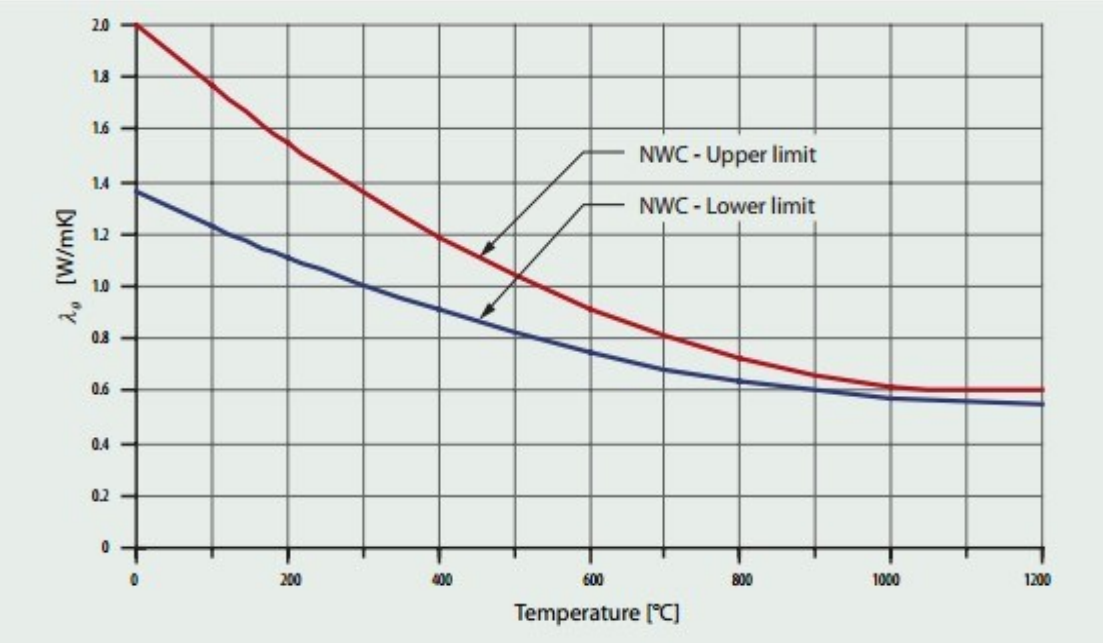

Figure 2.15: Thermal conductivity of concrete as function of temperature (Simms, 2016).

2.3.3.4 Density

According to the European standards, the relationship of the concrete's density with increasing temperature is predominately affected by the loss of free water. However, for static loading, the concrete's density does not depend on the temperature. The expression below is used to estimate the variation of concrete's density during any thermal analysis (Eurocode 4, 2005):

$\rho_{c,\theta} = 2354 - 23.47\ (T_s/100)$

2.3.4 b) Mechanical Properties

The European standards illustrates the reduction of strength with increasing temperatures for normal weight concrete (see Figure 2.16). It is clearly visible that an increase in temperatures causes a decrease in the concrete's compressive strength. The expression below describes the concrete's stress-strain relationship under uniaxial compressive forces at extreme temperatures (Eurocode 4, 2005).

$$\sigma_{c,\theta} = \frac{3.\varepsilon_{c,\theta} f_{c,\theta}}{\varepsilon_{cu,\theta}(2+(\varepsilon_{cu,\theta})3)} \qquad \varepsilon \leq \varepsilon_{cu,\theta}$$

Where:

$f_{c,\theta}$ = is the compressive strength of concrete at temperature $\theta_c (=k_{c,\theta} f_c)$ f_c
= is the compressive strength of concrete at ambient temperature.

ε_c = is the concrete's strain

$\varepsilon_{cu,\theta}$ = is the concrete's strain in relation with $f_{c,\theta}$

θ_c = is the temperature of the concrete $\sigma_{c,\theta}$
= is the stress of the concrete

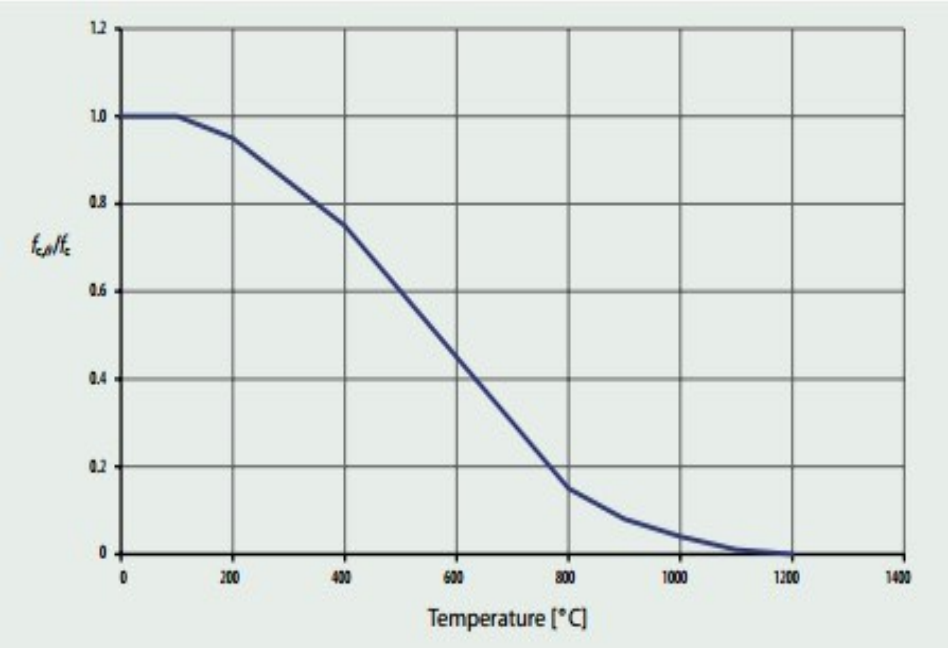

Figure 2.16: Reduction of strength for normal weight concrete at extreme temperatures (Simms, 2016).

Figure 2.17 below describes the stress-strain relationship for normal weight concrete at extreme temperatures as adapted from the EN 1994-1-2 (2005). It is evident that the concrete material reaches a peak compressive strength at very low temperatures, however, as the temperature increases, the compressive strength reduces very drastically while the concrete strains increase with the increasing temperatures. Simms (2016) recommends that in simple calculation models, the concrete's tensile strength can be disregarded.

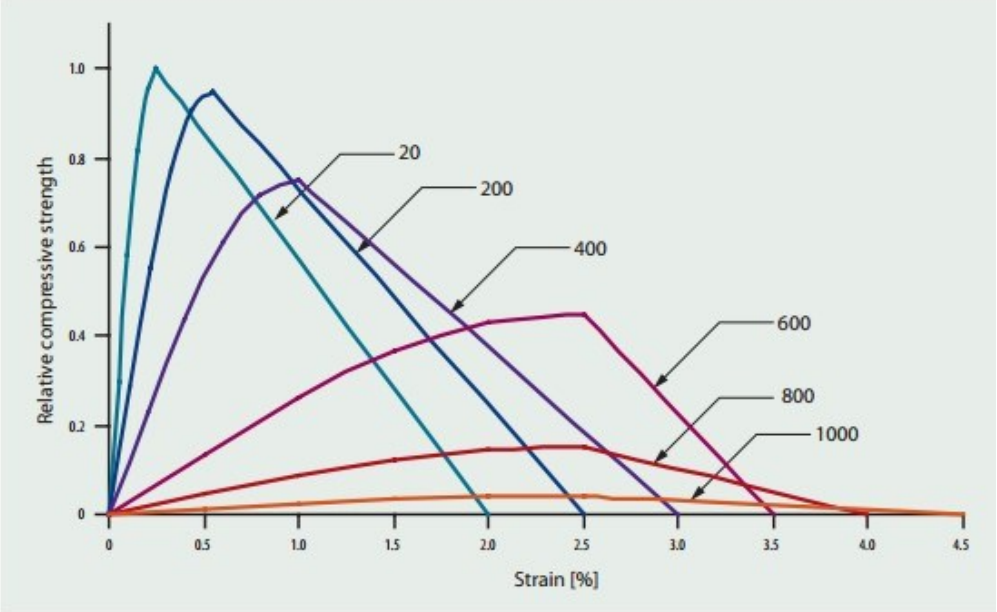

Figure 2.17: Stress-strain relationship for normal weight concrete at extreme temperatures (Simms, 2016).

2.4 Temperature in Fires

This section looks at a quick review of the development of natural fire, a range of available fire curves which are used for fire resistance testing, as well as the three types of heat transfer mechanisms.

2.4.1 Natural fire Overview

Through many years of research, a more realistic behaviour of a real fire approach has been developed. Similarly, to other fire tests, they are constituted of temperature versus time curves. The natural fire test considers that real fires in structural buildings grow and decay based on the balance of energy and as well the mass within each compartment (Oosthuizen, 2010).

Real fires can be described only by three phases, namely the growth, full development and decay phase as it is illustrated in Figure 2.18. The growth phase (as known as the pre-flashover) occurs immediately after the start of the fire, it is commonly referred to as the development stage of the fire. Afterwards, the flashover occurs when there is enough heat to cause the involvement of the whole compartment. Thereafter, the full development phase occurs when the whole compartment is under fire. During this phase, both the temperature and the energy released increases very quickly as all the combustible materials are being burnt. Lastly, the decay phase occurs where both the temperature and the energy released decreases since all the combustible materials have been burnt out (Oosthuizen, 2010).

According to Walls (2016), the temperature in the structural steel building can be as high as 1000℃ to 1200℃ and in some instances, the decay phase can result into structural failure. Figure 2.18 below illustrates the three phases of natural fire and the comparison of the atmospheric temperature with the standard fire curve.

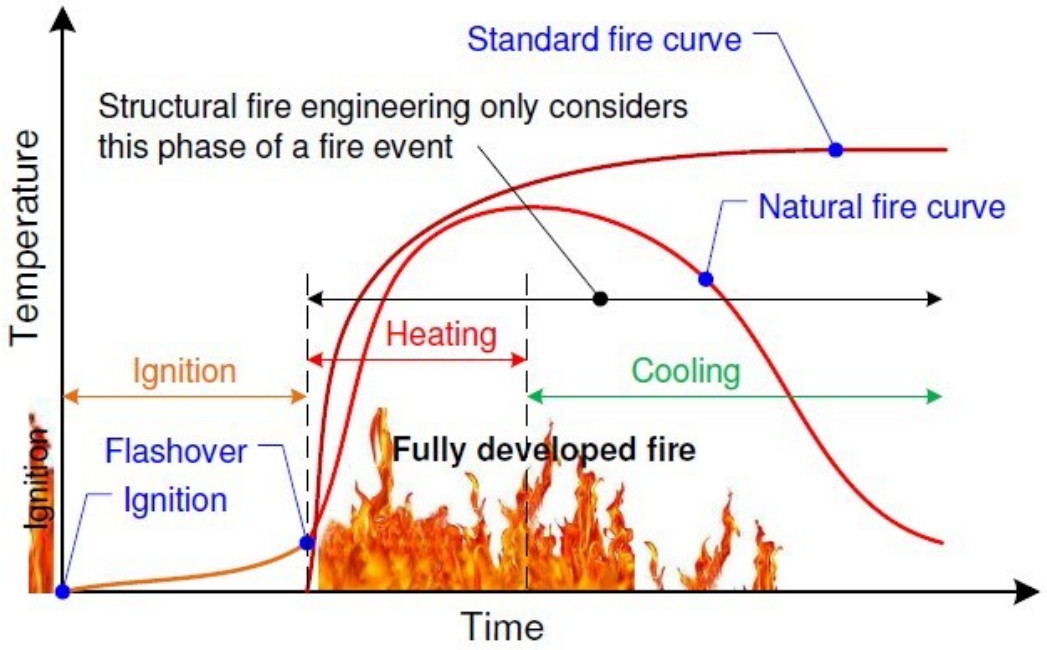

Figure 2.18: Temperature versus time of natural fire curve (Walls, 2016).

2.4.2 Standard Fire Curves

Most national fire design codes have adopted the standard fire curve (ISO Curves 834) as the standard design code and is utilized to test the fire resistance for the steel members. According to Walls (2016), the structural steel members behave differently in comparison with the global structure when the standard fire tests are performed. Furthermore, the standard fire curves are used to test structural elements (i.e. beams, columns etc.), non-structural elements (i.e. walls partitions, windows etc.) and building materials (i.e. steel, concrete etc.).

The equation below is used to illustrate the behaviour of a standard fire curve (Eurocode 3, 2001).

$$\theta_g = T_0 + 345 \log_{10}(8t + 1)$$

Where

θ_g = gas temperature [°C] t
= Time (in minutes)
T_0 = Ambient Temperature [20 °C]

The hydrocarbon fire curves are utilized in fire design buildings which contain higher content of hydrocarbon materials such as plastics, petroleum products, therefore the higher temperatures are to be expected. The equation below is used to elucidate the behaviour of the hydrocarbon fire curve (Eurocode 3, 2001).

$$\theta_g = 1080(1 - 0.325e^{-0.167t} - 0.675e^{-2.5t}) + T_0$$

Where

θ_g = gas temperature [°C] t
= Time (in minutes)
T_0 = Ambient Temperature [20 °C]

The external fire curves are utilized when structural elements are exposed to outside fires. This means that the structural elements are completely unexposed from the burning compartment and will be experiencing very low temperatures. The equation below is utilized to elucidate the behaviour of external fire curve (Eurocode 3, 2001).

$$\theta_g = 660(1 - 0.687e^{-0.32t} - 0.313e^{-3.8t}) + T_0$$

Where

θ_g = gas temperature [°C] t
= Time (in minutes)
T_0 = Ambient Temperature [20 °C]

2.4.3 Parametric Fire Curves

Parametric fire curves are also used to model the "realistic natural fires" by considering several variables (heating and cooling phases) which represent characteristics of a realistic fire model.

The parametric fire curves adopt simple models that consider the most important physical circumstances which will take place in case of fire in the building. Like other fire curves, the parametric fires are temperature-time curves (Vassart *et al.* 2014).

Most of the parametric fires considers the following variables/parameters:

- The nature of the compartment (geometry).
- The material properties in the compartment.
- The fire load (fuel) density.
- Ventilation conditions within the compartment.

Vassart *et al.* (2014) states that parametric fires are based on the theory that within the fire compartments, the temperature remains the same which means that the area of application is restricted. The parametric fire equation below is utilized only for a restricted floor area of 500 m^2 or less and the maximum height of 4 m (Eurocode 3, 2005).

$$\theta_g = 1325\ (1 - 0.324e^{-0.2t_*} - 0.204e^{-1.7t_*} - 0.472e^{19t_*}) + T0$$

Where:

θ_g = Temperature (°C)

t* = t • Γ [hr] t = time

[hr]

T_0 = ambient temperature [20 °C]

Γ = [O/b] ^{2} / (0.04/1160)^2 [°C]

b= $\sqrt{(pc\lambda)}$ with the following limits: 100≤b≥2200 [J/m^{2}s$^{1/2}$K]

P = density of boundary of enclosure [kg/m^3]

c = specific heat of boundary of enclosure [J/kgK]

λ = thermal conductivity of boundary of enclosure [W/mK]

O = opening factor: $Av\sqrt{h_{eq}}\ /A_t$ with the following limits: 0,02 ≤O ≤0,20 [m$^{1/2}$]

A_v = total area of vertical opening on all walls [m^2]

h_{eq} = weighted average of window heights on all walls [m]

A_f = total area of enclosure (walls, ceiling and floor, including openings) [m^2]

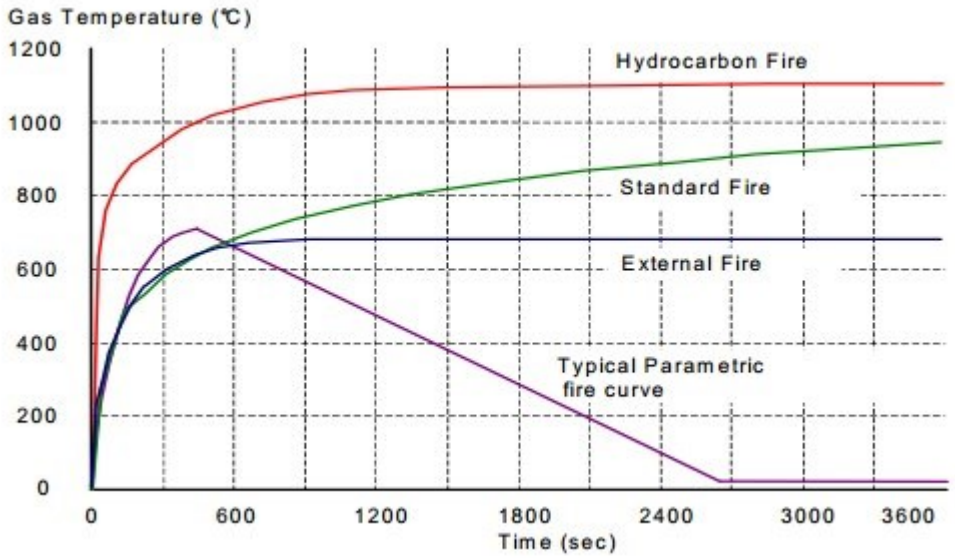

Figure 2.19: Nominal fire curves versus the parametric fire curve (Eurocode 3, 2001).

2.4.4 Heat transfer Mechanisms

According to Johnson (2017), temperature is basically the quantity of the molecular energy in a body. The second law of thermodynamics states that heat is transferred between two bodies or objects due to temperature imbalances. There are three basic heat transfer mechanisms which are defined as the conduction, convention and radiation mechanisms. The equation below indicates that when the heat is added to the object, its temperature changes. Figure 2.20 below shows the summary of the three heat transfer mechanisms.

$$Q = mc\Delta T$$

Where:

Q = Heat energy (J)

m = mass of a substance (kg)

c = specific heat (J/kg. °C)

ΔT = Change in temperature (°C)

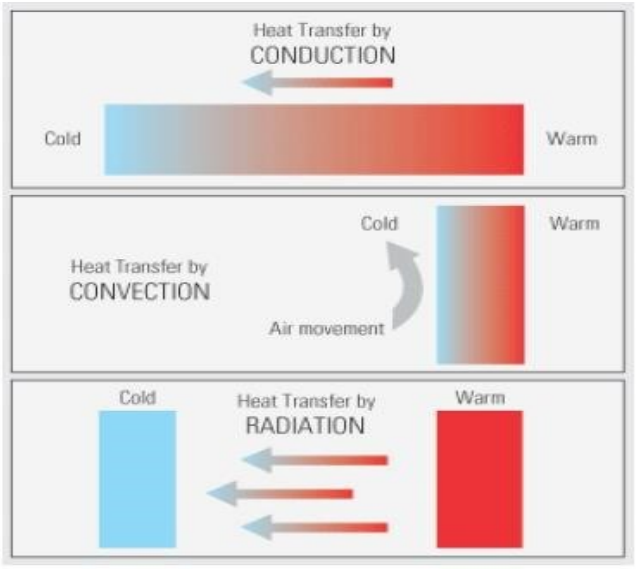

Figure 2.20: Heat transfer mechanisms (Qin, 2016).

2.4.4.1 Conduction

Most solid objects transfer heat through conduction mechanisms, which is defined as the transfer of heat when two or more bodies come into contact. Normally, materials which are good electrical conductors such as steel, aluminium, are also good heat conductors because of the free available electrons. Thermal conductivity (k) is the most important property which is utilized to determine the rate of conductivity thus the higher the conductivity, the more the material can transfer heat with ease.

2.4.4.2 Convection

Convection is the transfer of heat due to the movement of fluids in response to changes in its density. In addition, the changes in the fluid density are a result of temperature changes which creates fluid movement. This is termed as the natural convection. For a fire scenario, natural convection transfer of heat is caused by the buoyant forces which emerge from the temperature gradients in the air.

2.4.4.3 Radiation

Radiation is the transfer of heat by electromagnetic waves (such as ultraviolet light, infrared radiation, microwaves and visible light). Radiation can manoeuvre through a vacuum, some solids, and some liquids. Radiation is of great significance in a building fire scenario because it forms as the main mechanism which transfers the heat onto close buildings, fire to buildings compartments, and fire to surrounding cooler elements etc.

2.5 Basic principles of fire-resistant design

Eurocode 3 (2001) defines fire resistant design as the fire resistance time of structural members before yielding, when the standard fire curve is applied. The national building regulations states that the fire resistance design must be within the relevant time limits. According to the European codes, there are three categories which are used to describe the fire resistance, namely load bearing function, Integrity separating function and thermal insulating separating function.

2.5.1 Integrity separating function

The integrity separating function is defined as the ability of structural members to preserve their integrity without any separation when subjected to fire events. Figure 2.21 below describes this function further.

2.5.2 Load bearing function

The load bearing function is described as the ability of structural members to continue carrying the mechanical loadings even when it is subjected to fire events. The Figure below is utilized to present the function (Eurocodes 3, 2005).

2.5.3 Thermal Insulating separating function

Thermal insulating separating function is interpreted as the ability of structural members to resist thermal loadings when the standard fire curve is applied. However, this is assumed to be satisfied only for a limited temperature range of 140K to 180K for the side(s) which are not exposed to heat (Eurocode 3, 2005). The ASTM code (2007) assumes a temperature range of 140°C - 180°C at a single point for the unexposed side. Figure 2.21 below further explain these categories into detail (Eurocode 3, 2005).

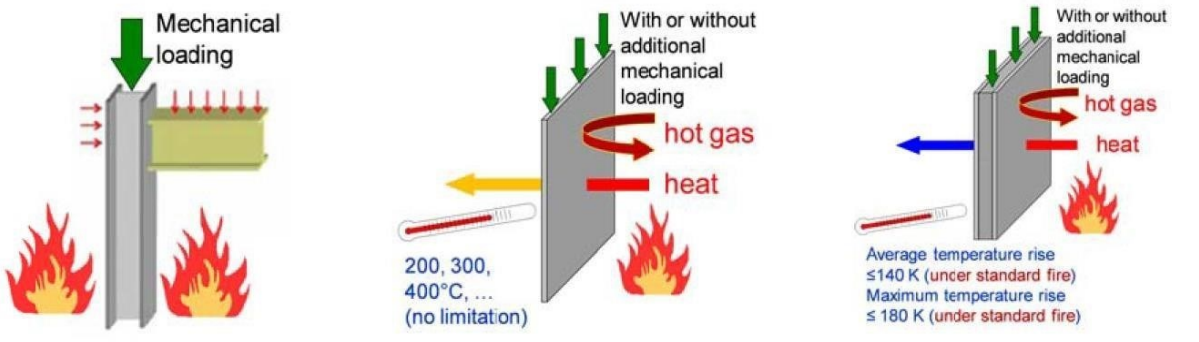

Criterion "R" – load bearing capacity

Criterion "I" – integrity separating function

Criterion "E" – thermal insulation separating function

Figure 2.21: Fire resistance criterion (Zhao, 2012).

2.5.4 Mechanical loads resistance

The EN 1993-1-2 and EN 1994-1-2 design codes cover the set of mechanical resistance and integrity criterion which must be fulfilled under any ambient conditions and/or parametric fires. Furthermore, the fire design codes define the material properties and basic rules for calculating the loads (actions) under fire situations. EN 1993-1-2 states that the dead (permanent) loads are utilized unfactored ($\gamma_{GA} = 1.0$) and the imposed (variables) loads are factored with a factor $\Psi_{1.1}$ in a range of 0.5-0.9 based on what the building is utilized for. The following expression serves as a requirement during any fire event at time t:

$$\boldsymbol{E_{fi,d,t} \leq R_{fi,d,t}}$$

Simms (2016) indicates that the influence of indirect actions such as resulting internal forces or moments caused by restrained thermal expansion and deformations, are negligible when a fire safety design is constructed from ISO curve 834 (standard fire curve). The following equation represents the reduction factor:

$$\boldsymbol{n_{fi,d,t} = \frac{E_{fi,d,t}}{R_d}}$$

The above expression is used during a global structure analysis design.

$$\boldsymbol{n_{fi,d,t} = \frac{E_{fi,d,t}}{E_d}}$$

Where:

E_d = is the design value based on the basic combinations of loads (Ultimate limit states).

$n_{fi,d,t}$ = is the reduction factor for the design load level.

The above expression is utilized during the structural member analysis. The expression is conservative hence, it is employed only when imposed loads are used in combination with the dead loads (Oosthuizen, 2010). The following expression shows reduction factor with both partial factors and characteristic loads:

$$\boldsymbol{n_{fi,d,t} = \frac{\gamma_{GA}.\, G_k + \Psi_{1.1}.\, Q_{k.1}}{\gamma_{G}.\, G_k + \gamma_{G.1}.\, G_{k.1}}}$$

2.5.5 Cross Section Classification

Under normal temperature conditions, the cross sections are divided into different classes based on which cross sections act collectively or singularly in compression. According to Vassart *et al.* (2014), structural steel design codes divide the steel members into four classes by considering-varying slenderness of their cross sections. Furthermore, the stress distribution for the members also determines the classification of the steel members. Below are there four classes of rolled shapes available for structural steel (Eurocode 3, 2005):

- Class 1: Plastic Design Sections – plastic hinges can be formed.
- Class 2: Compact Sections – plastic hinges cannot be formed however the plastic moment resistance can be developed.
- Class 3: Non-Compact Sections – subjected to buckling as it reaches the yield moment.
- Class 4: Slender Sections – subjected to local buckling before reaching yield moment.

In a fire event, the strength and the elastic modulus of the structural steel are greatly reduced at elevated temperatures hence, the more the risk of local buckling which may cause progressive collapse of the whole structure. Figure 2.22 below demonstrates the classification of the cross section for the structural steel at elevated temperatures.

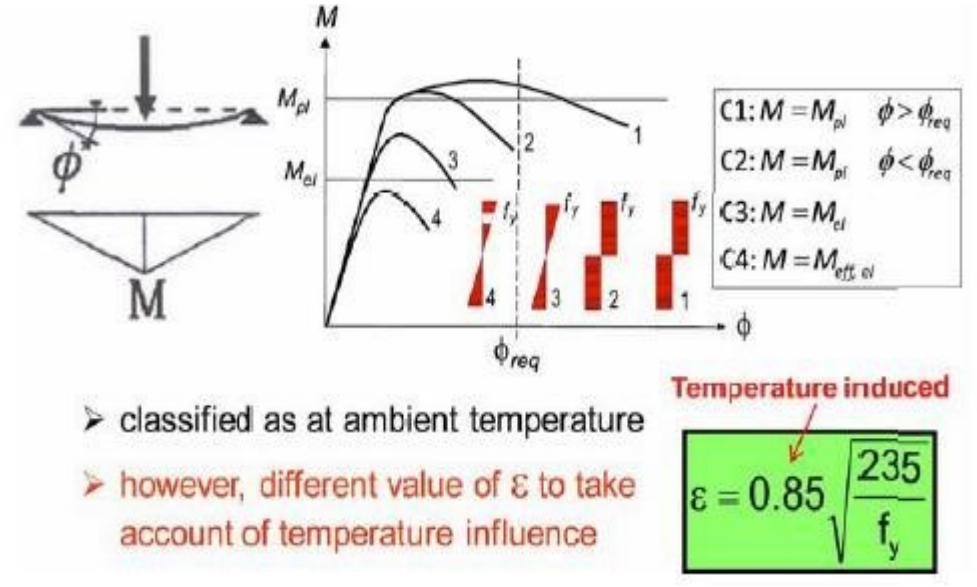

Figure 2.22: Classification of structural steel at elevated temperatures (Vassart *et al.* 2014).

Where:

ε = Classification of the class under fire exposure

f_Y = yield strength of the structural steel at ambient temperature

The coefficient 0.85 includes the effect of material properties when subjected to fire conditions and can be approximated by the equation, $\sqrt{\frac{k_{e,\theta}}{k_{y,\theta}}}$ (Simms, 2016).

2.6 Summary

A lot of research has been conducted on structural steel members but less efforts and focus on global structure. From the literature, it is shown that the global system analysis may experience a substantial deformation, however, it can resist collapse by transferring the loading to the surrounding members. According Oosthuizen (2010), the current analytic methods predict higher heating rates for the isolated steel members and a number of variables which can affect failure are not considered. This includes, 1) members of global structure that encounter axial and rotational restraint which may increase or decrease collapse probability. 2) members in a fire compartment tending to encounter expansion which results in lateral deformations and moments in columns.

Over the two decades, several computational studies on the behaviour of steel structures exposed to elevated temperatures have been conducted and have been compared with the findings from experiments/laboratory testing. The findings are as follows:

I. Steel structures at elevated temperatures tends to lose their stiffness and strength significantly.
II. The major reason for column failure under fire exposure was only due to the applied axial load and not under influence of connection stiffness and the moment applied.
III. The influence of boundary conditions (fixed or pinned) on the behaviour of structural elements under fire exposure was observed.
IV. The influence of restraints resulted in reduction of the frames limiting temperature.

The theoretical background presented in this chapter highlighted several key points (obtained from different sources including the Eurocodes) which are necessary to comprehend the structural steel performance under fire exposure.

Chapter 3: Simulation with ANSYS

3.1 Introduction

During any fire scenario, the heat transfer mechanism is of great importance to fully understand the performance of the whole structure against progressive collapse. Engineers can utilize several finite elements modelling tools to simulate models which can resemble the actual behaviour of the global structure or the structural elements under fire conditions. These modelling tools include ANSYS, ABAQUS, LS-DYNA and many more. In this study, ANSYS was used to study the behaviour of a multi-storey steel frame with concrete slabs exposed to elevated temperatures. The first two sections (section 3.2 and 3.3) on this chapter describe the finite elements method, then the ANSYS simulation steps are described into detail. Furthermore, section 3.4 describes the limitation of the ANSYS program and lastly, a short summary for the whole chapter is given in section 3.5.

3.2 Finite Element Method

Finite element analysis (FEA) is a computational tool which is utilized to study several engineering models under structural, vibration, heat transfer and dynamics analysis. These analyses are utilized to model real world scenarios and are used during prototype testing stages to predict how a prototype will behave. The finite element analysis features the use of a finite element modelling algorithm and it utilizes mathematical equations to simulate the analysis. The program works by dividing complex models into many finite elements which are known as mesh (Kandekar & Mahale, 2016).

3.3 ANSYS

ANSYS is a computational modelling tool which utilizes the Finite Element Analysis (FEA) principles to model and solve engineering related problems such as thermal, structural, magnetic etc. The software offers a chance to simulate complex models which are usually difficult to solve through the use of simple calculation models.

ANSYS allows users to create either a two/three-dimensional geometry model directly on ANSYS using the design modeller or through the use of programmes such as AutoCAD and then, the geometry can be imported into ANSYS for analysis. The boundary conditions and the mesh generation help to generate more accurate results which resembles the actual behaviour of the prototype (Kandekar *et al.* 2016). This allows users to create and stimulate model behaviour for any prototype with certainty prior to the manufacturing process. For thermal

analysis, material properties which are temperature dependent such as specific heat, thermal conductivity and thermal expansion can be imported during the simulation to ensure that the thermal behaviour of the material is incorporated. This offers more accurate outputs and results.

3.4 Modelling with ANSYS

When using any software, there are basic steps which must be carried out to ensure success of any analysis. The following Figure summarizes the steps which are carried out during the thermo-mechanical analysis on ANSYS.

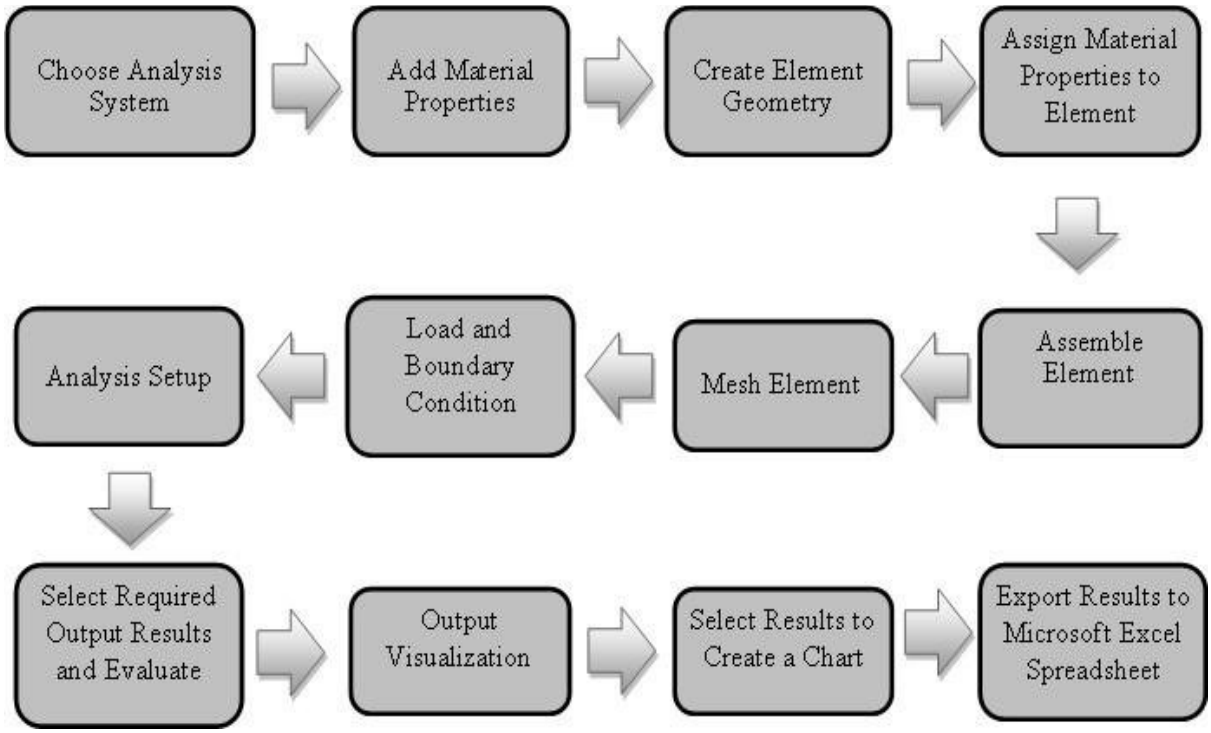

Figure 3.1: Simulation procedure with ANSYS.

Key words:

Structural Analysis: Is an analysis which is purely structural where only structural loads are applied.

Thermal analysis: Is an analysis where the thermal behaviour of any model is studied.

Thermo-mechanical analysis: Is a combination of both thermal and structural analysis.

Steady state analysis: Is a thermal analysis where the thermal behaviour of a model is studied but time is not considered.

Transient analysis: Is a thermal analysis where the thermal behaviour of a model is studied, however, time is considered.

3.4.1 Analysis System

For this study, the aim was to simulate a coupled thermo-mechanical analysis for the proposed geometry. Firstly, a transient thermal analysis was performed then a structural analysis was simulated afterwards. This is termed as the coupled thermo-mechanical analysis. The results from the transient thermal analysis are incorporated into the structural analysis. One of the outputs from transient thermal analysis is a temperature distribution which shows how temperature is distributed within the model structure.

3.4.2 Material Properties

For this study, the steel material properties with increasing temperatures were adopted from the European codes and inserted in ANSYS. These properties were mentioned above in the literature (Chapter 2) which include the thermal conductivity, specific heat, Young's modulus and stress-strain curves. By inserting these material properties with increasing temperature, this ensures that one has considered the plastic yield strength which is a failure criterion for steel material. In addition, since concrete slabs were adopted thus concrete material properties were also incorporated on the program, however, it should be noted that the focus of this study is mainly on the fire resistance of the steel against collapse.

3.4.3 Create Element Geometry

ANSYS offers an option for the user to construct the geometry using the design modeler within the program or the user can use programs such as AutoCAD, Solidworks to create any model and then, export it to ANSYS. For this study, the steel frame with concrete slabs was created using design modeler within ANSYS. The three-dimensional model of multi-storey steel frame was constructed using line bodies while the concrete slabs were constructed using shell elements. The line bodies were preferred over the solid elements. This was because a solid three-dimensional geometry would require a more proficient computer which was unavailable. In addition, the line bodies require less computational effort and time.

3.4.4 Assign Material Properties

ANSYS uses the default material properties which are considered at ambient temperature conditions (i.e., 20°C), this means that only the elastic yield strength will be displayed. The material properties which are adopted from the European codes were assigned to the models. These properties are of vital importance because this means that the plastic yield strength (failure criterion) will be considered during analysis. Hence, assigning the right materials

ensures that the material behaviour is modelled during the analysis. Material properties were considered for both concrete and steel in this study.

3.4.5 Assemble Element

ANSYS provides an option for the user to choose different contact interfaces between different parts of element geometry. Contacts interfaces available include bonded (fixed), frictionless, forced frictional sliding, rough and no separation connections. For this study, a bonded connection was chosen mainly because the study is focused on the thermal behaviour of the multi-storey steel frame and not in the simulation of the semi-rigid behaviour of the connections. However, future investigation must be conducted on the influence of connections against progressive collapse under fire conditions.

3.4.6 Mesh

Meshing is basically dividing the large model into many small units/finites. The smaller the mesh, the more accurate the results and the more time is required to simulate the model. For this study, a default mesh size with a minimum size face of 100mm and a maximum of 150mm was adopted because of the computational effort and time associated with smaller mesh sizes.

3.4.7 Loadings and Boundary Conditions

The loading and boundary conditions involves all the loading and support conditions assumed during the simulation. In this study, the uniform distributed loading was applied on the slabs during the static structural analysis. Fixed conditions were adopted for all ground floor columns at the bottom. For thermal analysis, a standard fire curve (ISO Curve 834) was applied as the source of heat for various fire cases and the ambient temperature of 20 ℃ was applied as the thermal boundary condition at the supports.

3.4.8 Analysis framework

This study focuses on a nonlinear analysis which considers a few non-linearities such as large displacements, contact mechanics etc. For this study, a Newton-Raphson iterative method is utilized to solve non-linear problem. The loading is applied in small increments to calculate the tangential stiffness matrix which gradually changes because of material non-linearities. ANSYS allows the user to choose the number of sub-steps that the program must take before yielding a solution. The more the sub-steps, the longer the computational time and the results are more accurate. However, this also relies on performance of the computer.

3.4.9 Select output results and evaluate

In this study, a thermomechanical analysis was performed and the output results from the coupled thermo-mechanical analysis were discussed. The temperature distribution was of significance results from transient thermal analysis as it displayed the temperature distribution across the model after heat was applied. Secondly, the displacements which were experienced by the model during the static structural analysis were also of vital importance. These results are then compared for the various cases which were investigated, and the findings are discussed in detail. In addition, ANSYS offers a range of output results which a user can select such as stresses, strains, and many more.

3.4.10 Select results to create a chart and Export results to Microsoft Excel

The results obtained by performing the coupled thermo-mechanical analysis were exported to Microsoft Excel spreadsheets to create graphical solutions which are used to compare different model cases. This enables the researcher to present the findings and as well give more accurate discussions.

3.4 Limitations of ANSYS

One of the limitations of ANSYS is that it does not possess a single simulation of thermomechanical analysis with one mesh and one solve. This is referred to as direct (strong) coupling approach. Therefore, for this study, the simulation is set in a way that the thermal analysis is performed firstly then output results from the thermal analysis are imported to the structural analysis which is performed afterwards. This is referred as sequential (weak) coupling approach. When weak coupling is present, this means that the results from the thermal analysis influences the mechanical parameters thus defining the behaviour of the material and therefore the structural analysis, and not vice-versa. Also, when strong coupling is present then the thermal parameters are dependent on the level of stresses/strains coming from the mechanical analysis. For this study, the weak coupling was assumed and to adopt a strong coupling approach would mean that a different modelling and solution method must be obtained, which will require a higher computational efficiency.

For this study, an implicit analysis was used for modelling due to financial and computational constraints. However, an explicit analysis is more appropriate for this kind of study due to its accuracy and competency against complex non-linear problems of this magnitude. In addition, the computational cost associated with numerical model, dense mesh, non-linear analysis and many more are more suited for the explicit analysis rather than the adopted implicit analysis.

Lastly, the equivalent strains (Von misses) which displays the failure criterion of the elements are not supported for line elements geometry.

3.5 Summary

ANSYS has several advantages in a number of engineering fields such as, it can be used to test a prototype before construction thus saving costs and improved efficiency. The aim of this research was to study the thermal behaviour against progressive collapse for the proposed geometry by using the coupled thermo-mechanical analysis. The problem presented in this study was a non-linear analysis and the Newton-Raphson iterative method to solve this nonlinear problem. Several nonlinear conditions were adopted, including nonlinear stress strain curves which are necessary to display the plastic yielding of the model. Also, the relationship of the thermal and mechanical properties of steel with increasing temperature was also adopted during the simulation, which includes the young's modulus, thermal conductivity, specific heat, density etc. The fixed support conditions, thermal boundary conditions and loads (thermal and mechanical) were assigned during structural analysis. In this study, outputs such as temperature distribution and displacements are of interest as the display the thermal behaviour on the model. The findings are then presented using the graphical solutions and discussed in detail.

Chapter 4: Methodology

4.1 Introduction

The main objective of the study was to investigate the fire resistance against progressive collapse for a multi-storey steel frame with concrete slabs exposed to elevated temperatures using FEM, ANSYS. As mentioned above, fire engineering is complex field to fully comprehend and this chapter will present the procedure which was utilized to simulate models and obtaining the results. Section 4.2 presents the structural description which includes the dimension of the structural elements (i.e. columns and beams), the section properties as well as all the assumed loadings (thermal and mechanical loadings). Section 4.3 highlights the materials properties including the thermal properties which were adopted during the study and stress-strain laws with increasing temperature which shows plastic yielding for the model. Section 4.4 illustrates the model scenarios which were investigated during the simulations. This includes studying the performance of fire resistance of a multi storey steel frame against progressive collapse under fire conditions. In addition, this section highlights the conditions which were adopted when simulating models. Lastly, a summary for the chapter is found in section 4.5 to highlight the main points in this chapter.

4.2 Structural Description

A three-dimensional multi-storey building was modelled on ANSYS using implicit analysis. The model consists of a steel frame with concrete slabs and it was constructed using line bodies, which are also referred to as the beam elements. The steel frame structure had three stories of 4 m high, with three bays of 5 m along the short span, and four bays of 8 m along the long span, as demonstrated in Figure 4.1 and Figure 4.2. All the dimension of the beams and columns adopted in this study were obtained from the Southern African Steel Institute Construction (2013). The 254x254x132 I section was adopted for this study.

The multi-storey steel frame consisted of fixed supports at all the ground floor columns and all the connections between the slab, beams and columns were assumed to be rigid/fixed. According to Jiang *et al.* (2016), it is known that the type of connection affects the load redistribution action and the type of collapse mode which can occur in steel frames. Hence, fixed connections present advantages against collapse resistance of the building because of their ability to transfer high amounts of axial loads to the surrounding structural components to avoid global collapse of the structure. Only rigid connections were assumed in this study, but

other researchers have studied the effect of other connection types (such as the pinned connections) against progressive collapse under fire conditions (Jiang *et al.* 2018).

Table 3.1 illustrates the dimensions of the steel I section. The thickness of the concrete slab was 100 mm. The columns are laid out such that the x axis which the stronger axis was along the short span. This is a common layout in practice aimed to counteracts the lateral forces along the short span. Furthermore, it is well known from research that loads are mainly redistributed to the stronger axis (higher stiffness), which is usually the short span in most cases compared to the long span (Jiang *et al.* 2016). Therefore, for this study, it was expected that more loads are to be transferred to the short span because the columns are laid out that the greater stiffness was on the short span. It should be noted that all the column dimensions were assumed to have the same sizes even though the exterior columns take a smaller amount of the load (q) compared to the internal columns. The load ratio for corner column had load of 0.25, edge columns with load ratio of 0.5 and interior columns with load ratio of 1.

The Figure below illustrates the plan view of the multi-story building model which was simulated during the study:

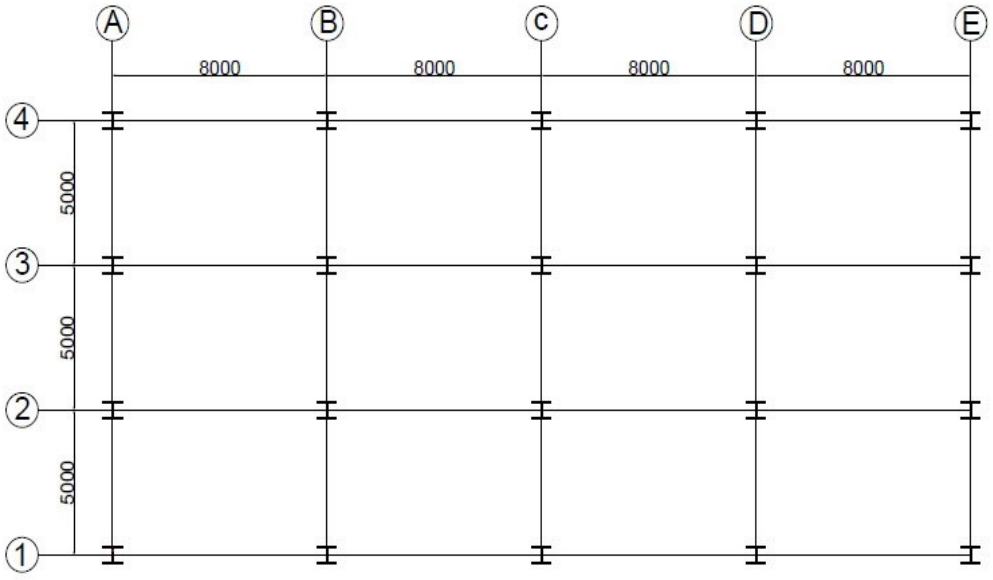

Figure 4.1: Plan view of the multi-story model which was simulated during the study.

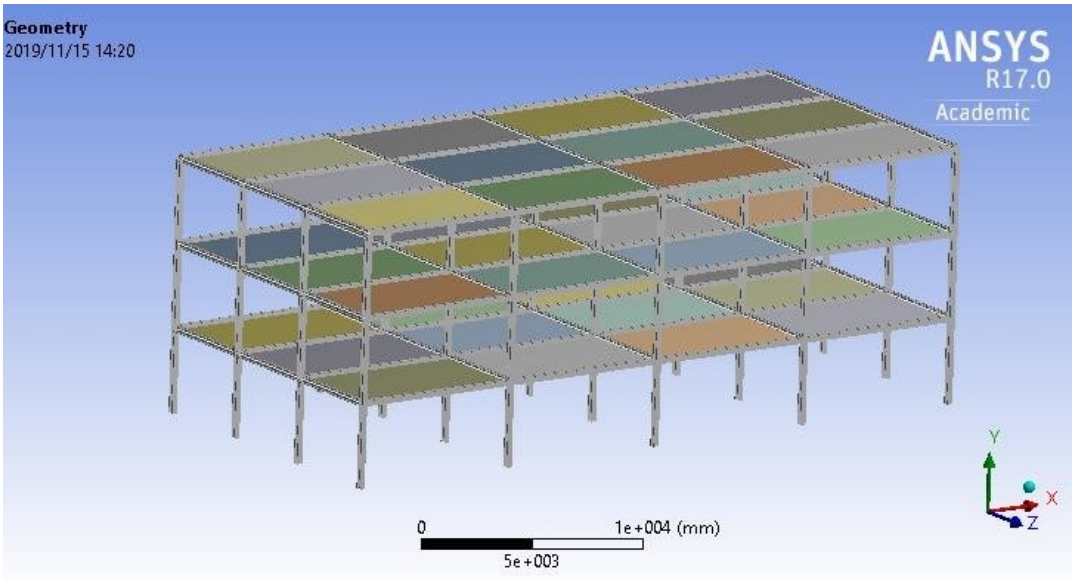

Figure 4.2: The FEA steel frame geometry (ANSYS, 2020).

Table 4.1: 254x254x132 I section properties (Southern African Steel Institute Construction, 2013)

Section Properties	**Dimensions**
Mass (kg/m)	132
Height (mm)	276.4
Breadth (mm)	261
Web thickness (mm)	15.6
Flange thickness (mm)	25.1
Web height (mm)	200
Cross sectional Area ($10^3\ mm^2$)	16.8

4.2.1 Element Mesh

As mentioned in the previous chapter, the smaller the mesh size, the more accurate the results and the more computational time the simulation requires. The minimum size of 100mm with 150mm maximum face size was selected as the mesh size for this study due to high computational effort and efficiency associated with using a denser mesh. The mesh of the steel frame consists of 77321 nodes and 68613 elements with each node consisting four degrees of freedom. Figure 4.3 below illustrate the element mesh size which was used during the study.

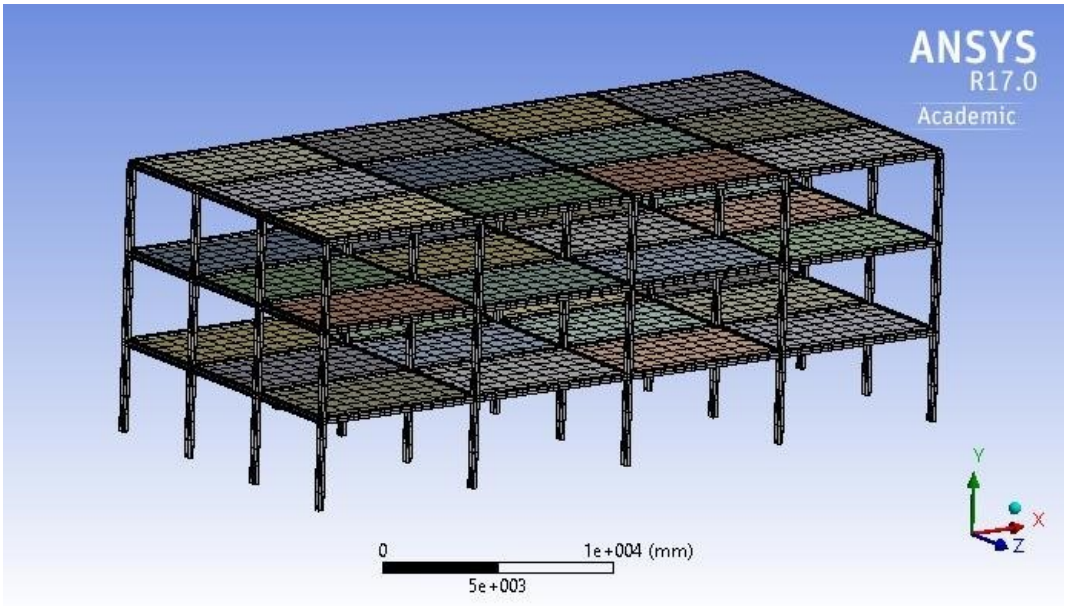

Figure 4.3: Element mesh size (ANSYS, 2020).

4.2.2 Loadings and Boundary conditions

In this study, both the live and dead loads were applied along with the thermal loads (standard ISO Curve 834). It should be noted that the thermal actions were firstly applied then the mechanical loadings were applied using the Newton Raphson iterative method. The following section consists of mechanical and thermal loadings which were adopted during the study.

4.2.2.1 Thermal loadings

The transient analysis was performed during this study, where a standard fire curve which is also referred as the ISO Curve 834 was applied for a duration of 90 minutes to act as source of heat. The transient analysis is the most preferred analysis as it considers time into account rather the steady state which does not consider time. The ambient temperature of 20 °C was applied as boundary thermal conditions. Figure 2.18 on chapter two (literature review) shows the standard fire curve which was assumed for this study.

4.2.2.2 Mechanical loadings

All the columns were only fixed at the bottom to disallow both translation and rotation. A live load (q) of 7 KN/m^2 was applied on each concrete slab for the single column fire scenario and A live load (q) of 3 KN/m^2 was applied for the compartment fire scenario. The self-weight of all the structural components was considered during the simulation as the dead load.

4.3 Materials Models

This section shows the material properties which were adapted from the Eurocode. The steel and the concrete materials properties were obtained from Eurocode 3 (2001) and Eurocode 4 (2005)

4.3.1 Steel Properties

This section presents the mechanical and the thermal properties of steel which were considered during the simulation of the models.

4.3.1.1 Mechanical Properties

Density = 7850 kg/m^3

Poisson ratio = 0.3

Elastic Young's Modulus = 200 GPa

Effectives Yield Stress = 355 MPa

Table 4.2: Plastic stress and strains values for steel at normal temperatures (20°C).

Stress (MPa)	**Strain (m/m)**
355	0
450	0.0565
490	0.0156233

Table 4.2 above demonstrates the plastic stress and strain values for the steel at normal temperatures (20°C). However, as mentioned above, as the temperature increases, the strength and young's modulus are greatly reduced. Figure 4.4 below demonstrates the relationship of stress-strain (von mises) with increasing temperatures for the steel. Generally, these graphs are known as the stress-strain laws. The plastic model was considered during the simulation to demonstrate the plastic yielding of the steel with increasing temperatures.

In addition, Figure 4.5 demonstrates the reduction of the Young's modulus under elevated temperatures.

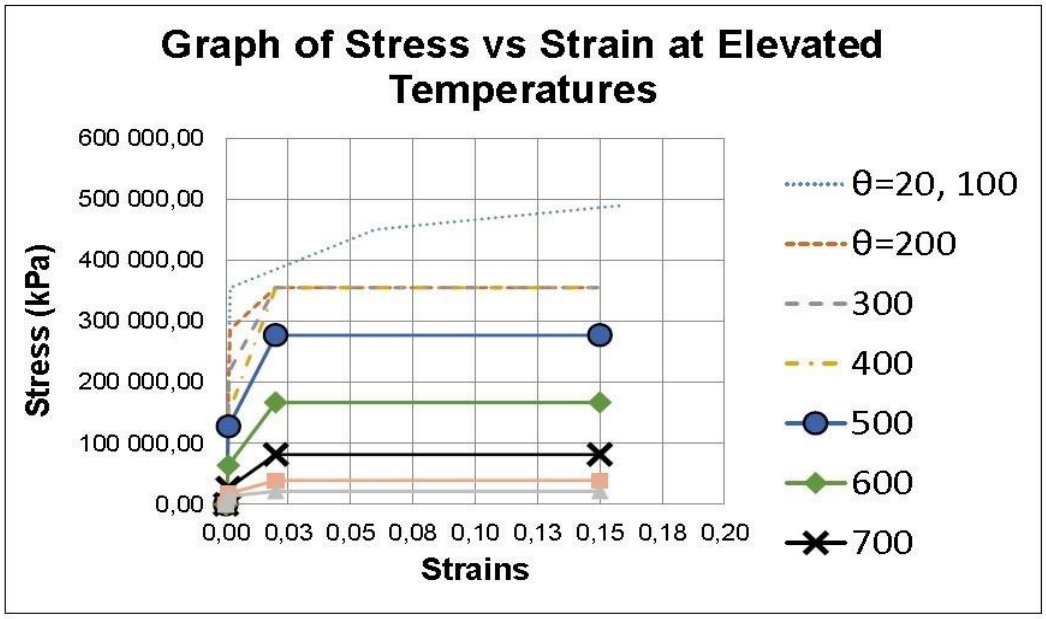

Figure 4.4: Stress-strain graph at elevated temperatures (Eurocode 3, 2001).

4.3.1.2 Thermal Properties

The following tables illustrates the steel thermal properties with increasing temperature (Eurocode 3, 2001).

Steel coefficient of thermal expansion = $12x10^{-6}/°C$

Table 4.3: Thermal Conductivity variation with increasing temperature (Eurocode 3, 2001).

Temperature (°C)	Conductivity (W/m°C)
20	53.33
100	50.67
200	47.34
300	40.01
400	40.68
500	37.35
600	34.02
700	30.39
800	27.30
900	27.30

Table 4.4: Specific Heat variation with increasing temperature (Eurocode 3, 2001).

Temperature (°C)	Specific Heat (J/Kg °K)
20	439.80
40	453.36
80	477.16
100	487.62
200	529.76
300	564.74
400	605.88
500	666.50
600	759.92
700	1008.16
735	5000
800	803.26
900	650.44

4.3.2 Concrete Properties

This section presents the mechanical and the thermal properties of concrete which were considered during the simulation of the models.

4.3.2.1 Mechanical Properties

It should be noted that the stress-strain and Young's modulus for concrete were taken as constants and not as a function of the temperature increase because the focus of this study was particularly on steel failure at elevated temperatures and not the concrete. The concrete mechanical properties are summarized as follows:

Density = 2300 kg/m^3

Poisson ratio = 0.18

Elastic Young's Modulus = 30 GPa

4.3.2.1 Thermal Properties

The following tables illustrates the concrete thermal properties with increasing temperature (Eurocode 4, 2005).

Concrete's coefficient of thermal expansion = $12x10^{-5}$/°C

Table 4.5: Thermal Conductivity variation with increasing temperature (Eurocode 4, 2005).

Temperature (°C)	Conductivity (W/m°C)
20	0.988
100	0.938
200	0.875
300	0.813
400	0.750
500	0.688
600	0.625
700	0.563
800	0.500
900	0.500

Table 4.6: Specific Heat variation with increasing temperature (Eurocode 4, 2005).

Temperature (°C)	Specific Heat (J/Kg °K)
20	900
40	900
80	900
100	900
150	950
200	1000
300	1050
400	1050
500	1100
600	1100
700	1100
735	1100
800	1100
900	1100

4.4 Modelling the Prototype steel frame – Fire Scenarios

The couple thermal-mechanical analysis was simulated on ANSYS program and the standard fire curve was applied to create different fire scenarios. As mentioned above, the model was constructed using beam elements together with shell elements and the section properties for these elements were defined. For this study, only the ground floor columns were heated because it was considered as the worst fire case compared to the upper floors. This was due to the fact that the ground floor columns carry the largest loads in comparison with the upper floor. The

columns were assumed to be unprotected, and all four sides of the column were exposed to elevated temperatures. In practise, the steel structures are always protected, and Cardington tests have proven that properly protected steel members will not fail under fire conditions. However, the aim of this research is to study the global progressive collapse modes due to column failure hence, a severe case of unprotected structural steel members was chosen.

In this study, it was considered that the global structural collapse modes were possibly caused by failure of the columns. Therefore, the thermal actions were applied to the columns to get more insights on the fire resistance of a multi-storey steel frame. According to Jiang *et al.* (2016:7), "the columns at the corner, or close to middle side of the long or short span of the structure have the highest chances of causing structural collapse thus, these columns must have access to alternative load path mechanisms". Therefore, in this study, these columns were chosen along with the interior columns. The main objectives of this research are to study the effect of fire location, influence of column load ratios and load redistribution action. Therefore, individual column and compartment fire (i.e. heating four columns within one compartment at the same time) scenarios were simulated on ANSYS while the beams and concrete slabs were at normal temperatures. It was recognized that a duration of 90 minutes heating of standard fire with maximum temperature of 1006 °C was proven to be enough for the study and was adopted for all the analysis below.

The different cases which were investigated during research are presented as follow.

4.4.1 Scenario 1 – Structural analysis

Firstly, a structural analysis of the proposed geometry without any application of fire was simulated. A uniformly distributed loading of 7 kN/m^2 was applied onto the concrete slabs for individual fire scenario and for compartment fires, a uniformly distributed loading of 3 kN/m^2 was applied onto the concrete slabs. The concept of performing structural analysis without fire was used to produce results which are then compared with different fire scenarios. The loading and boundary conditions as well as material and section properties mentioned above were adopted in this scenario as shown in Figure 4.2.

4.4.2 Scenario 2 – Coupled thermo-mechanical analysis

The coupled thermo-mechanical analysis was simulated on ANSYS where the standard fire curve was applied to the structure for a duration of 90 minutes and then, followed by the mechanical analysis where mechanical loads were applied onto the structure. The following cases demonstrates the fire scenarios which were investigated during the study.

4.4.2.1 Case 1: Column C2 (Internal column)

The standard fire curve was applied to an unprotected steel column (C2) on the interior panel for a duration of 90 minutes as shown on Figure 4.5. Only the internal ground floor column was exposed to heat while the beam and the slab remained at ambient temperatures. All the connection on the building were assumed to be rigid. The loading of 7 kN/m^2 was applied on the slab as the live loading and the self-weight of the structural elements was considered during simulation. It should be noted that the red colour indicates the heated columns and this applies to all the scenarios.

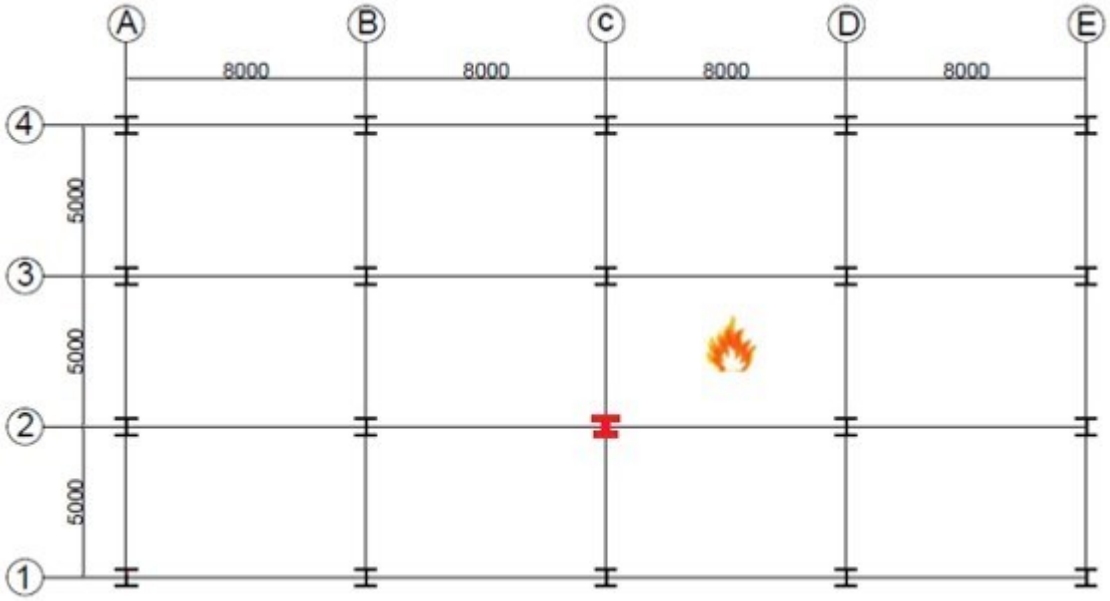

Figure 4.5: Ground floor interior column (C2) being heated.

4.4.2.2 Case 2: Column C1 (Long edge column)

The standard fire curve was applied to an unprotected steel column (C1) for a duration of 90 minutes as shown in Figure 4.6 below. The same mechanical loadings and boundary conditions mentioned above were adopted for this fire scenario.

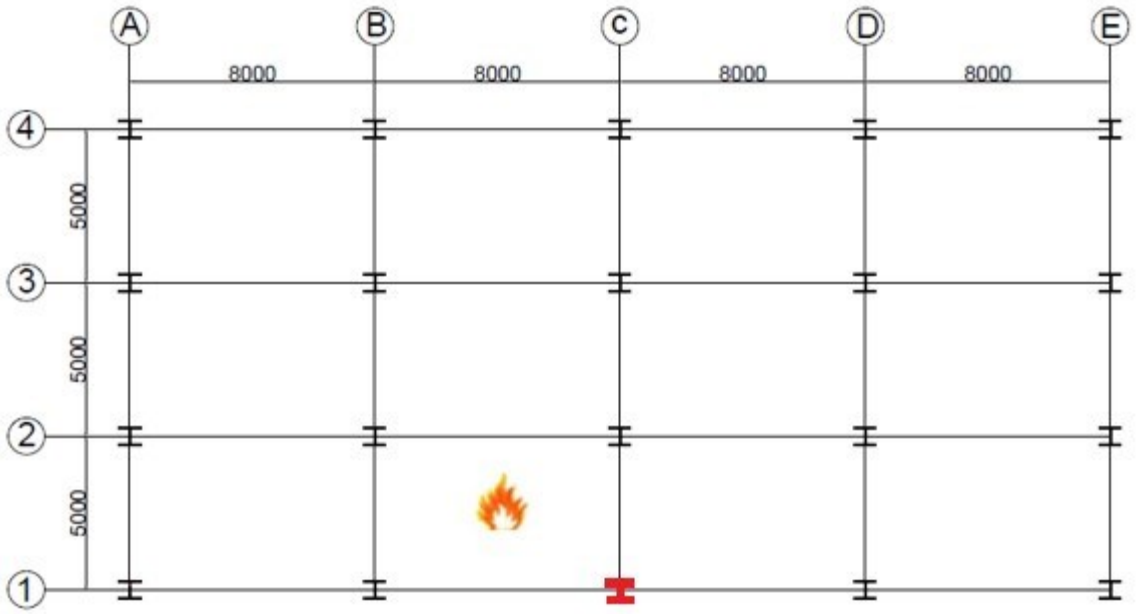

Figure 4.6: Ground floor edge column (C1) being heated.

4.4.2.3 Case 3: Column A2 (Short edge column)

The standard fire curve was applied to the steel column (A2) on the corner panel for a duration of 90 minutes as shown in Figure 4.7 below. The same mechanical loadings and boundary conditions mentioned on the above sections were adopted for this fire scenario.

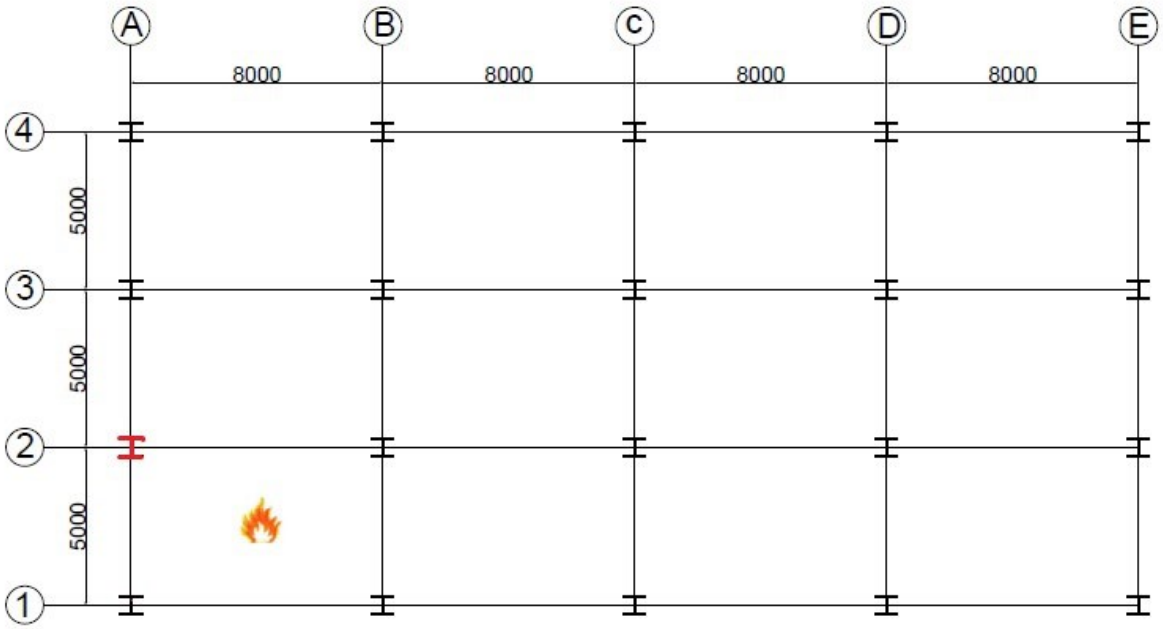

Figure 4.7: Ground floor edge column (A2) being heated.

4.4.2.4 Case 4: Column A1 (Corner column)

In this scenario, the standard fire curve was applied to the steel column (A1) on the corner panel for a duration of 90 minutes as shown in figure 4.8 below. The same mechanical loadings and boundary conditions mentioned on the above sections were also obeyed for this fire scenario.

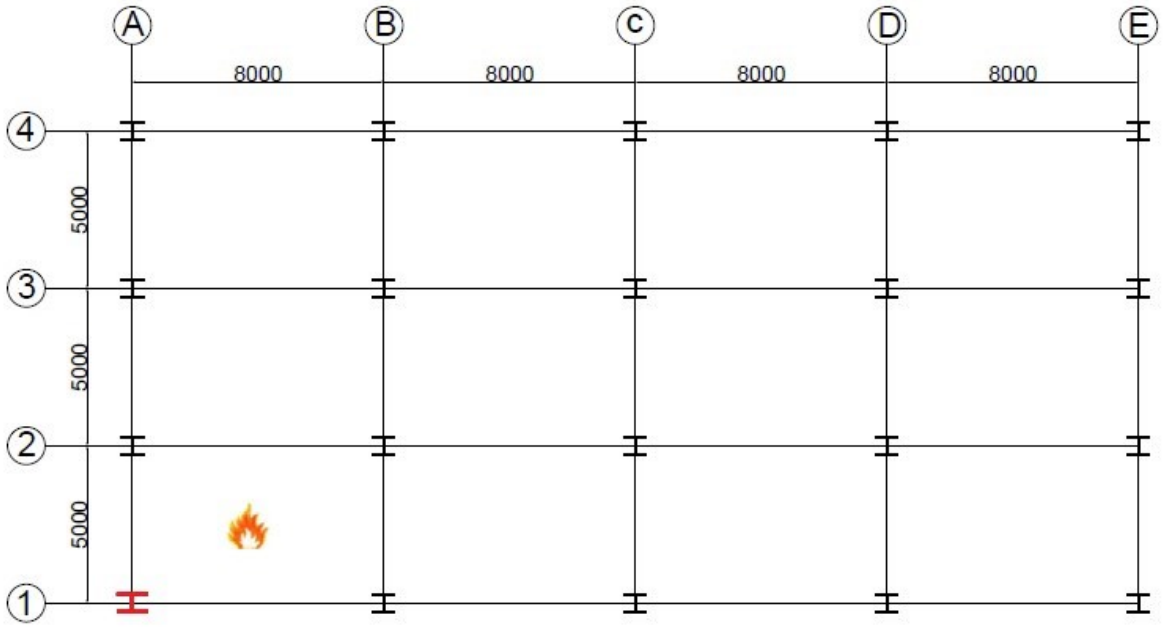

Figure 4.8: Ground floor corner column (A1) being heated.

4.4.2.5 Case 5: Short edge compartment fire

The standard fire curve was applied to the steel columns along the short edge for a duration of 90 minutes as shown in Figure 4.9. The heat was applied only to the four columns (indicated in red colour) within the same compartment at the same time. This is referred as compartment fires. All the connections on the building were assumed to be rigid. The loading of 3 kN/m^2 was applied on the slab as the live loading and the self-weight of the structural elements was considered during simulation. It should be noted that the loading, boundary and connection condition apply to all the compartment fire scenarios.

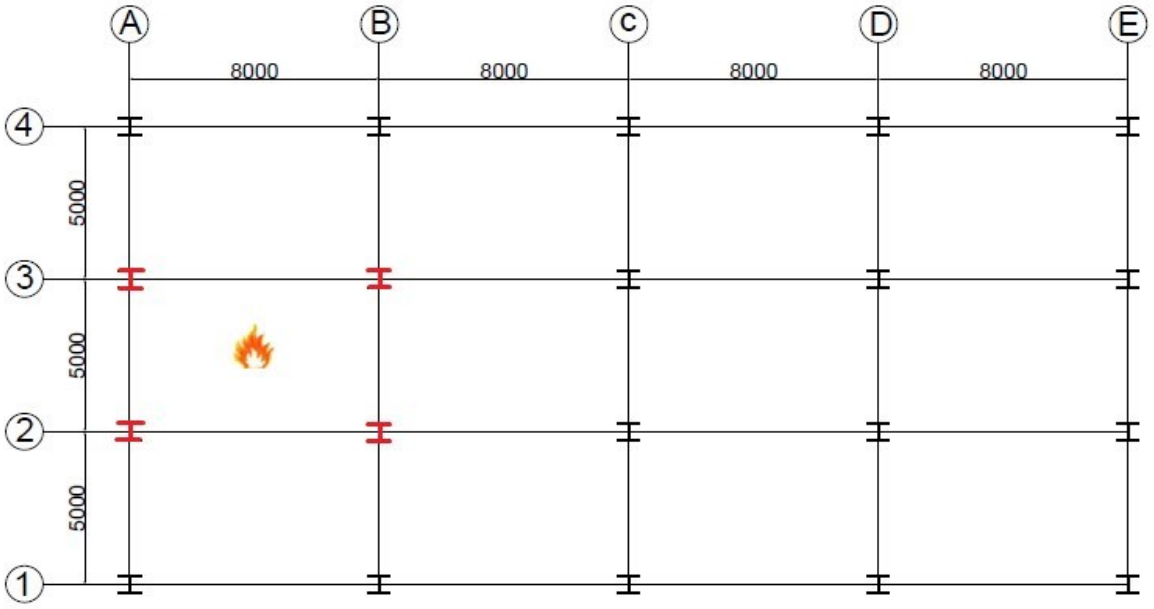

Figure 4.9: Ground floor edge panel along the short span being heated.

4.4.2.6 Case 6: Long edge compartment fire

The standard fire curve was applied to the steel columns along the long edge for a duration of 90 minutes as shown in Figure 4.10 below. The same mechanical loadings and boundary conditions mentioned on the above scenario were obeyed for this fire scenario.

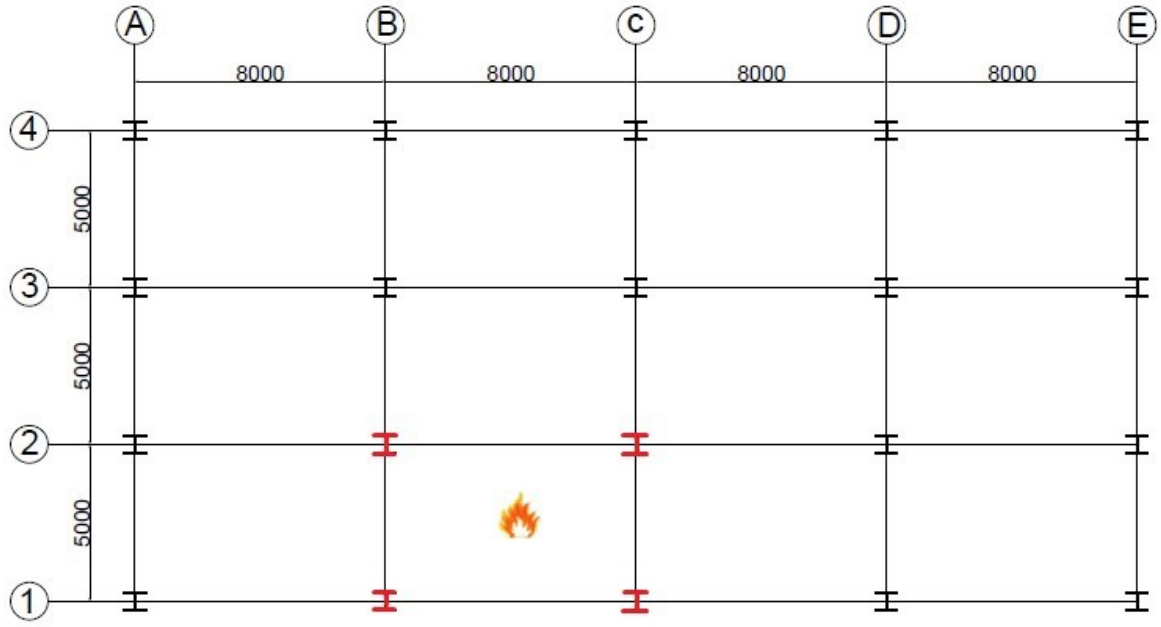

Figure 4.10: Ground floor edge panel along the long span being heated.

4.4.2.7 Case 7: Interior compartment fire

The standard fire curve was applied to the steel columns on the interior panel for a duration of 90 minutes as shown in Figure 4.11. The same mechanical loadings and boundary conditions mentioned on the above sections were adopted for this fire scenario.

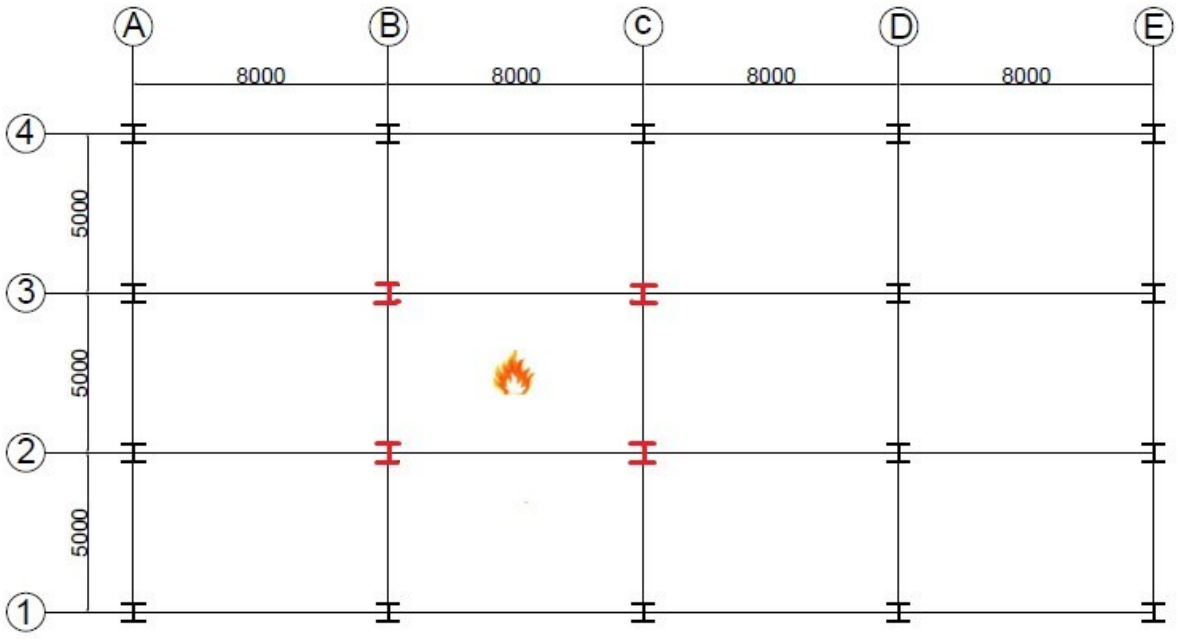

Figure 4.11: Ground floor internal panel being heated.

4.4.2.8 Case 8: Corner compartment fire

The standard fire curve was applied to the steel columns on the corner panel for a duration of 90 minutes as shown in Figure 4.12. The same mechanical loadings and boundary conditions mentioned on the above sections were adopted for this fire scenario.

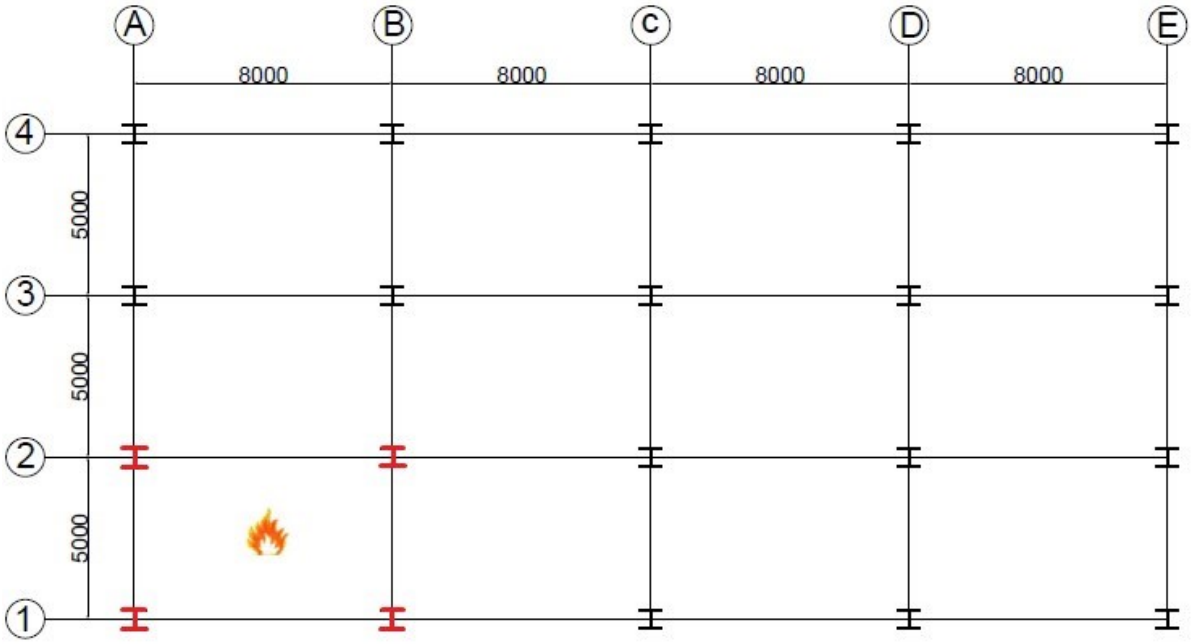

Figure 4.12: Ground floor corner panel being heated.

4.6 Summary

A multi-storey steel frame with concrete slabs was simulated on ANSYS using implicit analysis. The simulation was intended to investigate the behaviour against progressive collapse. The model was composed of beam and shell elements. The steel frame had three stories of 4 m high, with three bays of 5 m along the short span, and four bays of 8 m along the long span, as previously demonstrated in Figure 4.1 and Figure 4.2. All the connections in this study were assumed to be fixed connections. According to Jiang *et al.* (2016), the type of connection used influences the collapse modes and the load redistribution action. Hence, this assumption may result in non-conservative findings. The columns were oriented such that the stronger x-axis was along the short span, this is a common layout in practice to counteract the lateral forces on the short span. This orientation will influence the load redistribution action as it is known that loads are mainly transferred along the direction with stronger axis (larger stiffness).

The 254x254x132 I section steel material was selected for this study and the slab had a thickness of 100mm. The steel material thermal and mechanical properties with increasing temperature were adopted from Eurocode 3 (2001) while the concrete's material thermal and mechanical properties were selected from Eurocode 4 (2005). Firstly, a structural analysis (with no heat) was simulated on the model then afterwards, a coupled thermal-mechanical analysis was performed on ANSYS with the mesh of the steel frame consisting 77321 nodes and 68613 elements with each node consisting four degrees of freedom. The standard fire curve (ISO 834 curve) was applied on the columns for a duration of 90 minutes for various fire scenario. Afterwards, the mechanical loadings were applied on the slabs using the Newton-Raphson iterative method.

Two fire scenarios were investigated, namely, (i) individual fire scenario and (ii) compartment fire scenarios. The heating of individual columns located at corner (A1), short edge (A2), long edge (C1) and interior (C2) were first considered. Afterwards, compartment fires located at the corner, short edge and long edge and interior were also carried out. It should be noted that only the ground columns were heated as they were assumed to be worst case due to their large load ratio compared to upper floors. Furthermore, all the columns had similar sizes, which is unrealistic in practise because they perimeter columns always smaller than the interior column. Therefore, this assumption may lead to unconservative results.

Chapter 5: Results and Discussions

For fire design, the collapse resistance is measured against time, temperature, or strength. The previous chapter details the adopted methodology which was utilized to investigate the behaviour of a multi-storey steel frame against progressive collapse. This chapter is aimed to present the main findings of fire resistance against progressive collapse, which were obtained using the presented methodology in chapter four. In this chapter, section 5.1 presents the structural analysis results where only mechanical loads are applied. Afterwards, section 5.2 provides the results of a three-dimensional simulation model with individual column and compartment fires scenarios as illustrated on chapter four. Thereafter, the different models are compared and discussed into detail using the known theories in the fire engineering field. In addition, the uniform distributed loading versus displacement graphs, displacement and distribution figures are presented on this section. Lastly, a summary section is provided at the end of the chapter to summarize the main findings in this chapter.

5.1 Scenario 1: Structural analysis

As mentioned in the previous chapter, a structural analysis was performed when only the mechanical loadings were applied, and no heat was applied to any part of the structure as shown in Figure 4.2. The main findings are summarized on the following sub-section.

5.1.1 Case 1

The behaviour of the multi-storey steel frame was observed, and it is demonstrated on Figure 5.2 below. From UDL versus displacement graph, it is evident that there was no collapse due to the applied mechanical loadings as the graph shows a steady-linear curve. This is referred to as elastic behaviour. From the results obtained, a conclusion can be drawn that the global structure will resist the applied loading and will not yield any collapse. This was expected, since only live and dead loads are applied to the system.

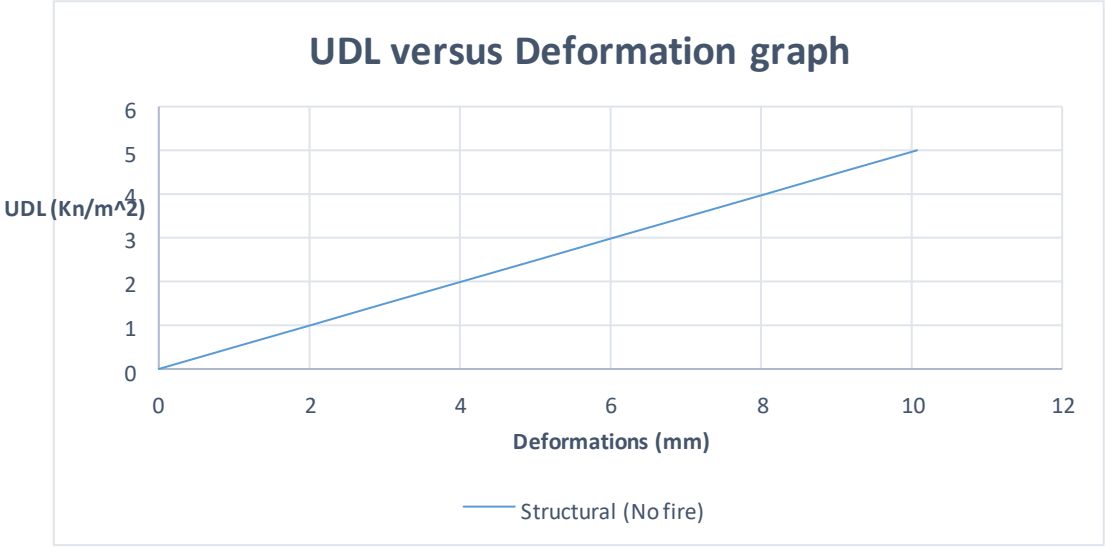

Figure 5.1: Udl versus displacement graph for structural analysis.

Furthermore, a displacement shape is shown on the Figure below to demonstrate the behaviour of the global structure and displacement values. The structure reaches a maximum vertical deformation of 10.073 mm which occurs along the corner slabs. It should be noted that all displacement Figures shown below are magnified by scale factor of 10 to clearly shown how the individual elements displaces under applied loadings.

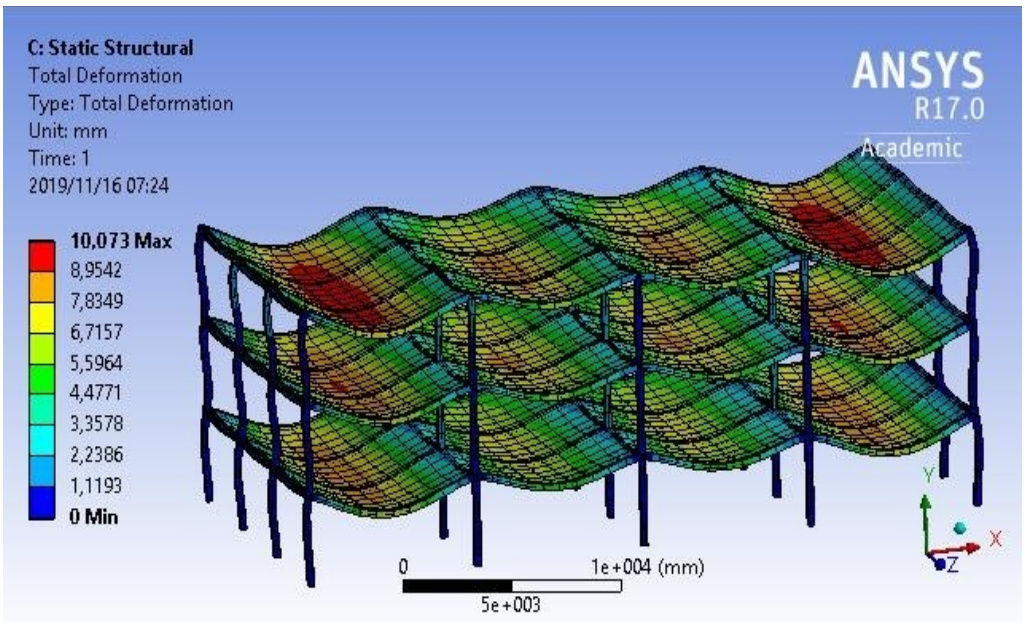

Figure 5.2: Displacement shape for structural analysis (ANSYS, 2020).

5.2 Scenario 2: Thermo-mechanical analysis

In this section, the thermo-mechanical results were obtained by heating the structural components as stated in the previous chapter are presented. This involves heating individual columns and compartment fires (i.e. four columns within the same compartment being heated at the same time). All the connections in this model are assumed to be rigid connections and the local failure of individual members was not analysed.

Furthermore, it must be noted that thermo-analysis on ANSYS works by running the thermal analysis firstly (i.e. apply thermal action such as standard fire curve) and static structural analysis afterwards, where static loads are being applied on the already heated structure. This analysis is the opposite of what happens in the real-life situations hence this may lead to unconservative results. The Newton-Raphson method was utilized to solve this non-linear problem through the application of the loading in small increments.

5.2.1 Case 1: Column C2 (Internal column)

A standard fire was applied to the internal column C2 for a duration of 90 minutes as mentioned in the previous chapter. Notice, only the ground floor columns were heated mainly because they carry much larger loads compared to the upper floor columns. Furthermore, it must be noted that all columns have the same sizes and the internal column carry much larger loads in comparison with the perimeter columns.

The heated column C2 experienced a reduction in its stiffness when under fire conditions as it clearly shows signs of yielding when compared to a non-heated column C2 which showed no signs of yielding or premature failure. For this study, premature failure was described as the condition where columns lose less than 100% of load carrying capacity due to high temperatures. The heated column C2 start yielding when 3,52 kN/m^2 was applied to the slabs with relatively small displacement as shown in Figure 5.3. As stated above, thermo-mechanical analysis is non-realistic to real life situation hence, it was the resultant for such findings as shown the Figure 5.3. The surrounding columns also, showed no signs of yielding when the internal column C2 was heated. The heated internal column C2 experienced premature buckling due to applied fire loads but the progressive buckling was restrained by the surrounding cooler columns through the action of load redistribution.

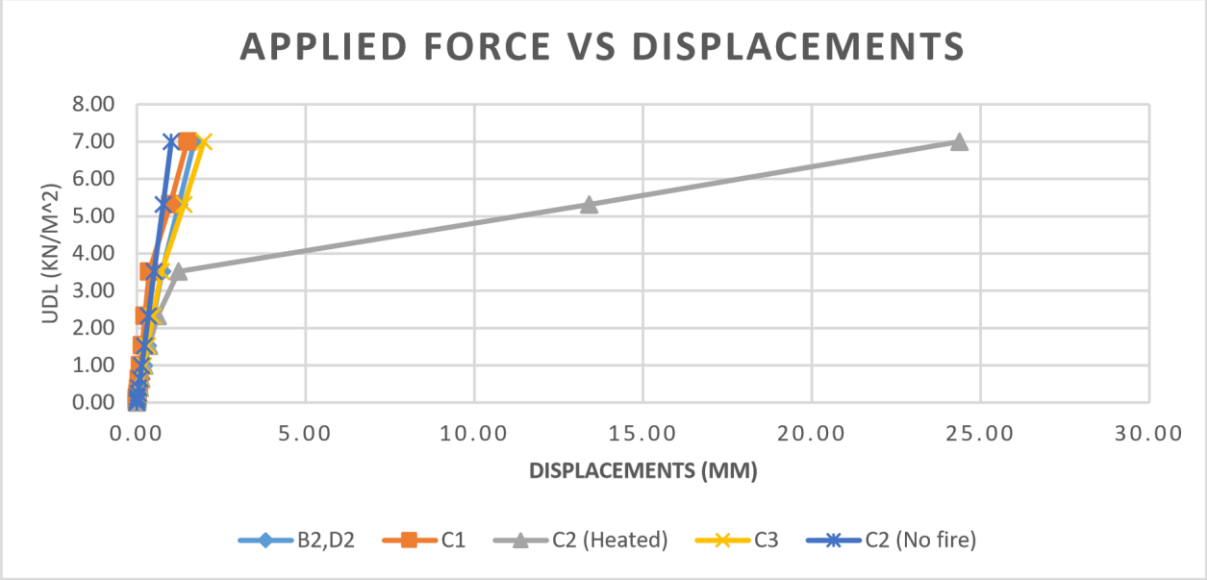

Figure 5.3: Udl versus deformation graph when the interior column C2 was heated.

The buckling of the heated column C2 was predominately controlled by the increase in compression and not by lateral displacements since the lateral displacement were significantly smaller to negligible. As mentioned above, all the columns have same sizes and the internal columns contain the largest load ratio (i.e. four times the corner columns and twice the edge columns), thus they are highly susceptible to buckling in comparison to other columns. In real life situation, the column sizes are not the same and for a similar load ratio scenario, the corner and edge column will buckle first.

The variation of axial loads when internal column C2 was heated are shown in the Table 5.1 below. The heated column C2 experienced a loss of its initial axial forces (expressed with a negative percentage) and these forces were redistributed to the surrounding columns. Column C1 and C3 engrossed most of the redistributed loading. More loads were transferred along the short span (i.e. column C1 with 139.80% and column C3 with 94.36% of additional loads), this is mainly due to orientation of the columns and in this case, the larger stiffness was in the short span direction thus more loads will be transferred in the direction with larger stiffness. In conclusion, an even load redistribution was experienced in this scenario as most of the columns were under compression.

Table 5.1: Load redistribution for the interior column (C2) fire.

Column Location	Intial axial load (Pi) kN	Final axial load (Pf) kN	Change in the load (Δ) kN	Change in the loading (%)
A1	188.01	280.54	92.53	49.22
A2	402.91	564.41	161.50	40.08
A3	402.91	571.46	168.55	41.83
A4	188.01	287.83	99.82	53.09
B1	429.04	562.33	133.29	31.07
B2	872.81	1408.90	536.09	61.42
B3	872.81	1177.50	304.69	34.91
B4	429.04	611.01	181.97	42.41
C1	409.14	981.13	571.99	139.80
C2	845.25	218.16	-627.09	-74.19
C3	845.25	1642.80	797.55	94.36
C4	409.14	542.90	133.76	32.69
D1	429.04	562.33	133.29	31.07
D2	872.81	1408.90	536.09	61.42
D3	872.81	1177.50	304.69	34.91
D4	429.04	611.01	181.97	42.41
E1	188.01	280.54	92.53	49.22
E2	402.91	564.41	161.50	40.08
E3	402.91	571.46	168.55	41.83
E4	188.01	287.83	99.82	53.09

In addition, the temperature distribution and the total displacements figure(s) are demonstrated below to show the behaviour of the global structure when the internal column C2 was heated. The maximum temperature which was reached was 1006 °C and the maximum total displacement of 25,685 mm.

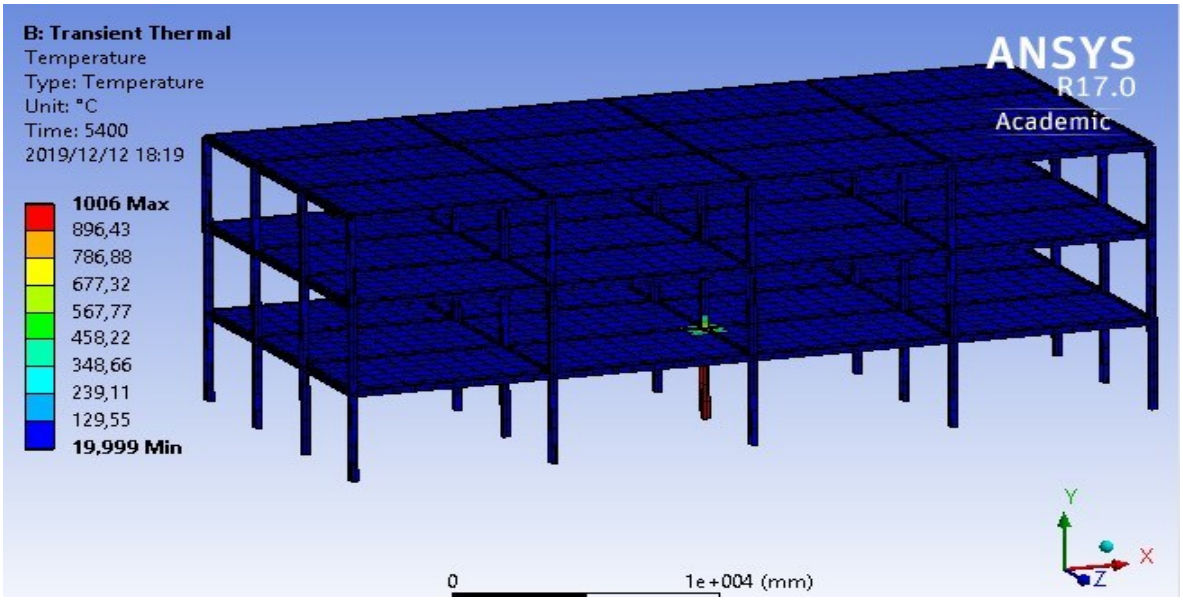

Figure 5.4: Pressure distribution shape when an internal column C2 was heated (ANSYS, 2020).

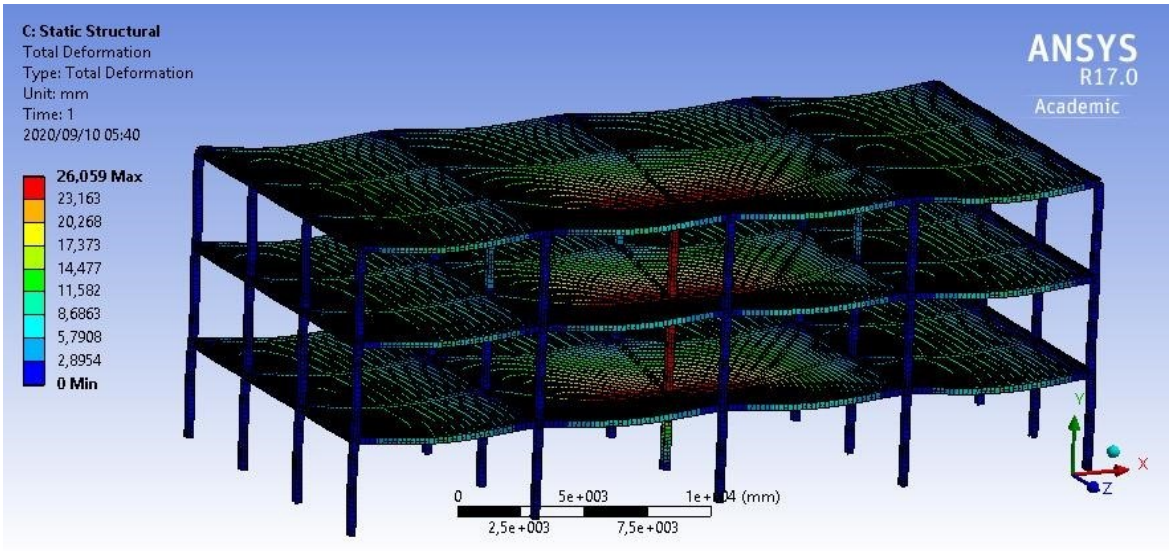

Figure 5.5: Displacement shape when an internal column C2 was heated (ANSYS, 2020).

5.2.2 Case 2: Column C1 (Edge column)

Similar to the internal column C2, the heated edge column C1 shows a reduction of its strength and stiffness compared to the non-heated edge column as shown in Figure 5.6. The heated column starts yielding as it reaches a uniform distributed loading of 3.52 kN/m^2 with relatively very small displacements. The reasoning for this phenomenon is similar to the above fire scenario. The heated edge column C1 experiences premature buckling, and the load redistribution mechanisms takes place to ensure the survival of the global structure where the surrounding column accumulated additional loads from heated column.

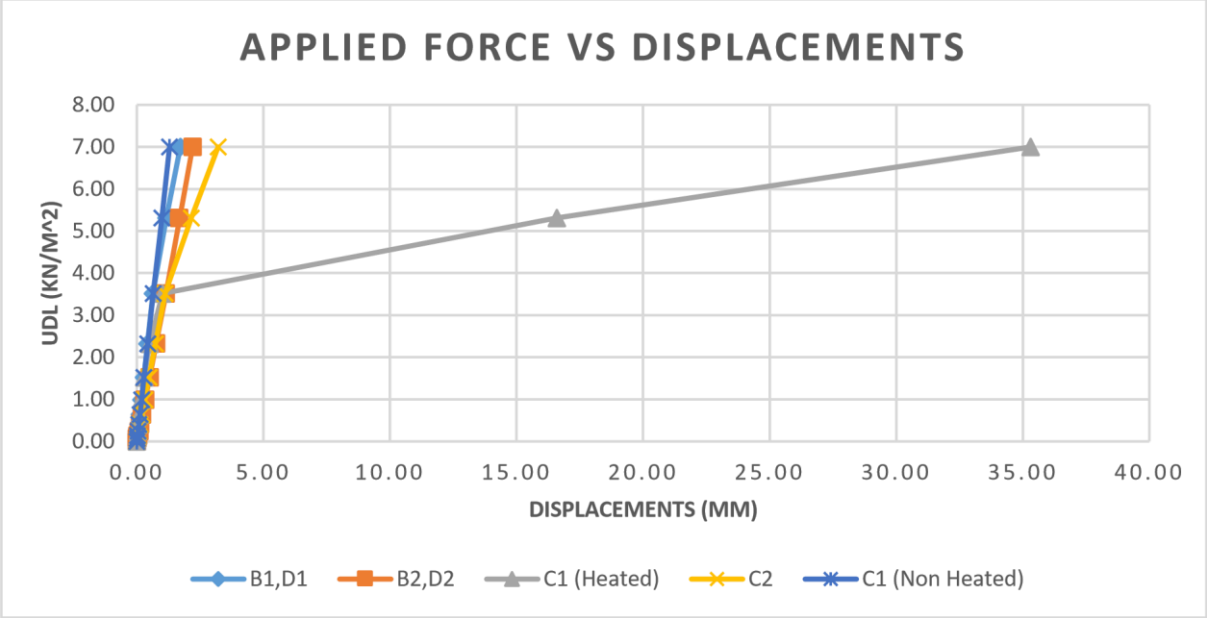

Figure 5.6: Udl versus deformation graph when the edge column C1 was heated.

The heated edge column C1 lost about 63.77% of its initial axial loads and from table 5.2, it is clearly visible that most of the loads were transferred along the short span (i.e. column C2 with 80.28% and column C3 with 32.64%) compared to the long span direction (i.e. column B1 and D1 with 75.90%). The reasoning behind this phenomenon was explained on the scenario above.

Table 5.2: Load redistribution for the long edge column (C1) fire.

Column Location	Intial axial load (Pi) kN	Final axial load (Pf) kN	Change in the load (Δ) kN	Change in the loading (%)
A1	188.01	268.16	80.15	42.63
A2	402.91	555.60	152.69	37.90
A3	402.91	562.38	159.47	39.58
A4	188.01	263.81	75.80	40.32
B1	429.04	754.69	325.65	75.90
B2	872.81	1113.90	241.09	27.62
B3	872.81	1184.70	311.89	35.73
B4	429.04	593.50	164.46	38.33
C1	409.14	148.24	-260.90	-63.77
C2	845.25	1523.80	678.55	80.28
C3	845.25	1121.10	275.85	32.64
C4	409.14	565.64	156.50	38.25
D1	429.04	754.69	325.65	75.90
D2	872.81	1113.90	241.09	27.62

D3	872.81	1184.70	311.89	35.73
D4	429.04	593.50	164.46	38.33
E1	188.01	268.16	80.15	42.63
E2	402.91	555.60	152.69	37.90
E3	402.91	562.38	159.47	39.58
E4	188.01	263.81	75.80	40.32

In addition, similar to heated column C1 scenario, the temperature distribution and the total displacements figures are utilized to illustrate the behaviour of the global structure when the edge column C1 was heated. The maximum temperature which was reached was 1006 °C and the maximum total displacement of 36,469 mm.

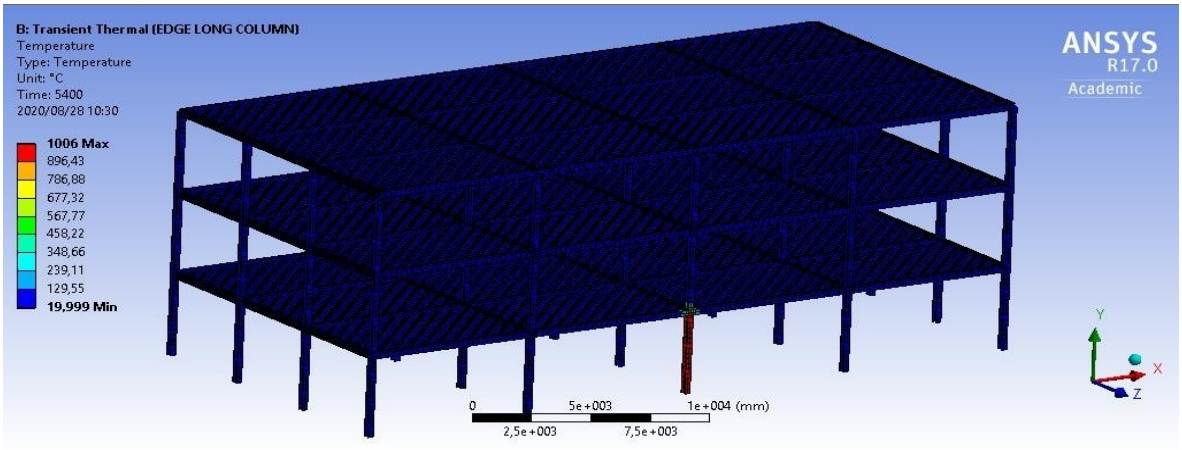

Figure 5.7: Pressure distribution shape when an edge column C1 was heated (ANSYS, 2020).

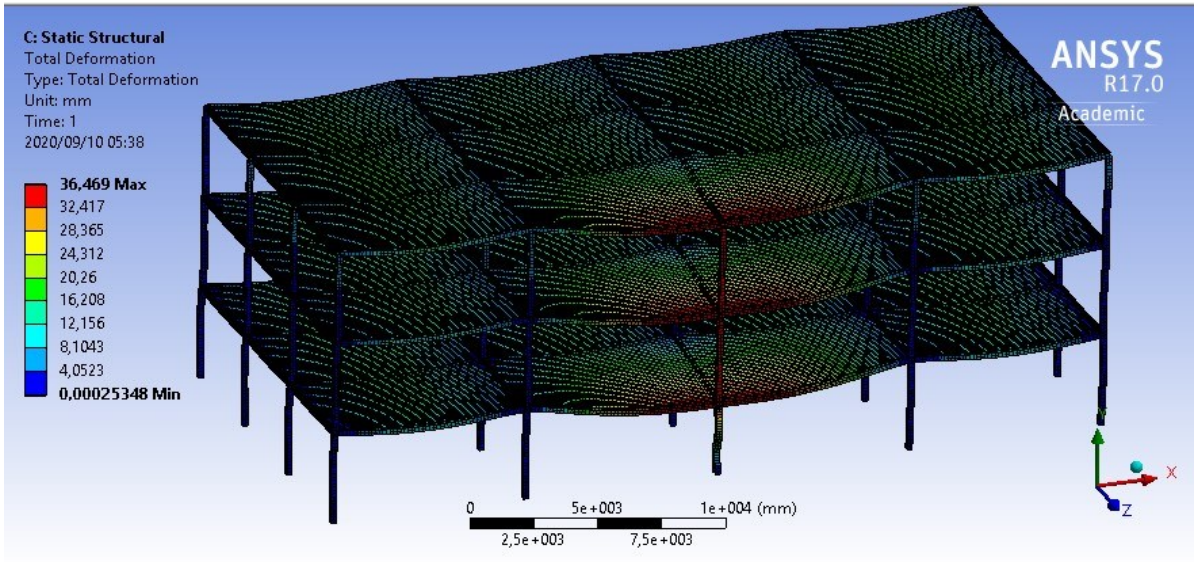

Figure 5.8: Displacement shape when an edge column C1 was heated (ANSYS, 2020).

5.2.3 Case 3: Column A2 (Edge column)

Figure 5.9 illustrates the uniform distributed loading versus displacement graph when the edge column A2 was under fire conditions. Similar to all the above scenario, the heated column shows a reduction of stiffness in comparison to the non-heated edge column. The heated column starts yielding as it reaches a uniform distributed loading of 3.52 kN/m^2 and it starts to experience premature buckling due to increasing compression. The heated column showed signs of yielding while non-heated columns remained in elastic condition with no sign of yielding. The progressive collapse of the structure was resisted by the load redistribution mechanisms as the surrounding columns accumulate additional loading without any showing signs of yielding as shown on Table 5.3.

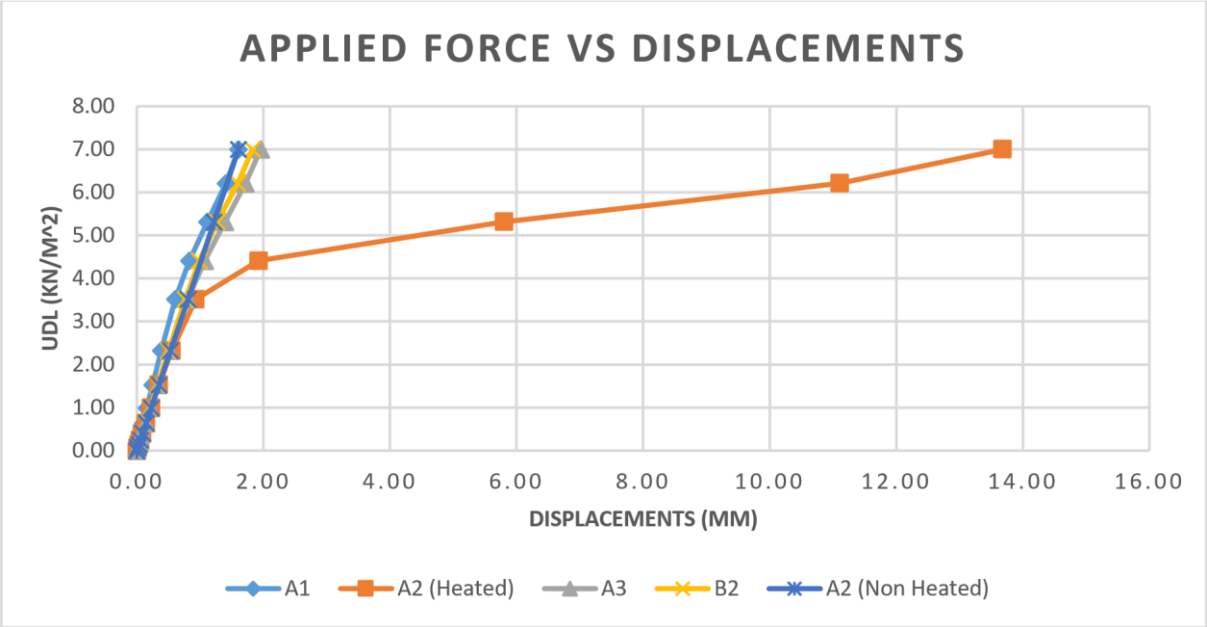

Figure 5.9: Udl versus deformation graph when the edge column A2 was heated.

On Table 5.3, the heated edge column A2 loss about 50.24% of its initial axial loads. In addition, it is noted most of the loads were transferred to the adjacent columns along the short span (i.e. column A1 with 140.16% and column A3 with 92.47%) compared to the long span direction (i.e. column B1 with 36.73% and column B2 with 50.39%). The phenomena of load redistribution and the orientation of column based on the stiffness were explained earlier in the section.

Table 5.3: Load redistribution for the short edge column (A2) fire.

Column Location	Intial axial load (Pi) kN	Final axial load (Pf) kN	Change in the load (Δ) kN	Change in the loading (%)
A1	188.01	451.53	263.52	140.16
A2	402.91	200.50	-202.41	-50.24
A3	402.91	775.49	372.58	92.47
A4	188.01	266.78	78.77	41.90
B1	429.04	583.58	154.54	36.02
B2	872.81	1316.60	443.79	50.85
B3	872.81	1193.20	320.39	36.71
B4	429.04	614.92	185.88	43.32
C1	409.14	587.60	178.46	43.62
C2	845.25	1171.30	326.05	38.57
C3	845.25	1175.30	330.05	39.05
C4	409.14	591.76	182.62	44.64
D1	429.04	617.10	188.06	43.83
D2	872.81	1218.30	345.49	39.58
D3	872.81	1218.20	345.39	39.57
D4	429.04	616.33	187.29	43.65
E1	188.01	285.12	97.11	51.65
E2	402.91	572.88	169.97	42.19
E3	402.91	573.65	170.74	42.38
E4	188.01	282.55	94.54	50.28

In addition, the temperature distribution, and the total displacements below illustrate the behaviour of the global structure when the edge column A2 was heated. The maximum temperature which was reached was 1006 °C and the maximum total displacement of 19,87 mm was experienced.

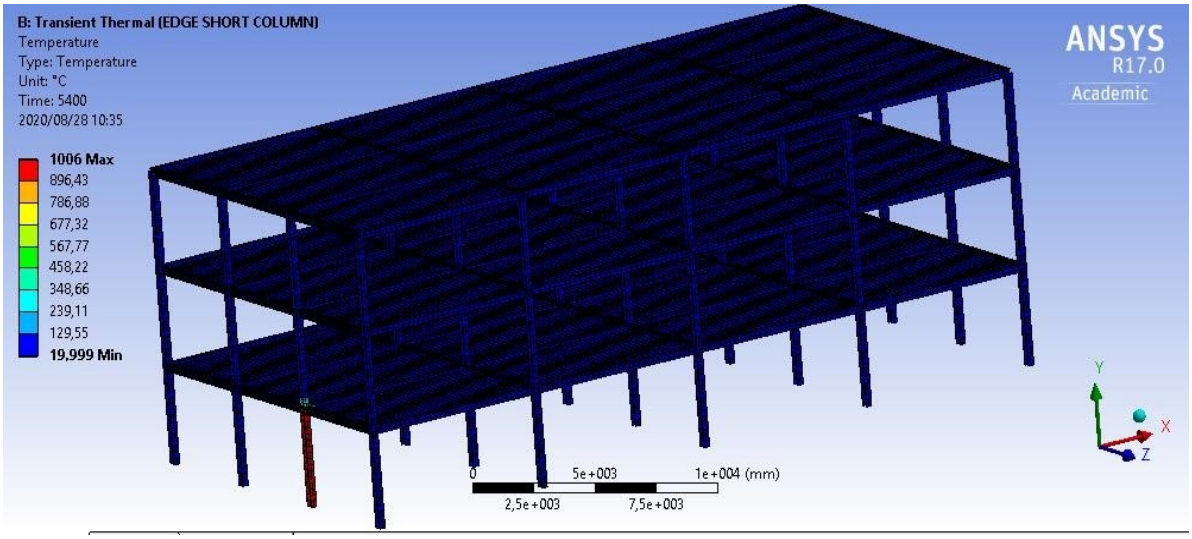

Figure 5.10: Pressure distribution shape when an edge column A2 was heated (ANSYS, 2020).

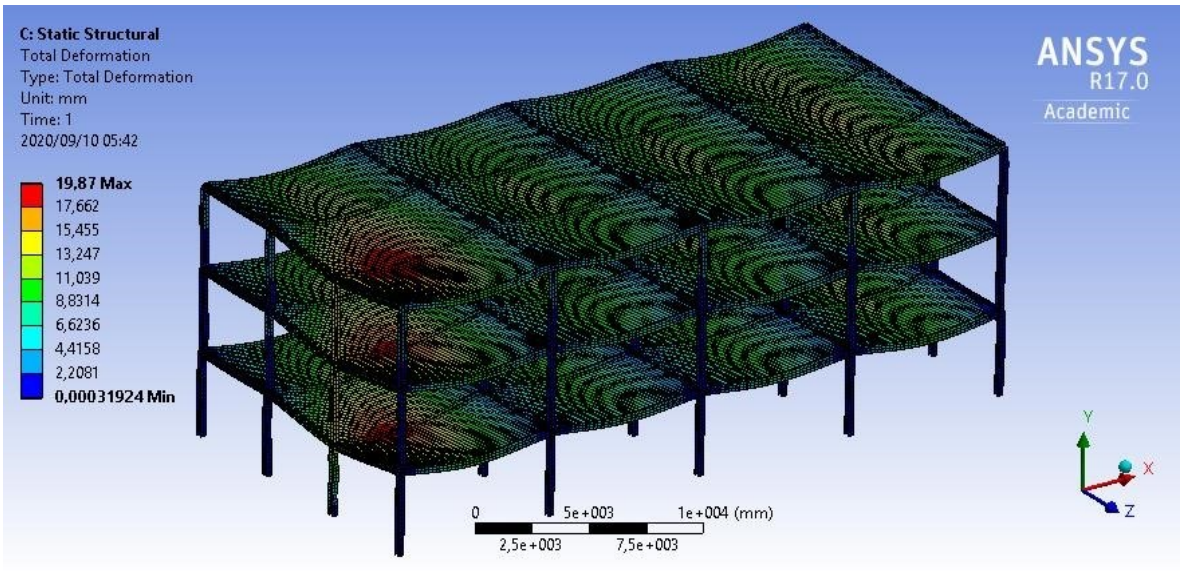

Figure 5.11: Displacement shape when the edge column A2 was heated (ANSYS, 2020).

5.2.4 Case 4: Column A1 (Corner column)

Similar to all the above scenario, the heated column shows a reduction of stiffness in comparison to the non-heated edge column and also, the heated column showed early signs of yielding as it reaches a uniform distributed loading of 5.31 kN/m^2. Furthermore, the heated column A1 starts to experience premature buckling due to increasing compression however the heated column lost smallest amounts axial loads (loss about one third of its loads) compared to other cases as shown on table 5.4. This is due to low load ratio applied to the column. The surrounding columns with the additional loading showed no signs of yielding when column A2 was heated and resistance to global failure was due to load redistribution mechanisms.

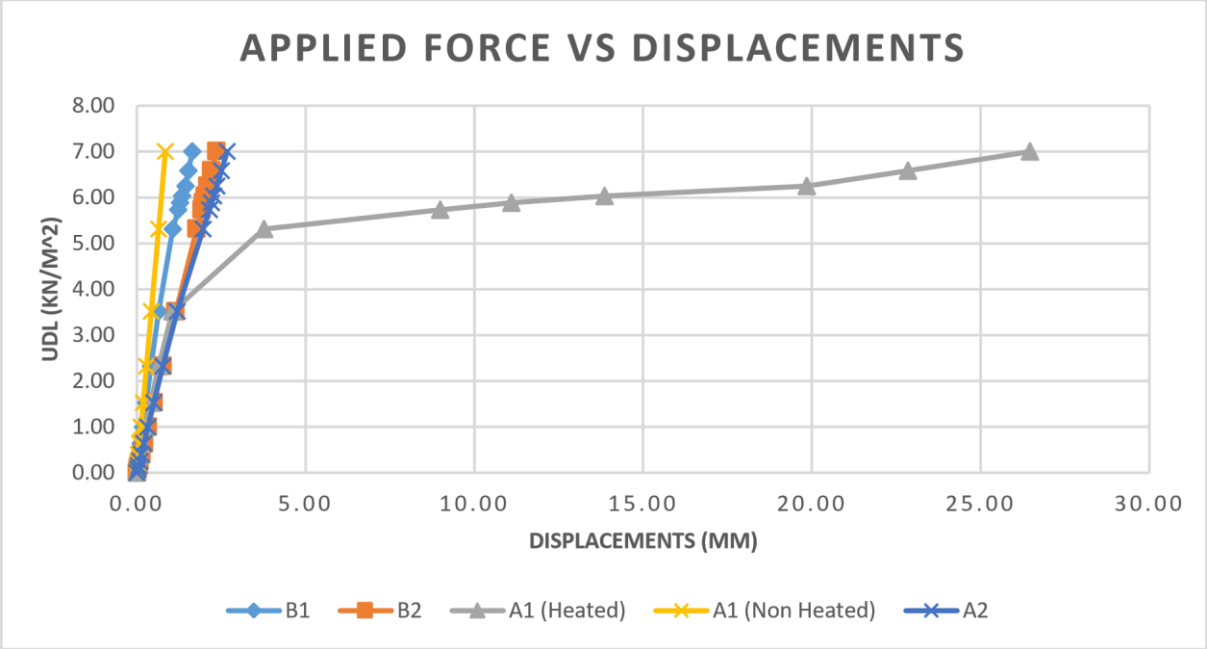

Figure 5.12: Udl versus deformation graph of the heated corner column A2.

The corner column A1 experienced loss of about 32.32% of its initial axial loads which is the lowest amongst all the above fire scenarios. This is due to column size and smaller load ratios on corner column compared to other columns. Similarly to the above cases, more of the loads were transferred to the adjacent columns along the short span (i.e. column A2 with 76.02% and column A3 with 35.27%) compared to the long span direction (i.e. column B2 with 31.09% and column C2 with 36.39%). Only the heated column experienced buckling and progressive collapse of the global structure was sustainable by the action of load redistribution mechanism.

Table 5.4: Load redistribution for the corner column (A1) fire.

Column Location	Intial axial load (Pi) kN	Final axial load (Pf) kN	Change in the load (Δ) kN	Change in the loading (%)
A1	188.01	127.24	-60.77	-32.32
A2	402.91	709.19	306.28	76.02
A3	402.91	545.03	142.12	35.27
A4	188.01	263.45	75.44	40.13
B1	429.04	686.27	257.23	59.95
B2	872.81	1144.20	271.39	31.09
B3	872.81	1188.90	316.09	36.22
B4	429.04	592.91	163.87	38.19

C1	409.14	571.80	162.66	39.76
C2	845.25	1152.80	307.55	36.39
C3	845.25	1156.90	311.65	36.87
C4	409.14	568.82	159.68	39.03
D1	429.04	601.23	172.19	40.13
D2	872.81	1193.50	320.69	36.74
D3	872.81	1194.00	321.19	36.80
D4	429.04	599.03	169.99	39.62
E1	188.01	268.16	80.15	42.63
E2	402.91	560.08	157.17	39.01
E3	402.91	559.00	156.09	38.74
E4	188.01	269.73	81.72	43.47

In addition, the temperature distribution, and the total displacements figures are illustrated below to display the behaviour of the global structure when the corner column A1 was heated. The maximum temperature which was reached was 1006 °C and the maximum experienced total displacement of 26.446 mm.

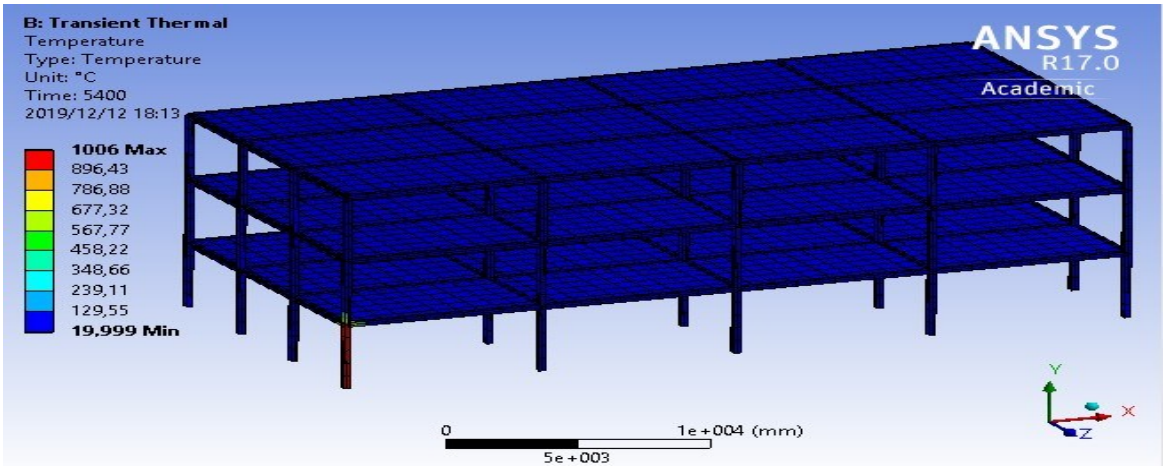

Figure 5.13: Pressure distribution shape when an edge column C1 was heated (ANSYS, 2020).

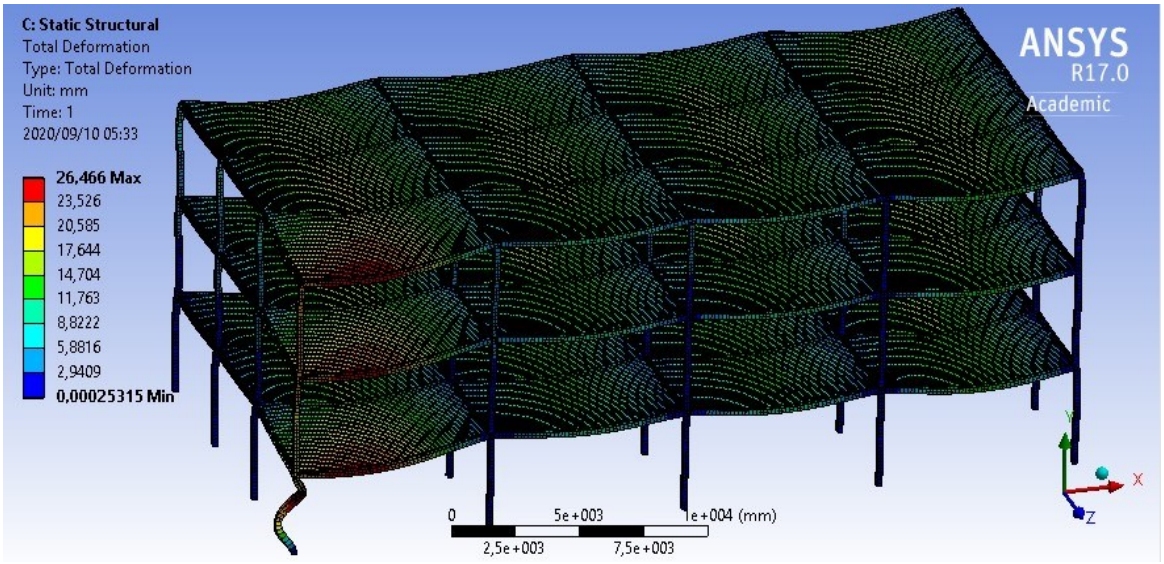

Figure 5.14: Displacement shape when a corner column A2 was heated (ANSYS, 2020).

In summary, only the heated columns experienced premature buckling and the buckling trend was resisted by the surrounding cooler columns as they engrossed the loads from the buckled column. No progressive collapse of frames was experienced when only a single column was heated, and this is mainly due to the load redistribution mechanisms. Most of the loads were transferred to the surrounding columns along the short span than the long span direction. The reason for this is the orientation of the column (i.e. axis with the stronger stiffness thus more loads transferred onto it).

In addition, the internal column C2 experienced the most loss of axial loads while the corner column A1 experienced the least loss of axial loads, this is because of the similar column size and the applied loading onto the columns in comparison with load bearing capacity (referred as load ratios). Furthermore, the heated columns started yielding at low displacement because the thermo-mechanical analysis is performed by primarily simulating the thermal analysis and then afterwards, the mechanical analysis is performed on an already heated structural elements. This is not realistic in real life situation. Therefore, more research must be conducted on this section by taking a realistic approach and also, by using a computation with sufficient efficiency. Furthermore, advance explicit modelling must be employed to investigate collapse (i.e. buckling failure where columns lose 100% of its initial axial loads) since the modelling used during the research could only model premature buckling.

5.2.3 Compartment fires

In this section, the compartment fires were investigated where four columns within the same compartment are heated at the same time which includes corner, edge, and internal compartments. The results obtained are summarized in the following sub sections below, which includes the uniform distributed load versus displacement graph, tables presenting axial load variation, pressure and displacement figures which illustrates how the global structure behaves under fire conditions. Please note that all displacement figures are magnified/scaled by a factor to clearly show how the structure displaces under the applied loading.

5.2.3.1 Case 5: Short edge Compartment fire

As mentioned in the previous chapter, a standard fire was applied to the fire compartments for a duration of 90 minutes. For this section, a uniformly distributed loading of 3 kN/m^2 was applied to the slabs. It must be noted that only the ground floor columns are heated mainly because they carry much larger loads compared to the upper floor columns and similar column sizes were adopted for this study.

From the graph, it can be noted that heated internal columns (B2 and B3) showed earlier signs of yielding compared to the other heated perimeter columns (A2 and A3) within the same edge compartment along the short span. The interior columns (B2 and B3) experienced premature buckling due to increasing compression. The surrounding cooler columns were in tension while the heated columns were in compression. It was interesting to notice that the heated perimeter columns along the short span did not buckle instead there was additional loads from the buckled interior columns. This was due to low load ratios and the condition of adopting similar column sizes. No progressive global collapse was observed and this resistance to global collapse was controlled by action of alternative load-transfer (also referred as load redistribution action). The earlier yielding of heated column under low loading with relatively very low displacement is attributed by how the simulation of thermo-mechanical is structured, i.e. the thermal actions were applied firstly then the structural loadings are applied afterwards. This does not represent an ideal life situation thus it results in odd findings.

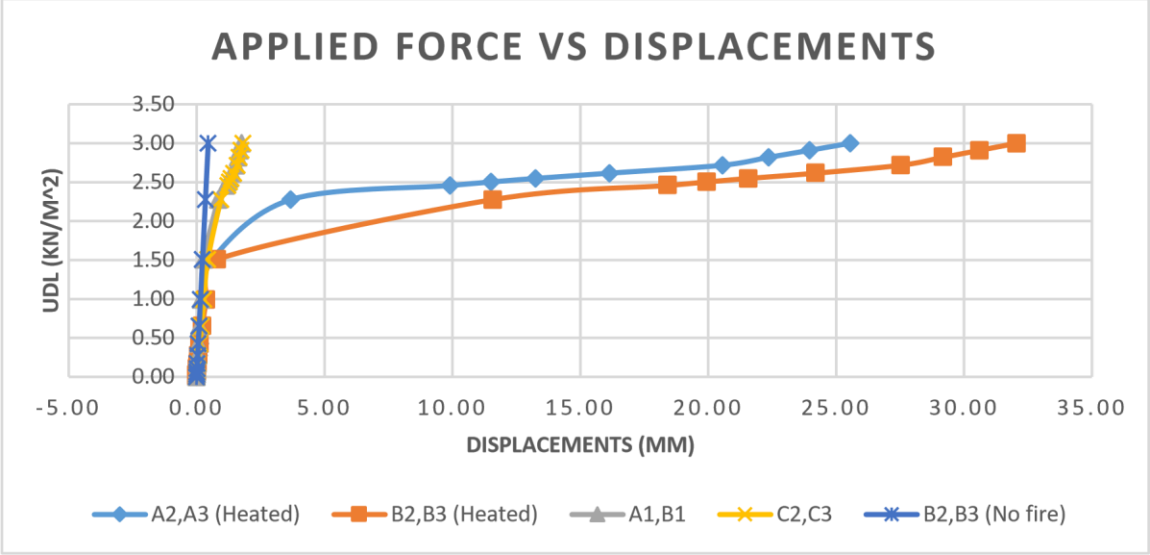

Figure 5.15: Udl versus deformation graph of the heated short edge compartment.

Furthermore, from the Table below, it is clearly visible that more loads were transferred to the short span columns (i.e. column B1, B4 carried most of the loads than column C2, C3 which are along the long span). As mentioned above, the direction which the loads will be transferred is controlled by several factors such the column orientation, types of supports and load-transfer path sequence. The collapse of the frame was sustained through a uniform distribution of loads which disallowed buckling of all four heated column by transferring the axial loads uniformly to the perimeter and interior columns. This mechanism was very pivotal to ensure that the axial loads did not accumulate on individual columns which would have resulted in progressive collapse. A load redistribution mechanism is indicated in the Table 5.5 in terms of change in the loading (%), which was calculated using the initial axial loads (Pi) on non-heated model and the final axial load (Pf) after the application of heat conditions. The heated columns are highlighted by red colour and the negative indicates decrease in axial load capacity.

Table 5.5: Load redistribution for the short edge compartment fire.

Column Location	Initial axial load (Pi) kN	Final axial load (Pf) kN	Change in the load (Δ) kN	Change in the loading (%)
A1	81.33	347.18	265.85	326.89
A2	171.79	209.74	37.95	22.09
A3	171.79	209.74	37.95	22.09
A4	81.33	347.18	265.85	326.89
B1	183.02	759.52	576.50	314.99
B2	375.33	226.28	-149.05	-39.71
B3	375.33	226.28	-149.05	-39.71
B4	183.02	759.51	576.49	314.99

C1	174.77	277.41	102.64	58.73
C2	362.28	870.89	508.61	140.39
C3	362.28	870.89	508.61	140.39
C4	174.77	277.41	102.64	58.73
D1	183.02	368.89	185.87	101.56
D2	375.33	700.91	325.58	86.74
D3	375.33	700.91	325.58	86.74
D4	183.02	368.89	185.87	101.56
E1	81.33	173.33	92.00	113.12
E2	171.79	342.28	170.49	99.24
E3	171.79	342.28	170.49	99.24
E4	81.33	173.33	92.00	113.12

In addition, the temperature distribution, and the total displacements figures are illustrated below to display the behaviour of the global structure when the edge compartment along the short was heated. The maximum temperature which was reached was 1006 °C and the maximum experienced total displacement of 37.583 mm. As expected, the maximum displacement was on the slabs within the heated compartment where the force was applied and the axial displacement on the columns are due to the applied loading on the slabs.

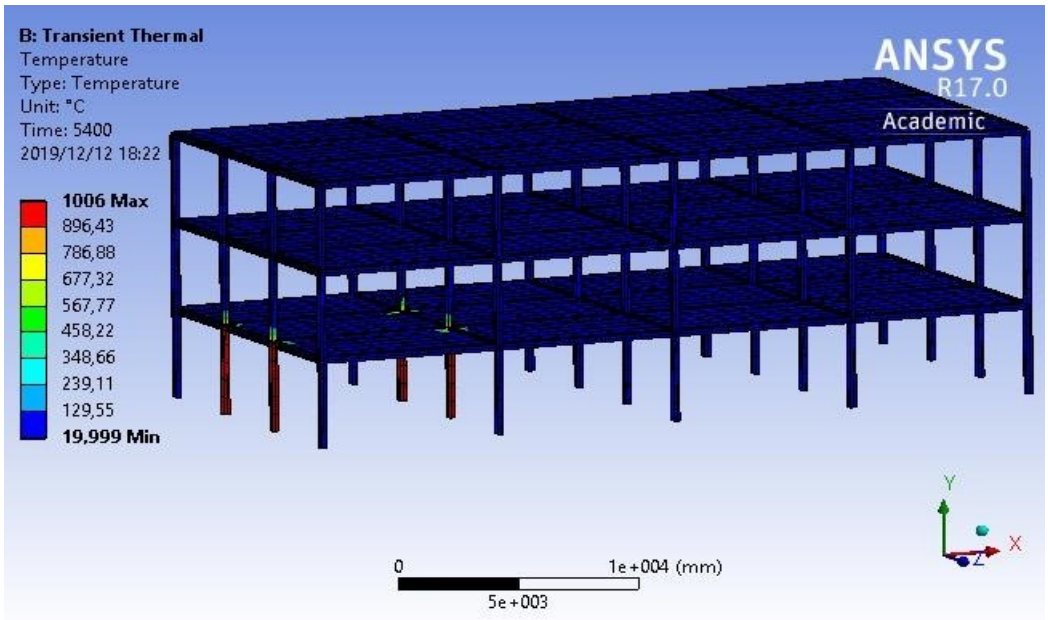

Figure 5.16: Pressure distribution when short edge compartment was heated (ANSYS, 2020).

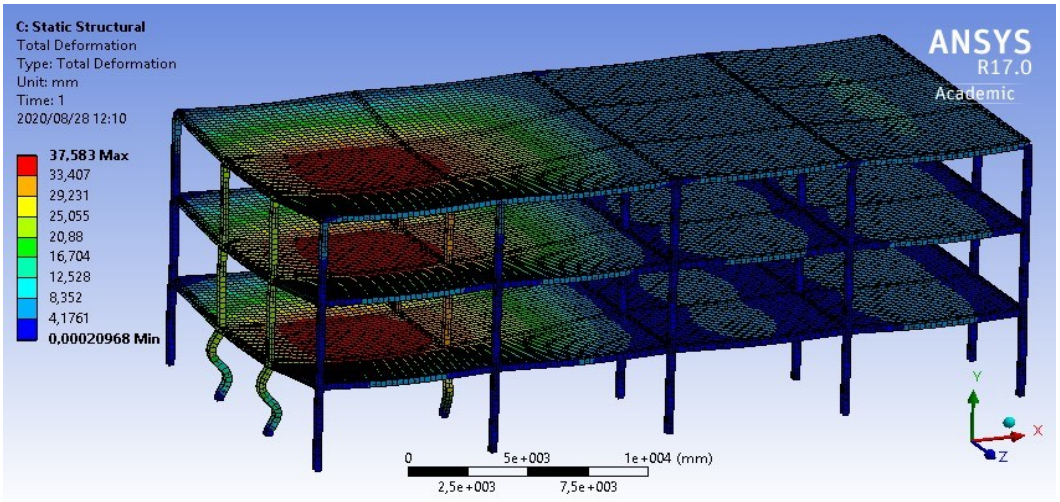

Figure 5.17: Displacement shape when short edge compartment was heated (ANSYS, 2020).

5.2.3.2 Case 6: Long edge Compartment fire

For the heated long edge fire compartment, it can be noted that only four heated columns showed signs of yielding. Similar to the short edge compartment fire, the interior columns (B2&C2) started to buckle prematurely due to increasing compression while the surrounding cooler columns remained in tension. The heated perimeter columns along the long span did not buckle instead there was additional loads from the buckled interior columns. As mentioned above, the interior columns are more prone to failure due to high load ratios in comparison with other columns. In addition, another contributing factor of this behaviour was adopting similar column sizes. The resistance to global collapse was controlled by the surrounding columns through the action of alternative load-transfer.

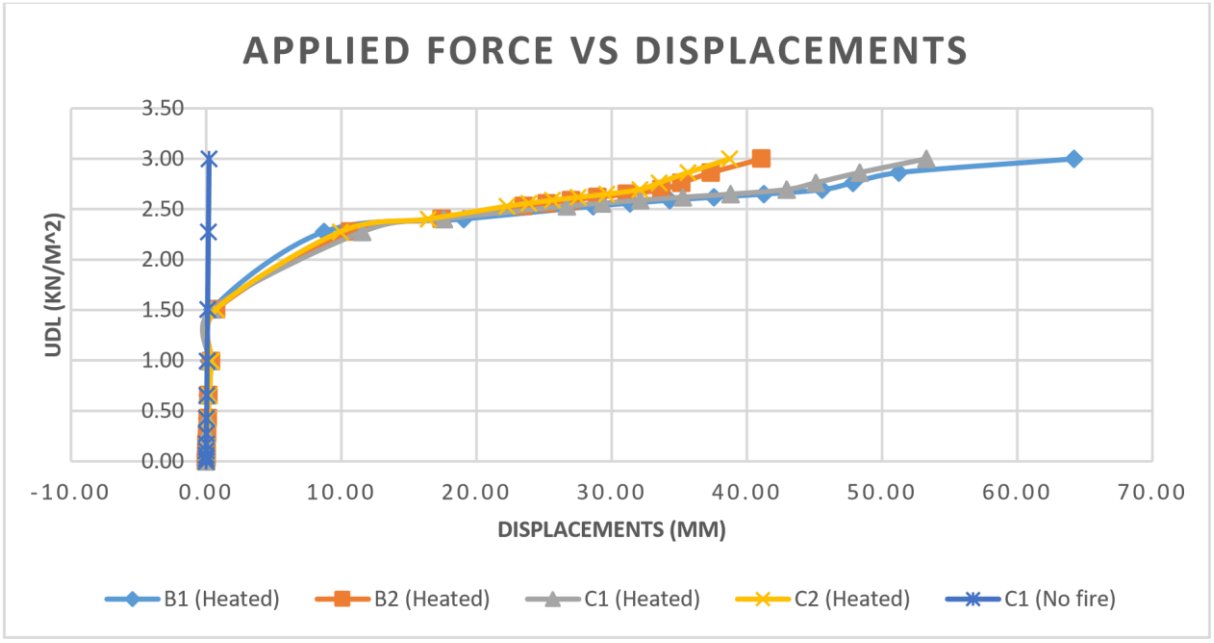

Figure 5.18: Udl versus deformation graph of the heated long edge compartment.

The collapse of the frame was sustained through a non-uniform distribution of loads which restricted buckling onto other columns by transferring most of the axial loads to the non-heated interior and perimeter columns all over the structure. This transfer of axial to all the non-heated ensured the survival of the global structure and also, this mechanism ensured that the axial loads did not accumulate on individual columns which would have resulted in buckling. Similar to the short edge compartment fire, more loads were transferred to the short span columns (i.e. column B3, C3 carried most of the loads than column A1, D1 which are along the long span).

A load redistribution mechanism is indicated in the table below in terms of changes in loading (%) and the heated columns are highlighted by red colour. The negative sign indicates a reduction of the compressive loading in the columns.

Table 5.6: Load redistribution for long edge compartment fire.

Column Location	Initial axial load (Pi) kN	Final axial load (Pf) kN	Change in the load (Δ) kN	Change in the loading (%)
A1	81.33	367.29	285.96	351.62
A2	171.79	453.02	281.23	163.71
A3	171.79	261.31	89.52	52.11
A4	81.33	104.00	22.67	27.88
B1	183.02	246.99	63.97	34.95
B2	375.33	236.17	-139.16	-37.08
B3	375.33	1319.80	944.47	251.64
B4	183.02	223.14	40.12	21.92
C1	174.77	250.36	75.59	43.25
C2	362.28	228.14	-134.14	-37.03
C3	362.28	1251.40	889.12	245.42
C4	174.77	222.76	47.99	27.46
D1	183.02	551.16	368.14	201.15
D2	375.33	858.21	482.88	128.65
D3	375.33	641.29	265.96	70.86
D4	183.02	328.97	145.95	79.75
E1	81.33	179.79	98.46	121.07
E2	171.79	324.72	152.93	89.02
E3	171.79	346.22	174.43	101.54
E4	81.33	157.75	76.42	93.97

The temperature distribution, and the total displacements figures are shown below to display the behaviour of the global structure when the long edge compartment was heated. The maximum temperature which was reached was 1006 °C and the maximum experienced total displacement of 65,149 mm.

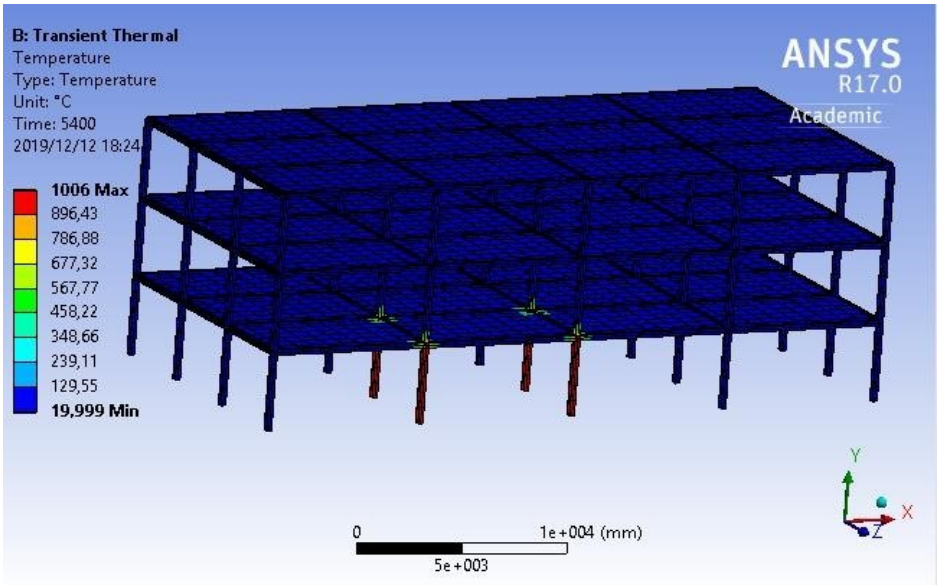

Figure 5.19: Pressure distribution when short edge compartment was heated (ANSYS, 2020).

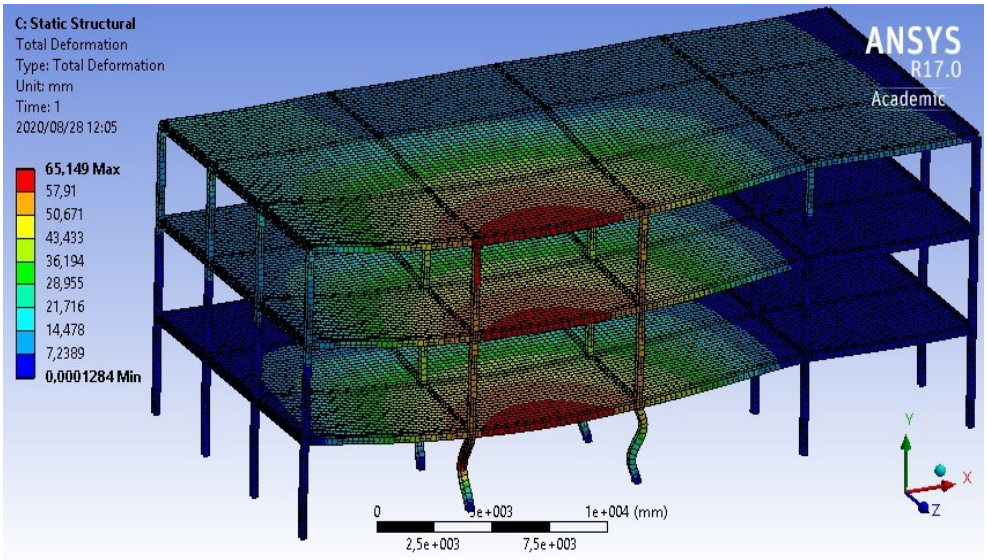

Figure 5.20: Displacement shape when long edge compartment was heated (ANSYS, 2020).

5.2.3.3 Case 7: Interior Compartment fire

For the interior compartment fire, it was interesting to note that all the heated interior columns showed uniform signs of yielding. The reason behind similar yielding patterns was due to the loading and similar column sizes assumption which were adopted in this study. In addition, a

more uniform load redistribution pattern to the surrounding cooler columns was observed in this scenario.

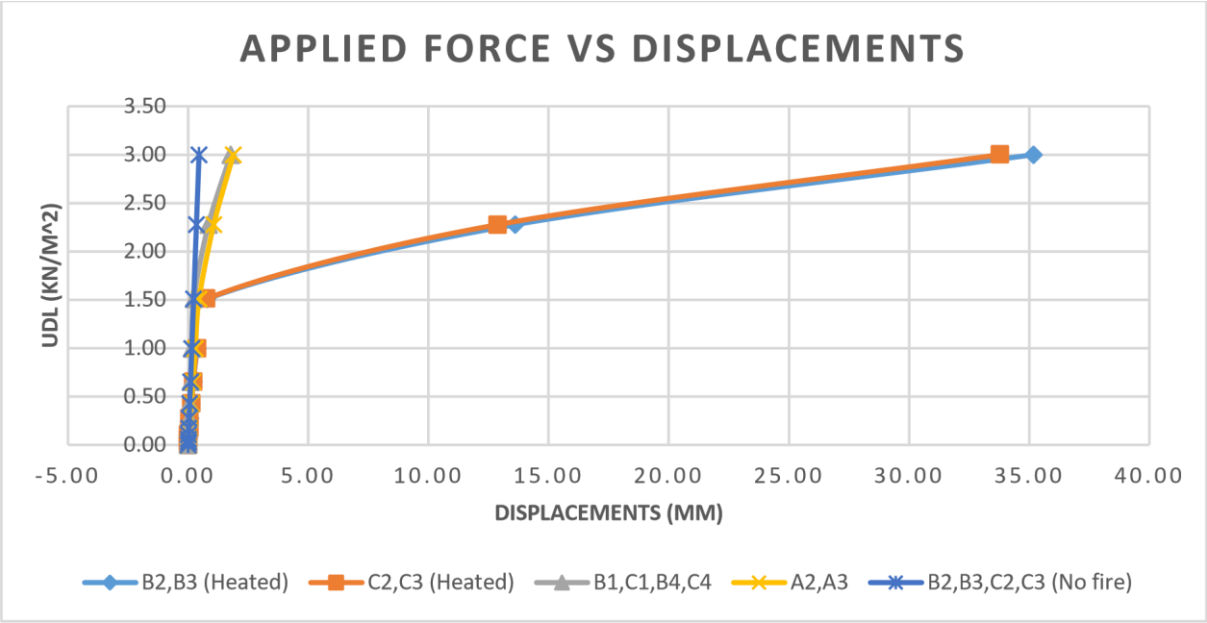

Figure 5.21: Udl versus deformation graph of the heated interior compartment.

Similar to the previous scenario, the heated interior columns started to buckle and its load bearing capacity diminished by almost 40%, however, it was interesting to note that additional perimeter columns (column A1 and A4) also, showed very minor reduction of its initial axial loading. The failure of edge columns (A1 and A4) is aggravated by the downward sagging of the slabs under tension forces resulting in lateral movement of the edge columns. However, the minor failure of the edge columns was not sufficient to results in global collapse. The uniform load redistribution pattern played an important role to disallow concentration of axial loads on individual column members and evenly distributed the axial loads through the structure as shown in the Table below. In addition, more loads were transferred to the column along the short span (i.e. Column B1 had 331.45% increase in its axial loading) compared to the columns along the long edge (i.e. Column A2 had 192.64% increase in its axial loading). The reasoning behind this pattern was based on the assumption adopted in this study which were highlighted in the previous sections.

Table 5.7: Load redistribution for the interior compartment fire.

Column Location	Initial axial load (Pi) kN	Final axial load (Pf) kN	Change in the load (Δ) kN	Change in the loading (%)
A1	81.33	81.29	-0.04	-0.05
A2	171.79	502.72	330.93	192.64

A3	171.79	502.72	330.93	192.64
A4	81.33	81.28	-0.05	-0.06
B1	183.02	789.64	606.62	331.45
B2	375.33	234.47	-140.86	-37.53
B3	375.33	234.47	-140.86	-37.53
B4	183.02	789.64	606.62	331.45
C1	174.77	748.71	573.94	328.40
C2	362.28	232.25	-130.03	-35.89
C3	362.28	232.25	-130.03	-35.89
C4	174.77	748.71	573.94	328.40
D1	183.02	285.21	102.19	55.84
D2	375.33	898.36	523.03	139.35
D3	375.33	898.36	523.03	139.35
D4	183.02	285.21	102.19	55.84
E1	81.33	175.21	93.88	115.44
E2	171.79	328.79	157.00	91.39
E3	171.79	328.79	157.00	91.39
E4	81.33	175.20	93.87	115.42

The temperature distribution, and the total displacements figures are shown below to display the behaviour of the global structure when the interior columns within the same compartment were heated. The maximum temperature which was reached was 1006 ℃ and the maximum experienced total displacement of 43,718 mm.

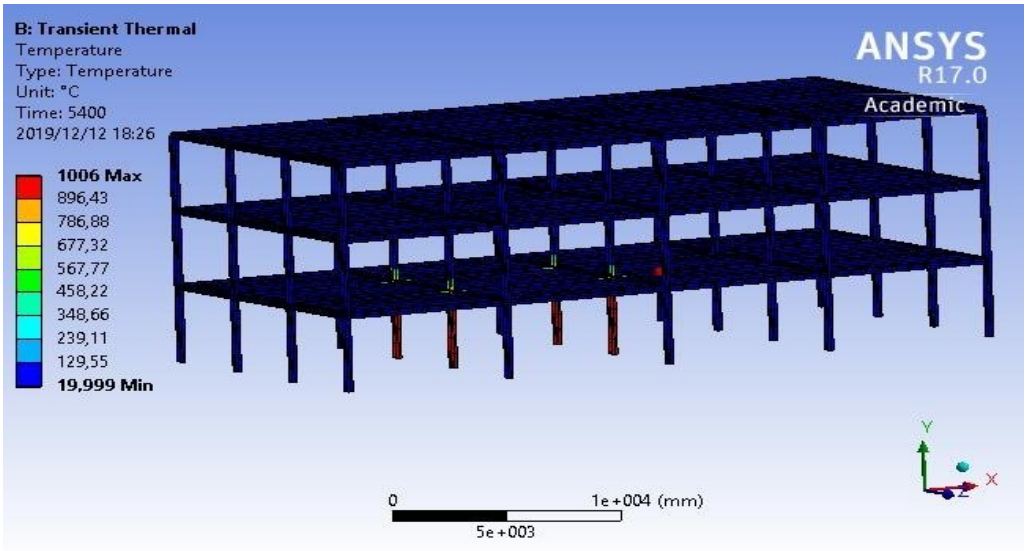

Figure 5.22: Pressure distribution when interior compartment was heated (ANSYS, 2020).

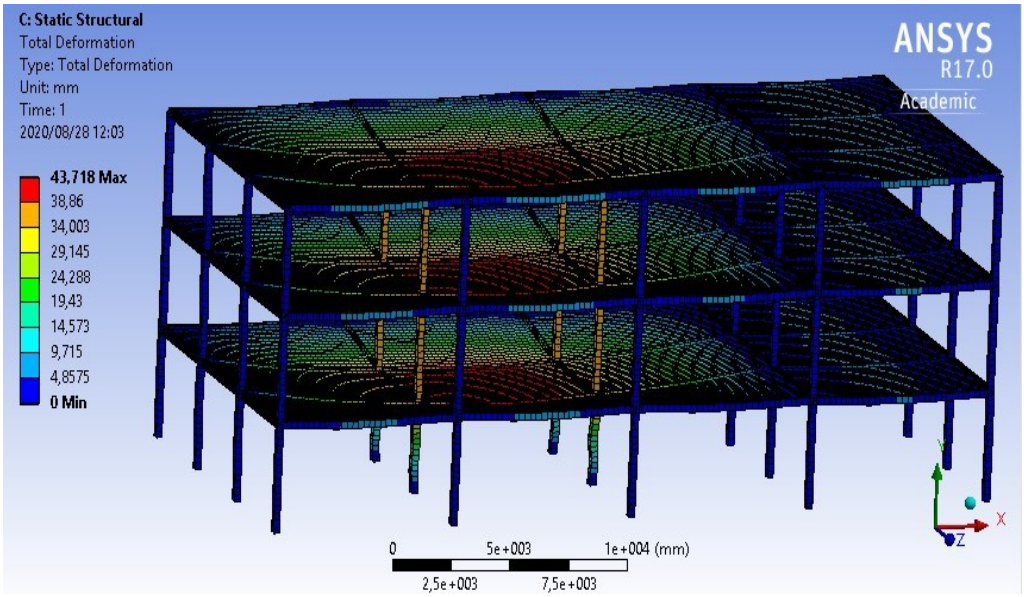

Figure 5.23: Displacement shape when interior compartment was heated (ANSYS, 2020).

5.2.3.4 Case 8: Corner Compartment fire

In this scenario, all of the four columns had signs of yielding due to reduction of the material's strength and stiffness under elevated temperatures as shown on Figure 5.24. However, only two columns (B2 and A1) out of the four heated columns showed signs of premature buckling as demonstrated on the table below. This is due to the reason that the interior columns are more prone to failure as they carry twice the loads compared to the perimeter columns. The structure resisted progressive collapse through the load redistribution mechanism.

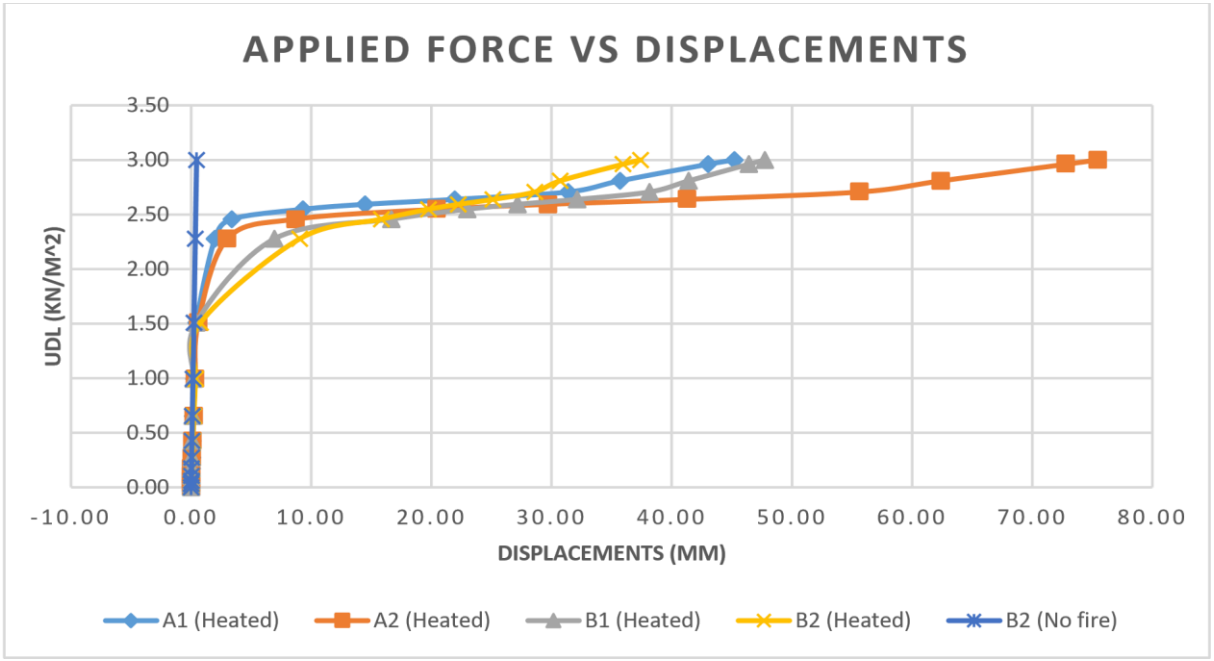

Figure 5.24: Udl versus deformation graph of the heated corner compartment.

Firstly, the heated interior column started to buckle due to larger load ratio and its load bearing capacity diminished by almost 40% and then it was followed by a non-heated corner column (column A1) which showed reduction of its initial axial loading by 37.69%. This was due to lateral movement of the column as the resultant of downward sagging of the slabs above the heated compartment fires which are subjected to tension forces. The lateral movement collapse mode was insufficient to induce progressive collapse of the structure, it was restricted by the load redistribution action as shown in the Table 5.8. The Table indicates that the axial loads on the heated columns reached their peak and start reducing which led to the surrounding columns accumulating these redistributed loads. In addition, it can be observed that more loads were transferred to the column along the short span (i.e. Column A2 had 277% increase in its axial loading) compared to the columns along the long edge (i.e. Column C1 had 73.11% increase in its axial loading). The reasoning behind this pattern was based on the assumption adopted in this study which were highlighted in the previous sections

Table 5.8: Load redistribution for the corner compartment fire.

Column Location	Initial axial load (Pi) kN	Final axial load (Pf) kN	Change in the load (Δ) kN	Change in the loading (%)
A1	81.33	223.68	142.35	175.03
A2	171.79	189.70	17.91	10.43
A3	171.79	647.64	475.85	277.00
A4	81.33	50.68	-30.65	-37.69
B1	183.02	254.04	71.02	38.80
B2	375.33	229.38	-145.95	-38.89
B3	375.33	1254.00	878.67	234.11
B4	183.02	231.49	48.47	26.48
C1	174.77	534.53	359.76	205.85
C2	362.28	832.89	470.61	129.90
C3	362.28	627.15	264.87	73.11
C4	174.77	309.48	134.71	77.08
D1	183.02	364.48	181.46	99.15
D2	375.33	695.99	320.66	85.43
D3	375.33	718.66	343.33	91.47
D4	183.02	360.15	177.13	96.78
E1	81.33	170.87	89.54	110.10

E2	171.79	344.75	172.96	100.68
E3	171.79	337.98	166.19	96.74
E4	81.33	174.96	93.63	115.13

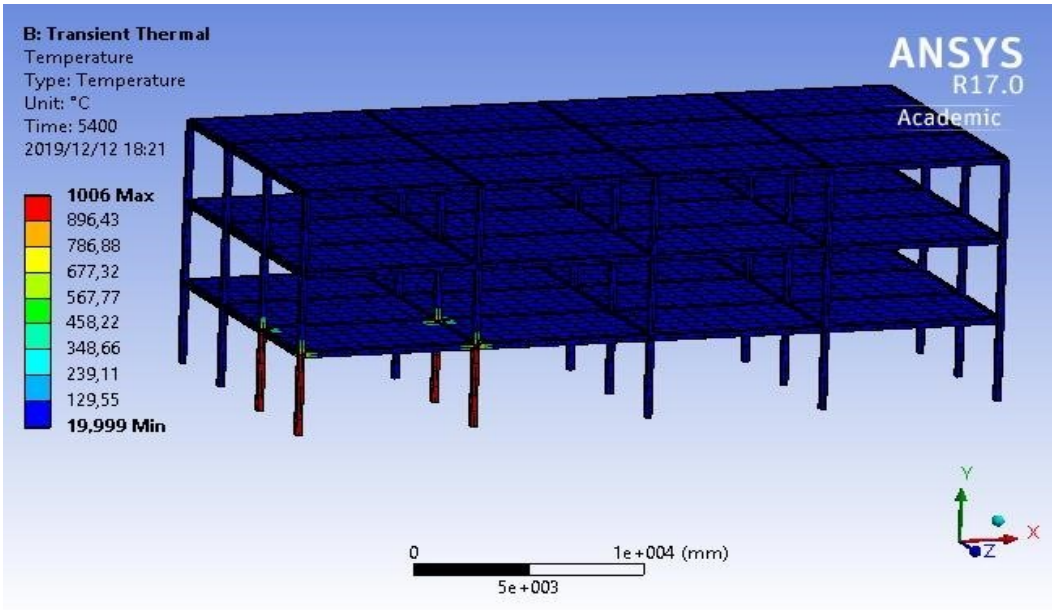

Figure 5.25: Pressure distribution shape when corner compartment was heated (ANSYS, 2020).

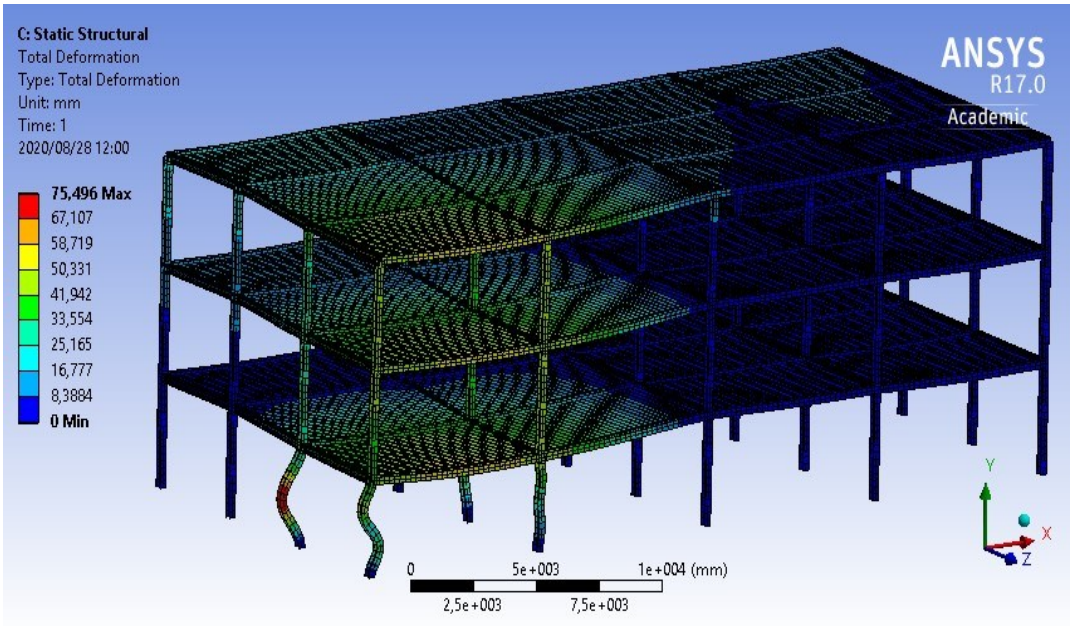

Figure 5.26: Displacement shape when corner compartment was heated (ANSYS, 2020).

5.3 Summary

In this study, an implicit mechanical and thermo-mechanical analysis was performed on a three-dimensional model to investigate the behaviour of a steel frame with concrete slabs against progressive collapse using ANSYS. The structural (non-heating condition) and thermo-mechanical analysis (heating condition) were simulated, and the findings were compared to understand the resistance of the global structure under fire conditions. As expected, under the influence of only mechanical loading (dead and live loads only), the columns showed no signs of yielding or failure and there was no progressive collapse observed. The uniform distributed loading versus displacement graph remained within elastic region and a steady linear curve which indicates that there are no signs of fatigue was obtained. The individual and compartment fires (i.e., four columns being heated at the same time within the same compartment) were investigated and columns at various locations were heated i.e., corner, long edge, short edge, and interior column.

When individual columns at various locations were heated, there was no progressive collapse observed, however, the heated columns experienced premature local buckling. This was due to material softening or an increase in compression on the heated column. The progressive collapse was restrained by the surrounding cooler structural elements which were in tension and the loads which were previously carried by the heated columns were redistributed to the surrounding columns as show on the Tables above. The interior columns showed to be more likely to cause progressive collapse however, this was due to column-load ratio (i.e., interior columns carry twice the load in comparison with the perimeter columns) and similar sizes assumption which was adopted in this study.

As well as for compartment fires, no progressive collapse was observed, however, premature local failure was also observed on the heated columns and for some non-heated perimeter columns. The short and long edge compartment fires showed only premature local failure of the heated columns. The interior and corner bay compartment fire showed premature local failure of heated and perimeter non-heated columns. This was due to lateral movement of the columns caused by the sagging of the slabs of the upper floors above the heated ground columns under tension forces. In all scenarios, the progressive collapse was restrained through the load redistribution action. The loads were transferred along the short span because the greater stiffness was along the short span. This is a common practice to reinforce the weaker short span against lateral loads. The uniform distributed loading versus displacement graph indicate that

solution did not give direct information about the collapse history and time during thermal loading. This may be associated to how the thermo-mechanical analysis was structured.

Chapter 6: Conclusion and Recommendations

6.1 Conclusions

The research was conducted to study the behaviour of a multi-storey building when it is exposed to elevated temperatures, using the finite element analysis program knowns as ANSYS. A thermo-mechanical analysis was performed on a three-dimensional steel multi-storey building which contain four spans, three bays and three stories high was created as the simulation model. The model was executed using line bodies constructed of beam and shell elements. The beams and the columns were composed of steel structures while the slabs were composed of concrete. Several objectives were studied including studying the outcomes of heating different locations whether it is a single columns or compartments. Furthermore, the effect of load ratios was also studied followed by the load redistribution mechanisms under heat exposure.

It should be noted that local failure or buckling of individual elements does not mean the progressive collapse of the global structure, however, individual collapse triggers the global progressive collapse. Furthermore, the heated column was subjected to local buckling and the axial loads increases until the peak value was reached then rapidly decreases to material degradation at high temperatures. It should be noted that the local failure was not analysed in this study. The mechanical and thermo-mechanical analysis were simulated during the study for various scenarios and the Newton-Raphson method was utilized to apply the loading in small increments.

The models showed several cases of local failure modes and the influence of redistribution of loads was also observed. In this study, all the heated columns were subjected to local premature buckling and the progressive collapse was resisted by the load redistribution mechanism through the redistribution of loads which were previously carried by the heated column to the surrounding cooler structural elements. Most of the loads which were previously carried by heated columns were mainly transferred along the short span rather than the long span as shown in Tables on the previous chapter. According to Jiang *et al.* (2016:6), "the load redistribution mechanism was influenced by span size, column orientation (bending stiffness), and the type of connection (fixed or pinned) used". In addition, the even or uneven redistribution pattern influences the concentration of loads on individual columns which may trigger progressive collapse.

Firstly, the mechanical analysis was simulated, where only mechanical loading (dead and live) only was applied, there was not any local buckling or collapse observed on the structure. This

was expected because no heat (thermal, accidental loading) was applied to the structure, therefore the structure should be able to carry its loading without any failure. The uniform distributed loading versus displacement showed a steady linear curve which is within the elastic region therefore indicating no failure. Thereafter, for fire scenario where various individual ground floor columns (i.e., interior, corner, short edge and long edge) were heated and the uniform distributed loading of 7 kN/m^2 was applied onto the slabs. The heated columns were only subjected to local premature buckling and no global progressive collapse was observed. The loads which were formerly carried by the heated columns were transferred to the surrounding cooler columns mainly along the short span. The heated interior column C2 lost the highest amount of axial loads (i.e., 74.15%) compared to any other individual column while the corner column A1 lost the least amount of axial loads (i.e. 32.32%). This indicates that the location of heated column has influence on the progressive collapse mode and that the failure of the interior column has a higher possibility to cause global collapse under fire condition. Note that this was because the interior columns carry larger amounts of loads than the corner and edge columns.

The almost similar case was observed when four columns were heated within the same compartment. The corner, interior, long edge and short edge compartment fires were investigated and a uniform distributed loading of 3 kN/m^2 was applied onto the slabs. The heated columns were subjected to local failure however no global collapse was observed. The survival of the structure was due to load-redistribution action which mainly transferred the loads to the surrounding columns mainly along the short span. For the short and the long compartment fire, the heated interior columns only showed signs of premature buckling as they lost at most 40% of its initial loads while the heated perimeter column engrossed additional loads. This was because of the load-ratio capacity as well as the assumption of adopting similar column sizes. In real life situation, the columns are not of similar sizes and the perimeter columns (corner and edge columns) are most likely to buckle first instead of the interior columns.

For the interior compartment fire, the heated interior columns (B2, B3, C2 and C3) also showed signs of premature buckling and it was interesting to note that the non-heated corner columns showed very minor signs of local buckling as they lost at most 0.06% of their initial loads. This was due to lateral movements of these columns induced by the downward sagging of the slabs above the heated ground floor columns under tension forces. This lateral drift collapse mode was not sufficient to result in global progressive collapse and it was restricted through a uniform

load redistribution pattern to the surrounding columns thus preventing concentration of loads on individual columns as shown on the Table 5.7. The corner compartment fire had similar findings with the interior compartment fire scenario and no progressive collapse mode was observed as well. The corner compartment fire resulted in premature buckling of only the heated interior column and the non-heated column (A4) showed signs of yielding due to lateral movement which was caused by the downward collapse of the slabs above the heated ground floor columns. This indicates that the location of compartment fires influences the lateral movement collapse mode.

The force versus displacement graphs shows that the heated columns experienced yielding at very low displacements. This was due to how the thermo-mechanical simulation is programmed, i.e., the thermal analysis was simulated firstly where thermal action are applied (in this case, Standard fire curve) and afterwards, the static structural analysis where structural loads (Dead and live loads) are applied. This indicates that the structural loads are applied on material that was already softened. From displacement Figures, it was observed that the maximum deflection occurred on the slabs where the loading was applied however the study was focused on the steel structures hence the displacements of the columns were only analysed.

In summary, there are two types of failure modes observed during the study namely (i) local failure of the heated columns (ii) lateral movement of columns due to downward sagging of the floors above the heated ground floor columns. The load-ratios as well as the location of the heated column had influence of the global progressive collapse and this was observed with the heated interior which were mostly likely to trigger progressive collapse. Furthermore, during compartment fire it was observed that the location of compartment fires on the lateral movement collapse mode.

6.2 Recommendations for future Studies

This study was conducted by using line bodies which are advantageous because the models which can be developed rely on the computational efficiency hence with line bodies there was less computational time compared to the solid models. However, there are major constraints of using the line bodies models such as the software was unable to model some behaviour features such as local buckling modes of webs or flanges as well the equivalent strains (Von misses) were not supported for a line body model. From the past fire events reviews in chapter 2, it can be noticed that the insulation was essential to prevent the collapse of the structural buildings in case of the fire event. However, during this study, an unprotected structural steel model which was exposed to fire conditions without any protection was adopted. This led to the overestimation of steel temperature due to lack of insulation. Thus, in future studies, fire insulations should be incorporated within the simulations. This can be advantageous because steel structure designers can only provide fire insulation to the areas where collapse was observed, thus saving money and improving the safety of the structural buildings.

In this study, a limited number of simulations were conducted due to the computational efficiency and the associated computational time. However, future studies should incorporate more possibilities of more fire scenarios in order to improve the reliability and the accuracy of the results. Due to financial constraints, only computational simulations were performed and no laboratory experiments were conducted. According to my knowledge, full scale structural response subjected to fire is very perplexing to be studied experimentally and laboratories in this direction are quite rare. Most of the experiments are mainly focused on the structural elements. Besides, very few places have laboratories that are able to conduct full scale fire experiments. In addition, finite element programs must include a couple structural-thermal analysis where one can simulate the structural analysis first and then, followed by thermal analysis afterwards. This is more reliable and realistic approach which associated with real life situation. Future studies must be conducted to determine the influence of inconsistent temperature distribution of the isolated members such as columns, within the global structural system.

In addition, more advanced explicit finite elements modelling packages such as LS-DYNA can be utilized to model progressive collapse as they are more effective and efficient when it comes to modelling complex nonlinear analysis such as column removal (progressive collapse). In most cases, the explicit dynamic analysis is utilized when the implicit analysis is not sufficient, and this includes complex problems of high non-linearity, transient dynamic forces etc.

However, these packages require more computational efficiency and time. In this study, the implicit analysis was performed on ANSYS due to financial and computational limitations. The conclusion drawn on this study may only apply to rigid steel frames with similar column sizes. Hence, more research must be conducted to study the behaviour of the multi-story steel buildings exposed to heat. This involves unequal column sizes, various type of boundary supports i.e., pin support, higher load ratio of the uniformly distributed loading as this seemed too small to cause global collapse.

Appendix A: References

Awatade M., Pise P., Jagatap D., Pawar Y., Kadam S., Deshmukh C., & Mohite D. 2016. Finite Element Modeling for Effect of Fire on Steel Frame. *Journals of Engineering Research and Application*, 2248-9622, Vol. 6.

Bless, C., Highson-Smith, C. & Kagee, A. 2006. *Fundamentals of social research methods: An African perspective*, Juta and Company Ltd.

Burgess I, Huang Z, & Sun R. 2011. Progressive collapse analysis of steel structures under fire conditions. *Fire Safety Journal* 46: 348-63.

Chen, D., & Tang, J. 2016. Finite element analysis of portal frames under fire conditions. 4th international conference on mechanical materials and manufacturing Engineering (MMME).

Davies J., & Wang Y. 2003. An experimental study of non-sway loaded and rotationally restrained steel column assemblies under fire conditions: analysis of test results and calculations. *Journal of Constructional Steel Research* 59 (2003), pp. 291-313

El-Heweity, M. 2012. Behavior of portal frames of steel hollow sections exposed to fire. *Alexandria Engineering Journal*. 51, 95-107, Alexandria University, Egypt.

EN 1991-1-1-2 2005. Eurocode 1: Actions on structures – Part 1-2: General actions – Actions on structures exposed to fire. Brussels: European Committee for Standardization.

EN 1991-1-7 2006. Actions on structures – Part 1-7: General actions-accidental actions. Brussels: European Committee for Standardization (CEN).

EN 1993-1-2 2005. Eurocode 3: Design of steel structures. General rules. Structural fire design. Brussels: European Committee for Standardization.

EN 1994-1-2 2005. Design Action of composite steel and concrete structures, Part 1-2: General Rules- Structural fire. Brussels: European Committee for Standardization (CEN).

EN 1994-1-2 2005. Eurocode 4: Basis Design Action on structures – EN 1991-2-2 Part 22: Actions on structures exposed to fire. Brussels: European Committee for Standardization

Eurocode 3 2001. Design of steel structures – Part 1-2: General rules – Structural fire design. Brussels: European Committee for Standardization.

Hibbler, R. 2014. *Mechanics of Materials 9th Edition*. Pearson Prentice hall Publishers, New Jersey, United States.

Jeffers A, Kotsovinos P, Rackauskaitue E, & Rein G. 2017. Structural analysis of multi-story steel frames exposed to travelling fires and traditional design fires. *Journals of Engineering Structures* 150 (2017) 271-287.

Jiang, J, & Li GQ, 2017. Disproportionate collapse of 3D steel framed structures exposed to various compartment fires. *Journal of Constructional Steel Research* 138 (2017) 594-607

Jiang, J, & Li GQ, 2016. Progressive collapse analysis of 3D steel frames with concrete slabs exposed to localized fire. *Journal of Engineering Structures*, 149 (2016) 1-14.

Jiang, J., Li, G.Q., Lou, G, & Wang C. 2018. Quantitative evaluation of progressive collapse process of steel portal frames in fire. *Journal of Constructional Steel Research*, 150 (2018) 277-287.

Jiang, J., & Usmani A.S. 2014. Modelling of steel frames structures in fire using OpenSees. *Journal Computational Structure* 188: 90-9.

Jiang, J, Li G.Q., & Usmani A.S. 2014. Effect of bracing systems on fire induced progressive collapse of steel structures using OpenSees. *Journal of Fire Technology*. 51:1249-1273. Jiang, J., Li G.Q., & Usmani A.S. 2014. Influence of fire scenarios on progressive collapse mechanisms of steel framed structures. *Journal of Steel Construction Research*. 7:169-72

Kandekar, S., & Mahale, H. 2016. Behavior of steel structures under the effect of fire loading. *Journal of Engineering Research and Applications*, Vol. 6: 2248-9622,

Kang-Hai, T., Wee-Siang, T., Zhan-Fei, H., & Guang-Hwee, P. 2007. Structural responses of restrained steel columns at elevated temperatures. Part 1: Experiments. *Engineering Structures* 29 (8) (2007), pp. 1641-1652.

Kolos, I., Lausova L., Michalcova, V., & Skotnicova, I. 2017. Numerical analysis of steel portal frame exposed to fire. *Journal of Structural and Physical Aspect of Construction Engineering*, 190 (2017) 237-242.

Kothari, C.R. 2004. *Research methodology: Methods and techniques*, New Age International.

LaiChan, S., & Lu, C. 2004. A simulation based on large deflections and inelastic analysis of steel frames under fire. *Journal of Constructional Steel Research*. 60: 1495-1524.

Lamont S., Rotter J., & Usmani A. 2001. Fundamental principle of structural behaviour under thermal effects. *Fire Safety Journal*, 36: 721-744.

Li, G, Wang, P, & Wang, Y. 2010. Behavior and design of restrained steel columns in fire. Part 1: Fire test. *Journal Constructional Steel Research*, 66 (2010) 1138-47.

Mekky, W., Porcari, G., & Zalok, E. 2015. Fire induced progressive collapse of steel building structures: A review of the mechanisms. *Fire Engineering Journals*, 82 (2015) 261-267.

Mahmoud, H., Memari, M. 2014. Performance of steel moment resisting frames with RBS connections under fire loading. *Engineering Structure Journals,* 75:126-38.

Oosthuizen, P. 2010. Assessment of steel structures subjected to fire conditions. Master thesis, Department of Civil Engineering, University of Cape Town, South Africa.

Preston, R., & Kirby, B. 1998. High temperature properties of hot-rolled, structural steels for use in fire engineering design studies, *Fire Safety Journal* 13 (1988), pp. 27-37.

Qin, C. 2016. Collapse of simulation of steel buildings under fire. Master's thesis, Department of Civil and Environmental Engineering, Colorate State University.

Simms W. 2012. Fire resistance design of steel framed buildings, Ch. 2-5, 5-39. Steel construction Institute Publishers Co., Berkshire, United Kingdom.

Sun R., Huang Z., & Burgess I. (2012) Progressive collapse analysis of steel structure under fire conditions, *Journals of Engineering Structure*, 34:400-413

Sun R., Huang Z., & Burgess I. (2012) The collapse behaviour of braced steel frames exposed to fire, *Journals of Construction Steel Research,* 72:130-142

Vassart, O. & Zhao, B. 2011. FRACOF Engineering Background. Report developed for the

Vassart, O., Zhao, B., Cajot, L., Robert, F., Meyer, U., Frangi., A., Poljanšek., M., Nikolova.,

Walls, R. 2016. A beam finite element for the analysis of structures in fire. PhD Engineering Dissertation, School of Civil Engineering, Stellenbosch University, Cape Town, Republic of South Africa.

Zhao, B. 2012. Fire resistance assessment of steel structures: Workshop 'structural fire design of buildings according to the Eurocodes' – Brussels: European Committee for Standardization

Appendix B: Additional Data

The following data represent the plasticity model for the structural steel with increasing temperatures.

Table B.1: Plastic Values for the Proportional Limit

θ (°C)	Proportional stress (Kpa)	Elasticity modulus (GPa)	Strain of the proportional limit	Plastic strain of the proportional limit
20	355 000,00	200,00	0,00177500	0,00000000
100	355 000,00	200,00	0,00177500	0,00000000
200	286 485,00	180,00	0,00159158	0,00000000
300	217 615,00	160,00	0,00136009	0,00000000
400	149 100,00	140,00	0,00106500	0,00000000
500	127 800,00	120,00	0,00106500	0,00000000
600	63 900,00	62,00	0,00103065	0,00000000
700	26 625,00	26,00	0,00102404	0,00000000
800	17 750,00	18,00	0,00098611	0,00000000
900	13 312,50	13,50	0,00098611	0,00000000

Table B.2: Plastic Values at the Yielding Strength.

θ (°C)	Stress strength (KPa)	Elastic strain at the initiation of the stress strength	Plastic strain at the initiation of the stress strength
20	490000,00	0,02	0,01755000
100	490000,00	0,02	0,01755000
200	355000,00	0,02	0,01802778
300	355000,00	0,02	0,01778125
400	355000,00	0,02	0,01746429
500	276900,00	0,02	0,01769250
600	166850,00	0,02	0,01730887
700	81650,00	0,02	0,01685962
800	39050,00	0,02	0,01783056
900	21300,00	0,02	0,01842222

Table B. 3: Plastic Values at the Ultimate Strength.

θ (°C)	Stress strength at the end of diagrams (KPa)	Strain at the end of diagrams	Plastic strain at the end of the stress strength
20	490 000,00	0,15	0,14755000
100	490 000,00	0,15	0,14755000
200	355 000,00	0,15	0,14802778
300	355 000,00	0,15	0,14778125
400	355 000,00	0,15	0,14746429
500	276 900,00	0,15	0,14769250
600	166 850,00	0,15	0,14730887
700	81 650,00	0,15	0,14685962
800	39 050,00	0,15	0,14783056
900	21 300,00	0,15	0,14842222

Appendix C: Bibliography

Awatade M., Pise P., Jagatap D., Pawar Y., Kadam S., Deshmukh C., & Mohite D. 2016. Finite Element Modeling for Effect of Fire on Steel Frame. *Journals of Engineering Research and Application*, 2248-9622, Vol. 6.

Bacinskas, D, Cefarelli, G, Cuoto, C, Faggiano, B, & Ferrarp, A. 2015. Analyses of structures under fire. *Journal of Constructional Steel Research* 109, 101-114.

Björkstand, L. 2012. Single storey building exposed to fire – an integrated approach for analytical evaluation of steel structures exposed to fire. Masters Science in Engineering Technology Fire Engineering, Luleȁ University of Technology, Sweeden.

Bless, C., Highson-Smith, C. & Kagee, A. 2006. *Fundamentals of social research methods: An African perspective*, Juta and Company Ltd.

Abu, A. K., & Buchanan, A. H. 2017. Structural design for fire safety, John Wiley & Sons.

Burgess I, Huang Z, & Sun R. 2011. Progressive collapse analysis of steel structures under fire conditions. *Fire Safety Journal* 46: 348-63.

Chen, D., & Tang, J. 2016. Finite element analysis of portal frames under fire conditions. 4th international conference on mechanical materials and manufacturing Engineering (MMME).

Davies J., & Wang Y. 2003. An experimental study of non-sway loaded and rotationally restrained steel column assemblies under fire conditions: analysis of test results and calculations. *Journal of Constructional Steel Research* 59 (2003), pp. 291-313

El-Heweity, M. 2012. Behavior of portal frames of steel hollow sections exposed to fire. *Alexandria Engineering Journal*. 51, 95-107, Alexandria University, Egypt.

EN 1991-1-1-2 2005. Eurocode 1: Actions on structures – Part 1-2: General actions – Actions on structures exposed to fire. Brussels: European Committee for Standardization.

EN 1991-1-7 2006. Actions on structures – Part 1-7: General actions-accidental actions. Brussels: European Committee for Standardization (CEN).

EN 1993-1-2 2005. Eurocode 3: Design of steel structures. General rules. Structural fire design. Brussels: European Committee for Standardization.

EN 1994-1-2 2005. Design Action of composite steel and concrete structures, Part 1-2: General Rules- Structural fire. Brussels: European Committee for Standardization (CEN).

EN 1994-1-2 2005. Eurocode 4: Basis Design Action on structures – EN 1991-2-2 Part 22: Actions on structures exposed to fire. Brussels: European Committee for Standardization

Eurocode 3 2001. Design of steel structures – Part 1-2: General rules – Structural fire design. Brussels: European Committee for Standardization.

Feeney, M., & Lim, L. 2015. The application of advanced finite elements analysis for structural fire design. International conference on performance based and life cycle structural Engineering (PLSE 2015).

Huang Z., Tan K, Toh W., & Phng G. 2007. Structural responses of restrained steel columns at elevated temperatures. Part 1: Experiments. *Journals Engineering Structure*, 29 (2007) 1641-52.

Hibbler, R. 2014. *Mechanics of Materials 9th Edition*. Pearson Prentice hall Publishers, New Jersey, United States.

Jeffers A, Kotsovinos P, Rackauskaitue E, & Rein G. 2017. Structural analysis of multi-story steel frames exposed to travelling fires and traditional design fires. *Journals of Engineering Structures* 150 (2017) 271-287.

Jiang, J, & Li GQ, 2017. Disproportionate collapse of 3D steel framed structures exposed to various compartment fires. *Journal of Constructional Steel Research* 138 (2017) 594-607

Jiang, J, & Li GQ, 2016. Progressive collapse analysis of 3D steel frames with concrete slabs exposed to localized fire. *Journal of Engineering Structures*, 149 (2016) 1-14.

Jiang, J., Li, G.Q., Lou, G, & Wang C. 2018. Quantitative evaluation of progressive collapse process of steel portal frames in fire. *Journal of Constructional Steel Research*, 150 (2018) 277-287.

Jiang, J., & Usmani A.S. 2014. Modelling of steel frames structures in fire using OpenSees. *Journal Computational Structure* 188: 90-9.

Jiang, J, Li G.Q., & Usmani A.S. 2014. Effect of bracing systems on fire induced progressive collapse of steel structures using OpenSees. *Journal of Fire Technology*. 51:1249-1273. Jiang, J., Li G.Q., & Usmani A.S. 2014. Influence of fire scenarios on progressive collapse mechanisms of steel framed structures. *Journal of Steel Construction Research*. 7:169-72

Kalogeropoulos, A., Drosopoulos, G., & Stavroulakis G.E. 2012. Thermal stress analysis of a three-dimensional end plate steel joint. *Construction and Building Materials Journal*. 29: (2012) 619-626.

Kandekar, S., & Mahale, H. 2016. Behavior of steel structures under the effect of fire loading. *Journal of Engineering Research and Applications*, Vol. 6: 2248-9622.

Kang-Hai, T., Wee-Siang, T., Zhan-Fei, H., & Guang-Hwee, P. 2007. Structural responses of restrained steel columns at elevated temperatures. Part 1: Experiments. *Engineering Structures* 29 (8) (2007), pp. 1641-1652.

Kolos, I., Lausova L., Michalcova, V., & Skotnicova, I. 2017. Numerical analysis of steel portal frame exposed to fire. *Journal of Structural and Physical Aspect of Construction Engineering*, 190 (2017) 237-242.

Kothari, C.R. 2004. *Research methodology: Methods and techniques*, New Age International.

LaiChan, S., & Lu, C. 2004. A simulation based on large deflections and inelastic analysis of steel frames under fire. *Journal of Constructional Steel Research*. 60: 1495-1524.

Lamont S., Rotter J., & Usmani A. 2001. Fundamental principle of structural behaviour under thermal effects. *Fire Safety Journal*, 36: 721-744.

Lausova L., Kolos I., Michalcova V., Skotnicova I. 2017. Numerical analysis of steel portal frame exposed to fire. University of Ostrava, Faculty of Civil Engineering, Ostrava, Czech Republic.

Li, G, Wang, P, & Wang, Y. 2010. Behavior and design of restrained steel columns in fire. Part 1: Fire test. *Journal Constructional Steel Research*, 66 (2010) 1138-47.

Lin, J. 2015. Fundamentals of Materials Modelling for Metals Processing Technologies: Theories and Applications, World Scientific Publishing Company Pte Limited.

Long, T, McAllister, T, Gross, J, & Hurley, M. 2010. Best Practise Guidelines for Structural Fire Resistance Design of Concrete and Steel Buildings. National Institute of Standard and Technology, United State.

Mahmoud, H., Memari, M. 2014. Performance of steel moment resisting frames with RBS connections under fire loading. *Engineering Structure Journals,* 75:126-38.

Mekky, W., Porcari, G., & Zalok, E. 2015. Fire induced progressive collapse of steel building structures: A review of the mechanisms. *Fire Engineering Journals*, 82 (2015) 261-267.

Mosta, S., & Drosopoulos, G. 2018. Failure behaviour of a fire protected steel element. *Frattura ed integritiá strutturale*, 46 (2018) 124-139; DOI: 10:3221/IGF-ESIS.46.13

Oosthuizen, P. 2010. Assessment of steel structures subjected to fire conditions. Master thesis, Department of Civil Engineering, University of Cape Town, South Africa.

Preston, R., & Kirby, B. 1998. High temperature properties of hot-rolled, structural steels for use in fire engineering design studies, *Fire Safety Journal* 13 (1988), pp. 27-37.

Qin, C. 2016. Collapse of simulation of steel buildings under fire. Master's thesis, Department of Civil and Environmental Engineering, Colorate State University.

Rackauskaite, E., Kotsovinos, P., Jeffers, A & Rein, G. 2017. Structural analysis of multistorey steel frames exposed to travelling fires and traditional design fires. Department of Mechanical Engineering, Imperial College London, London, United Kingdom.

Simms W. 2012. Fire resistance design of steel framed buildings, Ch. 2-5, 5-39. Steel construction Institute Publishers Co., Berkshire, United Kingdom.

Sun R., Huang Z., & Burgess I. (2012) Progressive collapse analysis of steel structure under fire conditions, *Journals of Engineering Structure*, 34:400-413

Sun R., Huang Z., & Burgess I. (2012) The collapse behaviour of braced steel frames exposed to fire, *Journals of Construction Steel Research,* 72:130-142

Steel Building in Europe Manuals: Multi-storey steel Buildings. Part 2: Concept Design

Steel Building in Europe Manuals: Multi-storey steel Buildings. Part 3: Actions

Steel Building in Europe Manuals: Multi-storey steel Buildings. Part 4: Detailed Design

Steel Building in Europe Manuals: Multi-storey steel Buildings. Part 6: Fire Engineering

Tide, R. 1998. Integrity of structural steel after exposure to fire. *Engineering Journal, American Institute of Steel Construction,* Vol 35, pp 26-38.

Vassart, O. & Zhao, B. 2011. FRACOF Engineering Background. Report developed for the Leonardo Da Vinci Programme: Fire Resistance Assessment of Partially Protected Composite Floors (FRACOF), Bordeaux, France, European Commission, Education and Culture DG.

Vassart, O., Zhao, B., Cajot, L., Robert, F., Meyer, U., Frangi., A., Poljanšek., M., Nikolova., B., Sousa, L., & Dimova, S. 2014. Eurocodes: Background & Applications Structural Fire Design. Luxembourg. doi, 10**,** 85432.

Walls, R. 2016. A beam finite element for the analysis of structures in fire. PhD Engineering Dissertation, School of Civil Engineering, Stellenbosch University, Cape Town, Republic of South Africa.

Zhao, B. 2012. Fire resistance assessment of steel structures: Workshop 'structural fire design of buildings according to the Eurocodes' – Brussels: European Committee for Standardization